MULTIPLE-ACCESS WITH ULTRA-WIDEBAND IMPULSE RADIO

MODULATION USING SPREAD SPECTRUM TIME HOPPING AND

BLOCK WAVEFORM PULSE POSITION MODULATED SIGNALS

by

Fernando Ramírez-Mireles

A Dissertation Presented to the

FACULTY OF THE GRADUATE SCHOOL

UNIVERSITY OF SOUTHERN CALIFORNIA

In Partial Fulfillment of the

Requirements for the Degree

DOCTOR OF PHILOSOPHY

(Electrical Engineering)

Dedication

To Miroslava, my lovely and brave wife who was with me when I most needed her.

To Tania, our wonderful daughter who made us a family and bring with her the light of her smile.

Acknowledgments

I want to give special thanks to Dr. Robert A. Scholtz for being the chairman of my Ph.D. committee. His guidance and advice during my doctorate endeavors changed the course of my professional life. I am grateful to Dr. Charles A. Weber for being a member of my committee. He contributed with valuable insights into the communication signals design problem. I owe thanks to Dr. Gary Rosen for being the external member of the committee. The time he spent attending my qualifying and defense is very much esteemed. I must express my gratitude to Dr. Robert Gagliardi for providing me with an invaluable learning experience. He taught me sound communications engineering principles. I want to thank Dr. Keith Chugg and Dr. Antonio Ortega for helpful technical discussions related with my dissertation.

I was fortunate to meet special people that rendered gently support and very much needed friendship in this long academic journey. I am especially beholden to Ph.D. candidate Chan-Kyung Park, Dr. Enrique Nava, Dr. Janette Murillo, Dr. Tony Liu, Mrs. Sunny Liu, Dr. Eduardo Esteves, Dr. Pablo Valle, Mrs. Norma Valle and Mrs. Milly Montenegro.

My classmates at the Communication Sciences Institute, Dr. Senthil Sengodan, Dr. Moe Z. Win, Dr. Joungheon Oh, Dr. George Chrisikos, Dr. Gent Paparisto, Dr. Jeng-Hong Chen, and Ph.D. candidates Jean-Marc Cramer, Carlos Corrada, Achilleas Anastasopoulos, Prokopios Panagiotou, and Anchung Chang, contributed to enrich my professional experience. The assistance of Mrs. Milly Montenegro, Mrs. Edith Ross and Ms. Mayumi Trasher was invaluable to run administrative dealings.

The signal propagation data used in the numerical example in chapter 6 was measured at Time Domain Corp., and was kindly provided to me by Dr. Moe Z. Win. My graduate studies were mainly supported by the Conacyt grant. This

Contents

List Of Tables

List Of Figures

symbols definition

List of Notations

$w(t)$	Basic UWB impulse used to convey information
$\sqrt{E_s}\, w_{tx}(t)$	Reference signal in CRcvr receiver
$\sqrt{E_a}\, \tilde{w}(u,t)$	Reference signal in PRake receiver
$\sqrt{E_a^{(K)}}\, \tilde{w}^{(K)}(u,t)$	Reference signal in MRake receiver
K	Number of fingers in MRake receiver
$x^{(\nu)}(t)$	User ν^{th}'s signal
$X_{m,d_m^{(\nu)}}^{(\nu)}(t)$	TH PPM signal
$C_m^{(\nu)}(t)$	TH signal
$S_i(t)$	PPM signal
δ_i^k	Time shift value
$\gamma_w(\tau)$	Normalized signal correlation function of $w(t)$
α_{ij}	Normalized signal correlation value of $S_i(t)$
Λ	Matrix containing α_{ij} values
$F_s(f)$	Power spectrum density of PPM signals
$Q(z)$	Gaussian tail integral
N_u	Number of users
UBP_e	Union bound on the symbol error probability
UBP_b	Union bound on the bit error probability
$\mathbf{SNR}_{\text{out}}(N_u)$	Multiple-access symbol SNR
$\mathbf{SNRb}_{\text{out}}(N_u)$	Multiple-access bit SNR
$C_{\text{IR}}(N_u)$	Multiple-access capacity of IR
$\text{DF}(N_u)$	Multiple-access degradation factor

AWGN	Additive white Gaussian noise
CRcvr	Correlation receiver
EC	Equally correlated
IR	Impulse radio
IR-AWGN	Free space propagation IR channel
IR-MP	Wireless indoor IR multipath channel
MRake	Mismatched Rake
MTSK	Multiple-TSK modulation
NO	N-orthogonal
OR	Orthogonal
PPM	Pulse position modulation
PRake	Perfect Rake
Rake	Rake receiver
SNR	Signal-to-noise-ratio
TH	Time hopping
TSK	Time-shift-keyed modulation
UWB	Ultra-wideband

Abstract

Impulse radio (IR) is an ultra-wideband (UWB) modulation that uses waveforms that consist of trains of time-shifted subnanosecond pulses. Data is transmitted using pulse position modulation at a rate of many pulses per symbol. Multiple access capability is achieved using spread spectrum time hopping. Impulse radio promises to be a viable technique to build relatively simple and low-cost, low-power transceivers that can be used for short range, high speed multiple-access communications over the multipath indoor wireless channel.

In [8] the single-user multiple-access performance of IR assuming free space propagation conditions and additive white Gaussian noise (AWGN) was studied. The analysis assumed that binary pulse-position-modulated (PPM) signals based on binary time-shift-keyed (TSK) modulation are detected using a correlation receiver. The analysis in [8] is quite similar to that for code-division multiple-access made in [44] and is based on the fact that both designs use single-channel correlation receivers for phase-coherent detection of the bit waveform.

In this dissertation we generalize the ideas in [8] to investigate the use of block-waveform signals to increase the data transmission rate supported by the system without degrading the multiple-access performance for a given number of users, or to increase the number of users supported by the system for a given multiple-access performance and bit transmission rate. More specifically, we present three M-ary block-coded PPM signal designs and analyze the multiple-access performance of IR

using these PPM signals. We also discuss some of the tradeoffs between performance and receiver complexity. Using this idealized analysis, numerical examples given in chapter 5 show that IR modulation is potentially able to support hundreds of users, each transmitting at a rate over a Megabit per second at bit error rates as low as 10^{-8}. Similarly, it is shown that IR is potentially able to support thousands of users, each transmitting at a rate about ten Kilobits per second at bit error rates in the order of 10^{-4}. In either case, the combined transmission rates give a transmission capacity of over 500 Megabits per second using receivers of moderate complexity.

We also include an assessment of the performance of IR modulation in the presence of dense multipath (no multiple-access interference is considered in this assessment). Numerical results in chapter 6 show that for a particular set of $M = 4$ signals and symbol error probability of 10^{-3}, the performance in the presence of multipath using a mismatched Rake receiver with $K = 10$ fingers is, on average, just 3 dB worse than performance in the absence of multipath using a correlation receiver.

Chapter 1

Introduction

This chapter briefly describes the ultra-wideband spread spectrum impulse radio modulation rationale and the targeted application. It lists some of the research problems and results that can be found in the literature. It also describes the objective of this research.

1.1   Motivation for impulse radio modulation

Short range, high speed multiple-access communications over the multipath indoor wireless channel is a technical challenge [1]. This channel is impaired with deep multipath nulls (fading) produced by dense multiple path signals arriving at the receiver with different time delays that can be as small as fractions of nanoseconds [2]. For the signals to survive these nulls, an increase in the transmitted power (fading margin) and/or the use of diversity techniques [3] [4] is required. Frequency diversity can be achieved by using signals with bandwidths on the order of G-Hz to allow a Rake receiver to be operable in this environment [5].

One convenient way to generate this UWB communication signals is to use sub-nanosecond pulses.[1] The technology for receiving and generating such pulses controlling their relative position in the time axis with great accuracy is now available [6] [7]. Impulse radio modulation uses UWB waveforms that consist of trains of time-shifted subnanosecond pulses. Data is transmitted using PPM data modulation at a rate of many pulses per symbol, and multiple-access capability is achieved using spread spectrum (SS) time hopping (TH). The TH PPM combination results in non-constant envelope, "carrier-less" UWB modulated waveforms that can be received by correlation detection literally at the antenna terminals, making a relatively simple and low-cost, low-power transceiver viable [8].

Although an IR system and a CDMA system operating with the same bandwidth can be shown to be quite comparable when used in a multiple-access environment, the current impulse technology gives an advantage to IR on the basis of achievable effective processing gains for the two systems [9]. In IR, an effective processing gain of about 50 (30) dB paired with a data transmission rate of about 9.6 (1024) Kilo bits per second is automatically achievable with the use of subnanosecond pulses, allowing a large number of users to be accommodated in the system. These large processing gains are essential for IR equipment to be operable license-free, and be able to coexist with a large number of services with narrower bandwidths without significant mutual interference.

In comparison to a fast-frequency hopping receiver operating with the same processing gain, IR has an edge in uncoded error-probability because of its coherence.

---

[1]Depending on the pulse shape and the definition of bandwidth, the range of frequencies occupied goes from a few hundred of K-Hz to a few G-Hz.

Finally, when compared with other technologies capable of supporting G-Hz bandwidths, IR has an advantage over infrared technology since radio communication can easily penetrate the structure of buildings facilitating wireless communications. Also, impulse radio potentially is cheaper than millimeter wave communications for the same short-range communications environment.

1.2   Current research areas

The same qualities that make IR technologically attractive [8] [10] also provide the communication design challenges [11] [12], yielding a rich source of research problems . Among them are UWB channel propagation measurements [13] [14], channel modeling, including multipath angle of arrival characterization [17] [15] [16] [18], PPM signal selection [19] [20] [21] [23] [22] [34], PPM signal design [24] [25] [26], TH sequence design, fast TH sequence acquisition and tracking, demodulation and synchronization with limited radiated power, multiple-access performance calculation [8] [27] [28] [29] [31] [32], receiver implementation issues [33] [34] [36] [24] [25] [26] [35], as well as network issues [37] [38] [39] [40]. Other possible research topics are listed in section 7.2.

1.3   Objective of this research

In this dissertation we analyze and quantify the benefits of using block-coded PPM signals in IR modulation. We present three M-ary block-coded PPM signal designs. We analyze the multiple-access performance of IR using these PPM signals and discuss some of the tradeoffs between performance and receiver complexity. Finally, we conclude this thesis making an assessment of the performance of IR modulation

in the presence of dense multipath (no multiple-access interference is considered in this assessment).

This thesis is organized as follows. Chapter 2 describes the channel and signal models. In chapter 3 the demodulation processing when TH-PPM signals are used to transmit information is discussed. In chapter 4 we describe three block waveform PPM signal designs. In each case the construction method is given, the performance is analyzed, and receiver simplification is discussed. In chapter 5 we analyze the single-user multiple-access performance of IR using block-waveform PPM signals. In chapter 6 we investigate the performance of IR modulation in the presence of dense multipath. Chapter 7 contains the conclusions and future research.

Chapter 2

Channel, signals and multiple-access interference models

This chapter begins with a description of the assumed channel model and the characteristics of the impulse waveform used to carry information. It then discusses the structure and properties of the TH PPM communications signals used in IR. Finally, it describes the assumed statistical properties of the multiple-access interference.

2.1 Channel model

The model assumed is a channel with free space propagation conditions and AWGN, and is denoted IR-AWGN. The transmitted pulse is $w_{tx}(t) \triangleq \int_{-\infty}^{t} w(\xi)d\xi$ and the received pulse is $Aw(t-\tau)+n(t)$.[1] The constants A and τ represent the attenuation and propagation delay, respectively, that the signal experiences over the link path between the transmitter and receiver. The noise $n(t)$ is AWGN with two-sided power density $\frac{N_o}{2}$ Watts/Hz.

---

[1] The combined effect of the channel and the antenna system is modeled as a derivation operation. Hence, the received pulse is the derivative of the transmitted pulse.

2.2 Signals models

2.2.1 Impulse signal

The UWB signal $w(t)$ is the basic subnanosecond impulse used to convey information. It has duration T_w seconds, two-sided bandwidth of W Hertz, and energy $E_w = \int_{-\infty}^{\infty} [w(t)]^2 \, dt$ Joules. The normalized signal correlation function of $w(t)$ is

$$\gamma_w(\tau) \triangleq \frac{1}{E_w} \int_{-\infty}^{\infty} w(t)w(t-\tau)dt > -1 \; \forall \tau. \tag{2.1}$$

The minimum value of $\gamma_w(\tau)$ will be denoted $\gamma_{\min}$, and $\tau_{\min}$ will denote the smallest value of τ in $[0, T_w]$ such that $\gamma_{\min} = \gamma_w(\tau_{\min})$. The correlation value between $w(t-\tau_i)$ and $w(t-\tau_j)$, $i \neq j$, is given by $\gamma_w(\tau_i - \tau_j)$. Note that the signals $w(t-\tau_i)$ and $w(t-\tau_j)$ are linearly independent, hence they can never be antipodal.

2.2.2 TH-PPM signals

The TH PPM signal conveying information exclusively in the time shifts is

$$x^{(\nu)}(t) = \sum_{k=0}^{\infty} w\big(t - kT_f - c_k^{(\nu)}T_c - \delta_{d_{\lfloor k/N_s \rfloor}^{(\nu)}}^k\big). \tag{2.2}$$

The superscript (ν), $(1 \leq \nu \leq N_u)$ indicates user-dependent quantities. The index k is the number of time hops that the signal $x^{(\nu)}(t)$ has experienced, and also the number of impulses that has been transmitted. The impulse duration satisfies $T_w << T_f$, where T_f is the frame (impulse repetition) time and equals the average time between pulse transmissions. The $\{c_k^{(\nu)}\}$ is the pseudo-random time-hopping sequence assigned to user ν. It is periodic with period N_p (i.e., $c_{k+lN_p}^{(\nu)} = c_k^{(\nu)}, \forall k, l$ integers) and each sequence element is an integer in the range $0 \leq c_k^{(\nu)} \leq N_h$. The time hopping code provides an additional time shift to each impulse, each time shift

6

being a discrete time value between $0 \leq c_k^{(\nu)} T_c < N_h T_c$ seconds. The time shift corresponding to the data modulation is $\delta_{d_{\lfloor k/N_s \rfloor}^{(\nu)}}^k \in \{\tau_1 = 0 < \tau_2 < \ldots < \tau_{N_d}\}$, with τ_{N_d} small relative to T_f. To simplify the analysis, we further assume that

$$N_h T_c + 2(\tau_{N_d} + T_w) < T_f/2. \tag{2.3}$$

The data sequence $\{d_m^{(\nu)}\}$ of user ν is an M-ary ($1 \leq d_m^{(\nu)} \leq M$) symbol stream that conveys information in some form. Impulse radio is a fast hopping system, which means that there are N_s impulses transmitted per symbol. The data symbol changes only every N_s hops, and assuming that a new data symbol begins with pulse index $k = 0$, the index of the data modulating pulse k is $\lfloor k/N_s \rfloor$ (Here the notation $\lfloor q \rfloor$ denotes the integer part of q). Hence (2.2) can be written as

$$x^{(\nu)}(t) = \sum_{m=0}^{\infty} X_{m,d_m^{(\nu)}}^{(\nu)}(t), \tag{2.4}$$

where

$$X_{m,d_m^{(\nu)}}^{(\nu)}(t) \triangleq \sum_{k=mN_s}^{(m+1)N_s-1} w(t - kT_f - c_k^{(\nu)} T_c - \delta_{d_m^{(\nu)}}^k), \tag{2.5}$$
$$mN_s T_f \leq t \leq [(m+1)N_s]T_f,$$

where m indexes the number of transmitted symbols. If we define

$$C_m^{(\nu)}(t) \triangleq \sum_{k=mN_s}^{(m+1)N_s-1} T_c\, c_k^{(\nu)} p(t - kT_f), \tag{2.6}$$

where

$$p(t) = \begin{cases} 1, & \text{if } 0 \leq t \leq T_f \\ 0, & \text{otherwise} \end{cases} \tag{2.7}$$

7

and

$$S_i(t) \quad \triangleq \quad \sum_{k=0}^{N_s-1} w\big(t - kT_f - \delta_i^k\big), \quad i = 1, 2, \ldots, M, \tag{2.8}$$

then we can write

$$X_{m,d_m^{(\nu)}}^{(\nu)}(t) \quad = \quad S_{d_m^{(\nu)}}\big(t - mN_sT_f - C_m^{(\nu)}(t)\big), \tag{2.9}$$

i.e,

$$x^{(\nu)}(t) \quad = \quad \sum_{m=0}^{\infty} S_{d_m^{(\nu)}}\big(t - mN_sT_f - C_m^{(\nu)}(t)\big). \tag{2.10}$$

Hence the user's signal $x^{(\nu)}(t)$ is composed of a sequence of signals $X_{m,d_m^{(\nu)}}^{(\nu)}(t)$, where each frame-shifted $X_{m,d_m^{(\nu)}}^{(\nu)}(t)$ is a fast-hopped version of one of the M possible PPM symbol waveforms $\{S_i(t)\}$. A single symbol waveform has duration $T_s \triangleq N_sT_f$. For a fixed T_f, the M-ary symbol rate $R_s = T_s^{-1}$ determines the number N_s of impulses that are modulated by a given symbol. Note that when the hopping pattern in (2.6) is known, the signals in (2.8) and (2.9) have the same correlation properties

$$\int_{-\infty}^{\infty} X_{m,i}^{(\nu)}(\xi)\, X_{m,j}^{(\nu)}(\xi)\, d\xi = \int_{-\infty}^{\infty} S_i(\xi)\, S_j(\xi)\, d\xi \tag{2.11}$$

These properties will be discussed in the next section.

2.2.3   PPM signals

The PPM signal $S_i(t)$ in (2.8) represents the i-th signal in an ensemble of M information signals,[2] each signal completely identified by the sequence of time shifts

---

[2]The signal $S_i(t)$ is the received signal when $\int_{-\infty}^{t} S_i(\xi)d\xi$ is transmitted over the IR-AWGN channel in the absence of noise and interference.

$\{\delta_i^k ; k = 0, 1, 2, \ldots, N_s - 1\}$. The complete ensemble of signals $\{S_i(t)\}$ will be represented by the $M \times N_s$ matrix

$$\Delta = \begin{bmatrix} \delta_1^1 & \delta_1^2 & \cdots & \delta_1^k & \cdots & \delta_1^{N_s} \\ \delta_2^1 & \delta_2^2 & \cdots & \delta_2^k & \cdots & \delta_2^{N_s} \\ \vdots & \vdots & \ddots & \vdots & \vdots & \vdots \\ \delta_i^1 & \delta_i^2 & \cdots & \delta_i^m & \cdots & \delta_i^{N_s} \\ \vdots & \vdots & \vdots & \vdots & \ddots & \vdots \\ \delta_M^1 & \delta_M^2 & \cdots & \delta_M^k & \cdots & \delta_M^{N_s} \end{bmatrix}, \tag{2.12}$$

where each row corresponds to the time shifts $\{\delta_i^k ; k = 0, 1, 2, \ldots, N_s - 1\}$ defining the i-th signal. The correlation between $S_i(t)$ and $S_j(t)$ is defined as

$$\begin{aligned} R_{ij} &\triangleq \int_{-\infty}^{\infty} S_i(t) S_j(t) dt \\ &= \sum_{k=0}^{N_s-1} \int_{-\infty}^{\infty} w(t - \delta_i^k) \, w(t - \delta_j^k) \, dt \end{aligned} \tag{2.13}$$

since for $k \neq l$ the pulses are non overlapping (see (2.3)). In terms of the correlation properties of $w(t)$, we can write R_{ij} as

$$R_{ij} = E_w \sum_{k=0}^{N_s-1} \gamma_w(\delta_i^k - \delta_j^k). \tag{2.14}$$

The energy in the ith signal is

$$E_S = R_{ii} = \int_{-\infty}^{\infty} [S_i(t)]^2 = N_s E_w, \tag{2.15}$$

and the normalized correlation value is

$$\alpha_{ij} \triangleq \frac{R_{ii}}{E_S} = \frac{1}{N_s} \sum_{k=0}^{N_s-1} \gamma_w(\delta_i^k - \delta_j^k) \geq \gamma_{\min}. \tag{2.16}$$

The complete set of normalized correlation values α_{ij} corresponding to the ensemble of signals Δ is given by the $M \times M$ symmetric non negative definite correlation matrix

$$\Lambda \overset{\triangle}{=} \begin{bmatrix} 1 & \alpha_{21} & \cdots & \alpha_{M1} \\ \alpha_{21} & 1 & \cdots & \alpha_{M2} \\ \vdots & \vdots & \ddots & \vdots \\ \alpha_{M1} & \alpha_{M2} & \cdots & 1 \end{bmatrix}. \tag{2.17}$$

Note that the signals in the set $\{S_i(t)\}$ are linearly independent. Hence the dimensionality of the set $\{S_i(t)\}$ is always M,[3] and the signals $S_i(t)$, $S_j(t)$, $i \neq j$, can never be antipodal.

The power spectrum density of the ensemble of signals $\{S_i(t)\}$ for a wide sense stationary stream of iid symbols can be shown to be [42]

$$\begin{aligned} F_s(f) &= \frac{1}{T_s} \sum_{i=1}^{M} P_i \, |F_{S_i}(f)|^2 \; + \\ &\quad \frac{1}{T_s} |\sum_{i=1}^{M} P_i F_{S_i}(f)|^2 \left[-1 + \frac{1}{T_s} \sum_{m=-\infty}^{\infty} \delta(f - \frac{m}{T_s}) \right], \end{aligned} \tag{2.18}$$

where P_i is the probability of signal $S_i(t)$ being used, and $F_{S_i}(f)$ is the Fourier transform of $S_i(t)$ given by

$$F_{S_i}(f) = \int_{-\infty}^{\infty} S_i(t) \, \exp\left(-j2\pi ft\right) dt = F_w(f) \, F_i(f), \tag{2.19}$$

where

$$F_w(f) = \int_{-\infty}^{\infty} w(t) \, \exp\left(-j2\pi ft\right) dt \tag{2.20}$$

---

[3]The linear independence also implies that, when the signals are equicorrelated with $\alpha_{ij} = \alpha$, then necessarily $\alpha > \frac{-1}{M-1}$, i.e., we can not achieve the "simplex bound" for the maximum value of correlation [41].

and

$$F_i(f) = \int_{-\infty}^{\infty} \sum_{k=0}^{N_s-1} \delta(t - kT_f - \delta_i^k) \exp(-j2\pi ft)\, dt$$

$$= \sum_{k=0}^{N_s-1} \exp[-j2\pi f(kT_f + \delta_i^k)], \tag{2.21}$$

If we substitute (2.19) in (2.18) we get

$$F_s(f) = \frac{|F_w(f)|^2}{T_s} \left\{ \sum_{i=1}^{M} P_i\, |F_i(f)|^2 + \right.$$

$$\left. |\sum_{i=1}^{M} P_i F_i(f)|^2 \left[-1 + \frac{1}{T_s} \sum_{l=-\infty}^{\infty} \delta(f - \frac{l}{T_s}) \right] \right\}. \tag{2.22}$$

2.3   Multiple-access interference model

The following assumptions are made to facilitate our analytical treatment.

(a) We assume that the signals $x^{(\nu)}(t - \tau^{(\nu)})$, for $\nu = 1, 2, \ldots, N_u$ and $n(t)$ are independently generated.

(b) To estimate performance without choosing a hopping sequence family, we assume that the hopping sequences $\{c_k^{(\nu)}\}$, for $\nu = 1, 2, 3, \ldots, N_u$, and for all k, are samples of purely random sequences, and compute performance based on signal-to-noise ratios averaged over the hopping sequence variables. To guarantee that no hopping sequence random variable occurs more than once in a symbol time, we assume that $N_s \leq N_p$. Also, for many hops to occur in a symbol time, we further assume that $N_s \gg 1$. The elements of each user's hopping sequence will be modeled as random variables selected independently and uniformly from the time interval $[0, N_h T_c]$, and therefore the probability

density function of a time shift $c_k^{(\nu)} T_c$ produced by the element $c_k^{(\nu)}$ of the hopping sequence is approximated by

$$
p_{c_k^{(\nu)} T_c}(\varphi) = \begin{cases} (N_h T_c)^{-1}, & 0 \leq \varphi \leq N_h T_c \\ 0, & \text{otherwise} \end{cases}. \tag{2.23}
$$

(c) The time delay $\tau^{(\nu)}$ is related to the time when the νth radio starts transmitting in asynchronous operation, and its magnitude spans many frames T_f. We can model[4]

$$
\tau^{(\nu)} = \Phi T_f + \phi, \text{ where } \frac{T_f}{2} \leq \phi < \frac{T_f}{2}, \tag{2.24}
$$

hence Φ is the value of $\tau^{(\nu)}$ rounded to the nearest frame time, and ϕ is the error in this rounding process. Since ϕ is a round-off error of a large random variable, it is reasonable to assume that ϕ is uniformly distributed over it's range, therefore the probability density function of ϕ is

$$
p_\phi(\varphi) = \begin{cases} T_f^{-1}, & 0 \leq \varphi < N_h T_c \\ 0, & \text{otherwise} \end{cases}. \tag{2.25}
$$

A model for Φ won't be needed because the final calculations are independent of it.

(d) Since the received signal is modeled as the derivative of the transmitted signal, we assume that the impulse $w(t)$ satisfies the relation

$$
\int_{-\infty}^{\infty} w(\xi) \, d\xi = 0. \tag{2.26}
$$

(e) Let $\delta_m = \max \delta_i^k$, $i = 1, 2, \ldots, M$, $k = 0, 1, 2, \ldots, N_s - 1$, i.e, $\delta_m = \tau_{N_d}$. We will assume that δ_m is much smaller than both the time uncertainty parameter ϕ and the time hopping window width $N_h T_c$. We further assume that the data

---

[4]This model will be also valid for $\tau^{(\nu)} - \tau^{(1)}$.

modulation on the signals of users $2, 3, \ldots, N_u$ has no significant effect on the calculation of multiple-access interference statistics for user 1. Hence, the time shift values $\delta^k_{d^{(\nu)}_m} = 0$ for $\nu = 2, 3, \ldots, N_u$, and all k.

(f) To simplify the analysis we assume that the time interval over which the impulse $w(t)$ can be time hopped is less than a half a frame time so that

$$N_h T_c < \frac{T_f}{2} - \epsilon, \qquad (2.27)$$

where

$$\epsilon \triangleq 2(T_w + \delta_m) \qquad (2.28)$$

is two times the sum of widths of $w(t)$ and $w(t) - w(t - \delta_m)$.

These assumptions allow the use of the Central Limit Theorem [43] to conclude that the net effect of the ultra-wideband multiple-access interference caused by users $2, 3, \ldots, N_u$ in user one's correlation receiver can be modeled as a Gaussian random variable.

Chapter 3

Receiver signal processing and multiple-access performance

In this chapter we discuss the receiver signal processing and analyze the single-user multiple-access performance of IR using block-waveform TH-PPM signals. The multiple-access performance is analyzed in terms of the number of users supported by the system for a given bit error rate, bit transmission rate, and number of signals in the block waveform set.

The calculations made here are quite similar to the calculations in [8] for the single-user multiple-access performance of IR using binary PPM communications signals. The analysis in [8] is in turn quite similar to that for code-division multiple-access made in [44] and is based on the fact that both designs use single-channel correlation receivers for phase-coherent detection of the bit waveform.

In the present work we generalize the ideas in [8] to investigate the use of block-waveform signals to increase the data transmission rate supported by the system without degrading the multiple-access performance for a given number of users, or to improve the multiple-access performance of the system for a given number of users and bit transmission rate. Using this idealized analysis, numerical examples given in chapter 5 show that IR modulation is potentially able to support hundreds

of users, each transmitting at a rate over a Megabit per second at bit error rates as low as 10^{-8}, using receivers of moderate complexity. Similarly, it is shown that IR is potentially able to support thousands of users, each transmitting at a rate about ten Kilobits per second at bit error rates in the order of 10^{-4}. The combined transmission rate in either case gives a transmission capacity of over 500 Megabits per second.

3.1 Receiver signal processing

Consider a multiple-access system with N_u users transmitting IR modulation. The signal at the receiver $r(t)$ can be modeled as

$$r(t) = \sum_{\nu=1}^{N_u} A^{(\nu)} x^{(\nu)}(t - \tau^{(\nu)}) + n(t), \tag{3.1}$$

where $A^{(\nu)}$ is the attenuation of user ν's signal over the channel, $\tau^{(\nu)}$ represents time asynchronisms between the clocks of user ν's transmitter and the receiver, and the signal $n(t)$ represents non-multiple-access interference modeled as AWGN. Let's assume that the receiver wants to demodulate user one's signal representing the mth data symbol $d_m^{(1)}$, where $d_m^{(1)}$ is one of M equally-likely symbols. The received signal $r(t)$ in (3.1) can be viewed as

$$r(t) = A^{(1)} X_{m,d_m^{(1)}}^{(1)}(t - \tau^{(1)}) + n_{tot}(t), \ t \in \mathcal{T}_m, \tag{3.2}$$

where

$$\mathcal{T}_m \triangleq [mN_sT_f + \tau^{(1)}, (m+1)N_sT_f + \tau^{(1)}), \tag{3.3}$$

and

$$n_{tot}(t) \triangleq \sum_{\nu=2}^{N_u} A^{(\nu)} x^{(\nu)}(t - \tau^{(\nu)}) + n(t). \qquad (3.4)$$

When the receiver is perfectly synchronized to the first user signal, e.g., having learned the value of $\tau^{(1)}$ (or at least $\tau^{(1)} \bmod N_p T_f$), the receiver is able to determine the sequence $\{\mathcal{T}_m\}$ of time intervals, with interval $\mathcal{T}_m$ containing the waveform representing data symbol $d_m^{(1)}$ (or $d_m^{(1)} \bmod N_p$). In this case the detection problem becomes the coherent detection of M equal-energy, equally-likely signals in the presence of multiple-access interference in addition to AWGN. In this case the optimal receiver (multi-user detector) is a complicated structure that takes advantage of all of the receiver's knowledge regarding the characteristics of the multiple-access interference [45] [46].

Due to the complexity of the analysis, the multi-user detector will not be considered here. Instead, we will assume that $n_{tot}(t)$ is a zero-mean Gaussian random process (see section 2.3). Hence, the detection problem will be the coherent detection of M equal-energy, equally-likely signals in the presence of mean-zero Gaussian interference in addition to AWGN. A suboptimum receiver for this case is the M-ary correlation receiver [47]. This receiver is described in the next section.

3.2 Decoding of block waveform TH-PPM signals

The M-ary correlation receiver consists of M filters matched to the signals $\{X_{m,i}^{(1)}(t - \tau^{(1)})\}$, $i = 1, 2, \ldots, M$, $t \in \mathcal{T}_m$, followed by samplers and a decision circuit that selects the maximum among the decision variables

$$y_i = \int_{t \in \mathcal{T}_m} r(t) \, X_{m,i}^{(1)}(t - \tau^{(1)}) \, dt, \; i = 1, 2, \ldots, M. \qquad (3.5)$$

16

The error probability in decoding a symbol is the probability that an incorrect decision variable exceeds the correct one. When $d_m^{(1)} = j$ is sent, the conditioned symbol error probability is

$$\text{Prob}(\text{error}|d_m^{(1)} = j) = 1 - \text{Prob}(y_j \geq y_i |d_m^{(1)} = j), \ i = 1, 2, \ldots, i \neq j, \quad (3.6)$$

We can use the union bound [47] to upper bound the conditioned error probability in (3.6). This bound states that the probability that a particular y_j is less than the $M-1$ remaining decision variables is bounded from above by the sum of probabilities that y_j is less than y_i, $i = 1, 2, \ldots, M$, $i \neq j$, individually. The union bound implies that

$$\text{Prob}(\text{error}|d_m^{(1)} = j) \leq \sum_{\substack{i = 1 \\ i \neq j}}^{M} \text{Prob}(y_j \leq y_i |d_m^{(1)} = j). \quad (3.7)$$

The average error probability then satisfies

$$\begin{aligned}
\text{Prob}(\text{error}) &\leq \sum_{j=1}^{M} \text{Prob}(d_m^{(1)} = j)\text{Prob}(\text{error}|d_m^{(1)} = j) \\
&= \sum_{j=1}^{M} \frac{1}{M} \sum_{\substack{i = 1 \\ i \neq j}}^{M} \text{Prob}(y_j \leq y_i |d_m^{(1)} = j). \quad (3.8)
\end{aligned}$$

By properly pairing terms, we can rewrite 3.8 as

$$\text{Prob}(\text{error}) = \tfrac{1}{M}\sum_{j=1}^{M}\sum_{\substack{i=1 \\ i \neq j}}^{M} \text{PE}_{j,i}, \quad (3.9)$$

where

$$\text{PE}_{j,i} = \frac{1}{2}\text{Prob}(y_j \leq y_i |d_m^{(1)} = j) + \frac{1}{2}\text{Prob}(y_i \leq y_j |d_m^{(1)} = i) \quad (3.10)$$

The $\text{PE}_{j,i}$ is the probability of error in the binary test attempting to decide between the pair of signals $X^{(1)}_{m,j}(t)$ and $X^{(1)}_{m,i}(t)$. The observation variable in this binary test can be written

$$r_b(t) \;=\; A^{(1)} X^{(1)}_{m,d^{(1)}_m}(t - \tau^{(1)}) + n_{tot}(t),\ t \in \mathcal{T}_m,\ d^{(1)}_m \in \{i,j\}, \qquad (3.11)$$

and the decision variable in this binary test is

$$\begin{aligned}
y_{j,i} \;&=\; \int_{t \in \mathcal{T}_m} r_b(t) Y^{(1)}_{m,j,i}(t - \tau^{(1)}) dt \\
&=\; \int_{t \in \mathcal{T}_m} A^{(1)} X^{(1)}_{m,d^{(1)}_m}(t - \tau^{(1)}) Y^{(1)}_{m,j,i}(t - \tau^{(1)}) dt \;+\; n_{j,i}, \qquad (3.12)
\end{aligned}$$

where

$$Y^{(1)}_{m,j,i}(t - \tau^{(\nu)}) \;\stackrel{\triangle}{=}\; [X^{(1)}_{m,j}(t - \tau^{(\nu)}) - X^{(1)}_{m,i}(t - \tau^{(\nu)})], \qquad (3.13)$$

and

$$n_{j,i} \;\stackrel{\triangle}{=}\; \int_{t \in \mathcal{T}_m} n_{tot}(t)\, Y^{(1)}_{m,j,i}(t - \tau^{(1)})\, dt. \qquad (3.14)$$

The binary decision variable $y_{j,i}$ in (3.12) is a Gaussian random variable with two components. One produced by the correlation with the transmitted signal (which can be either $X^{(1)}_{m,j}(t)$ or $X^{(1)}_{m,i}(t)$), and one due to the Gaussian noise $n_{tot}(t)$. The conditioned mean of $y_{j,i}$ is

$$\begin{aligned}
m_{j,i} \;&\stackrel{\triangle}{=}\; \mathbf{E}\{y_{j,i} | d^{(1)}_m = j\} \\
&=\; \int_{t \in \mathcal{T}_m} A^{(1)} X^{(1)}_{m,j}(t - \tau^{(1)}) Y^{(1)}_{m,j,i}(t - \tau^{(1)}) dt \\
&=\; A^{(1)} E_s (1 - \alpha_{ji}), \qquad (3.15)
\end{aligned}$$

where $\mathbf{E}\{\cdot\}$ is the expected value operator. Here we have assumed that

$$\mathbf{E}\{n_{j,i}|d_m^{(1)} = j\} = \mathbf{E}\{n_{j,i}|d_m^{(1)} = i\} = 0. \tag{3.16}$$

The conditioned mean of $y_{j,i}$ when $d_m^{(1)} = i$ is $m_{i,j} = -m_{j,i}$. The variance of $y_{j,i}$ in the presence of N_u users is

$$\sigma_{j,i}^2(N_u) = \mathbf{E}\{[n_{j,i}]^2\}. \tag{3.17}$$

A symbol error is made in decoding when $d_m^{(1)} = j$ and $y_{j,i}$ is negative or when $d_m^{(1)} = i$ and $y_{j,i}$ is positive. Since $m_{i,j} = -m_{j,i}$ and $\sigma_{j,i}^2(N_u) = \sigma_{i,j}^2(N_u)$, the average probability of error in this binary test is simply

$$\mathrm{PE}_{j,i} = Q\left(\sqrt{\mathbf{SNR}_{\mathrm{out}}^{(j,i)}(N_u)}\right), \tag{3.18}$$

where

$$Q(z) = \int_z^\infty \frac{\exp\left(-\xi^2/2\right)}{2\pi} d\xi \tag{3.19}$$

is the Gaussian-tail integral, and

$$\mathbf{SNR}_{\mathrm{out}}^{(j,i)}(N_u) = \frac{m_{j,i}^2}{\sigma_{j,i}^2(N_u)} \tag{3.20}$$

is user one's output symbol signal-to-noise ratio (SNR) observed in binary communications in the presence of Nu users, when user one uses either $X_{m,j}^{(1)}(t)$ or $X_{m,i}^{(1)}(t)$ to communicate information. The bit SNR $\mathbf{SNRb}_{\mathrm{out}}^{(j,i)}(N_u)$ is related to the symbol SNR $\mathbf{SNR}_{\mathrm{out}}^{(j,i)}(N_u)$ by

$$\begin{aligned} \mathbf{SNRb}_{\mathrm{out}}^{(j,i)}(N_u) &= \frac{1}{\log_2(M)} \mathbf{SNR}_{\mathrm{out}}^{(j,i)}(N_u) \\ &= \frac{1}{\log_2(M)} \frac{m_{j,i}^2}{\sigma_{j,i}^2(N_u)}. \end{aligned} \tag{3.21}$$

19

Using (3.18) in (3.9), the union bound on the symbol error probability is

$$\text{UBP}_e(N_u) \triangleq \frac{1}{M} \sum_{\substack{i=1 \\ i \neq j}}^{M} \sum_{j=1}^{M} Q\left(\sqrt{\mathbf{SNR}_{\text{out}}^{(j,i)}(N_u)}\right). \tag{3.22}$$

If only the desired transmitter is active $(N_u = 1)$, then $n_{tot}(t) = n(t)$ is AWGN and

$$\mathbf{E}\{n_{j,i}|d_m^{(1)} = j\} = \int_{t \in \mathcal{T}_m} \underbrace{\mathbf{E}\{n(t)|d_m^{(1)} = j\}}_{\mathbf{E}\{n(t)\}=0} Y_{m,j,i}^{(1)}(t - \tau^{(1)}) \, dt = 0, \tag{3.23}$$

and

$$\sigma_{j,i}^2(1) = \int_{t \in \mathcal{T}_m} \int_{\xi \in \mathcal{T}_m} \mathbf{E}\{n(t)n(\xi)\}$$
$$Y_{m,j,i}^{(1)}(t - \tau^{(1)})Y_{m,j,i}^{(1)}(\xi - \tau^{(1)})d\xi dt$$
$$= N_o E_s(1 - \alpha_{ji}). \tag{3.24}$$

Hence

$$\mathbf{SNR}_{\text{out}}^{(j,i)}(1) = \frac{(A^{(1)})^2 E_s}{N_o}(1 - \alpha_{ji}). \tag{3.25}$$

When more than one user is present, the calculation of $\mathbf{SNR}_{\text{out}}^{(j,i)}(N_u)$ in (3.20) requires the evaluation of the variance in (3.17) and the verification that the expected value in (3.16) is indeed zero. This calculation is made in the next subsection.

3.2.1 Evaluation of the moments of n_{ji}

For clarity in the notation, we will assume $m = 0$ in the mathematical expression involving the desired user $(\nu = 1)$, and will drop the index m from these expressions.

Also, for clarity in the calculations, random quantities will be indexed by the *random index* u.[1] From the definition of n_{ji} in (3.14) we can write

$$n_{j,i}(u) \;=\; \sum_{\nu=2}^{N_u} A^{(\nu)} n_{j,i}^{(\nu)}(u) + n_{j,i}^{(1)}(u), \qquad (3.26)$$

where

$$n_{j,i}^{(\nu)}(u) \;\triangleq\; \int_{t \in \mathcal{T}_0} x^{(\nu)}\big(u, t - \tau^{(\nu)}(u)\big)\, Y_{j,i}^{(1)}\big(u, t - \tau^{(1)}\big)\, dt \qquad (3.27)$$

is the component of $n_{j,i}(u)$ caused by multiple-access noise from the νth user, for $\nu = 2, 3, \ldots, N_u$, and

$$n_{j,i}^{(1)}(u) \;\triangleq\; \int_{t \in \mathcal{T}_0} n(u, t) Y_{j,i}^{(1)}\big(u, t - \tau^{(1)}\big) dt \qquad (3.28)$$

is the component of $n_{ji}(u)$ caused by receiver noise and other forms of non-impulsive interference.

Recall from (2.2) that the νth user's signal is

$$x^{(\nu)}\big(u, t - \tau^{(\nu)}(u)\big) = \sum_{k=0}^{\infty} w\big(t - \tau^{(\nu)}(u) - kT_f - c_k^{(\nu)}(u)T_c - \delta^k_{d^{(\nu)}_{\lfloor k/N_s \rfloor}(u)}\big), \qquad (3.29)$$

and from (3.13) that

$$
\begin{aligned}
Y_{j,i}^{(1)}\big(t - \tau^{(1)}\big) \;&=\; \big[X_j^{(1)}\big(t - \tau^{(1)}\big) - X_i^{(1)}\big(t - \tau^{(1)}\big)\big] \\
&=\; \sum_{k=0}^{N_s-1} w\big(t - \tau^{(1)} - kT_f - c_k^{(1)}(u)T_c - \delta_j^k\big) \;- \\
&\qquad \sum_{k=0}^{N_s-1} w\big(t - \tau^{(1)} - kT_f - c_k^{(1)}(u)T_c - \delta_i^k\big)
\end{aligned}
$$

---

[1]In this notation the deterministic signal $a(t)$ is a function of the time index t, the random variable $a(u)$ is a function of the random index u, and the random process $a(u,t)$ is a function of both u and t.

$$= \sum_{k=0}^{N_s-1} v_{k,j,i}(t - \tau^{(1)} - kT_f - c_k^{(1)}(u)T_c), \qquad (3.30)$$

where

$$v_{k,j,i}(t) \quad \triangleq \quad w(t - \delta_j^k) - w(t - \delta_i^k) \qquad (3.31)$$

for $i, j = 1, 2, \ldots, M$, $i \neq j$, and $k = 0, 1, 2, \ldots, N_s - 1$. Therefore

$$
\begin{aligned}
n_{j,i}^{(\nu)}(u) &= \int_{\tau^{(1)}}^{\tau^{(1)}+N_sT_f} \sum_{k=0}^{\infty} \sum_{l=0}^{N_s-1} w\bigl(t - \tau^{(\nu)}(u) - kT_f - c_k^{(\nu)}(u)T_c - \delta_{d_{\lfloor k/N_s \rfloor}^{(\nu)}(u)}^k\bigr) \\
&\qquad v_{l,j,i}(t - \tau^{(1)} - lT_f - c_l^{(1)}(u)T_c)\, dt \\
&= \sum_{l=0}^{N_s-1} \int_{\tau^{(1)}+lT_f}^{\tau^{(1)}+(l+1)T_f} \sum_{k=0}^{\infty} w\bigl(t - \tau^{(\nu)}(u) - kT_f - c_k^{(\nu)}(u)T_c - \delta_{d_{\lfloor k/N_s \rfloor}^{(\nu)}(u)}^k\bigr) \\
&\qquad v_{l,j,i}(t - \tau^{(1)} - lT_f - c_l^{(1)}(u)T_c)\, dt \\
&= \sum_{l=0}^{N_s-1} \int_{-c_l^{(1)}(u)T_c}^{-c_l^{(1)}(u)T_c+T_f} v_{l,j,i}(\theta) \sum_{k=0}^{\infty} \\
&\qquad w\bigl(\theta - (\tau^{(\nu)}(u) - \tau^{(1)}) - (k-l)T_f - \\
&\qquad [c_k^{(\nu)}(u) - c_l^{(1)}(u)]T_c - \delta_{d_{\lfloor k/N_s \rfloor}^{(\nu)}(u)}^k\bigr)\, d\theta.
\end{aligned}
$$

$$(3.32)$$

We now use some of the assumptions made in section 2.3. By assumption (e) we make $\delta_{d_{\lfloor k/N_s \rfloor}^{(\nu)}(u)}^k = 0$ for $\nu = 2, 3, \ldots, N_u$, and by assumption (c) we make $\tau^{(\nu)}(u) - \tau^{(1)} = \Phi(u)T_f + \phi(u)$, $|\phi(u)| < \frac{T_f}{2}$, hence

$$
\begin{aligned}
n_{j,i}^{(\nu)}(u) &= \sum_{l=0}^{N_s-1} \int_{-c_l^{(1)}(u)T_c}^{-c_l^{(1)}(u)T_c+T_f} v_{l,j,i}(\theta) \\
&\qquad \sum_{k=0}^{\infty} w\bigl(\theta - \phi(u) - [k - (l - \Phi)]T_f - [c_k^{(\nu)}(u) - c_l^{(1)}(u)]T_c\bigr)\, d\theta.
\end{aligned}
$$

$$(3.33)$$

Noting that the integrand is always zero for $k \neq l - \Phi$ and that $v_{l,j,i}(\theta)$ is non-zero for $|\theta| \leq \epsilon$ (i.e., only for a few nanoseconds), we can write

$$
\begin{aligned}
n_{j,i}^{(\nu)}(u) &= \sum_{k=0}^{N_s-1} \int_{-\infty}^{\infty} v_{k,j,i}(\theta) w(\theta - \phi(u) - \Omega_k(u)) \, d\theta \\
&= \sum_{k=0}^{N_s-1} n_{k,j,i}^{(\nu)}(u),
\end{aligned}
\tag{3.34}
$$

where

$$
n_{k,j,i}^{(\nu)}(u) \;\; \triangleq \;\; \int_{-\infty}^{\infty} w(\theta - \phi(u) - \Omega_k(u)) \, v_{k,j,i}(\theta) \, d\theta
\tag{3.35}
$$

and

$$
\Omega_k(u) \;\; \triangleq \;\; [c_{k-\Phi(u)}^{(\nu)}(u) - c_k^{(1)}(u)]T_c.
\tag{3.36}
$$

Being the difference of two independent, continuous time-shift sequence variables (see assumption (b)), the probability density function (p.d.f) of $\Omega_k(u)$ is given by

$$
\begin{aligned}
p_{\Omega_k(u)}(\varphi) &= \int_{-\infty}^{\infty} p_{c_{k-\Phi(u)}^{(\nu)}(u)T_c}(\xi) \, p_{c_k^{(1)}(u)T_c}(\xi - \varphi) \, d\xi \\
&= \begin{cases} (N_h T_c)^{-1} \left[1 - \frac{|\varphi|}{N_h T_c}\right], & |\varphi| < N_h T_c \\ 0, & \text{otherwise} \end{cases} \quad \text{for } \nu \neq 1 \; .
\end{aligned}
\tag{3.37}
$$

The random variables $\Omega_k(u)$ for distinct values of k are conditionally independent, given the value of the time shift parameter Φ.

We now verify that $\mathbf{E}\{n_{j,i}(u)\} = 0$. Since $\mathbf{E}\{n_{j,i}^{(1)}(u)\} = 0$, we just need to verify that $\mathbf{E}\{n_{j,i}^{(\nu)}(u)\} = 0$, for $\nu = 2, 3, \ldots, N_u$. Note that this result can be obtained

23

by averaging over $\phi(u)$ alone by using assumptions (c), (d) and (f). That is, the conditional expectation over $\phi(u)$, given the TH sequence random variables, is

$$
\begin{aligned}
\mathbf{E}\{w(\theta - \phi(u) - \Omega_k(u))\} &= T_f^{-1} \int_{-T_f/2}^{T_f/2} w(\theta - \varphi - \Omega_k(u))\, d\varphi \\
&= T_f^{-1} \int_{-T_f/2 - \Omega_k(u) + \theta}^{T_f/2 - \Omega_k(u) + \theta} w(\xi)\, d\xi.
\end{aligned}
\tag{3.38}
$$

The constraint in assumption (f) guarantees that

$$
[-\frac{\epsilon}{2}, \frac{\epsilon}{2}] \subset [-\frac{T_f}{2} - \Omega_k(u) + \theta, \frac{T_f}{2} - \Omega_k(u) + \theta],
$$

i.e, the interval where $w(\xi)$ is non-zero is contained fully within the region of integration, regardless of the sequence element values, and regardless of those values of θ for which $v(\theta)$ is non-zero. Therefore, the domain of the integral can be extended to cover the whole real line, and by using assumption (d), $\mathbf{E}\{n_{j,i}^{(\nu)}(u)\} = 0$, for $\nu = 2, 3, \ldots, N_u$.

Now that it has been verified that all the random variables on the right side of (3.26) has mean zero, and since they are independent by assumption (a), it follows that $n_{j,i}(u)$ has variance $\sigma_{j,i}^2(N_u)$ given by

$$
\sigma_{j,i}^2(N_u) = \sigma_{j,i}^2(1) + \sum_{\nu=2}^{N_u} (A^{(\nu)})^2 \mathbf{E}\{[n_{j,i}^{(\nu)}(u)]^2\}.
\tag{3.39}
$$

We can now evaluate $\mathbf{E}\{[n_{j,i}^{(\nu)}(u)]^2\}$. Since $n_{j,i}^{(\nu)}(u)$ has mean zero, it's variance, conditioned on the time shift parameter $\Phi(u)$, is given by

$$
\begin{aligned}
\mathbf{E}\{[n_{j,i}^{(\nu)}(u)]^2\} &= \mathbf{E}\{\sum_{k=0}^{N_s-1} n_{k,j,i}^{(\nu)}(u) \sum_{l=0}^{N_s-1} n_{l,j,i}^{(\nu)}(u)\} \\
&= \sum_{k=0}^{N_s-1} \sum_{l=0}^{N_s-1} \mathbf{E}\{n_{k,j,i}^{(\nu)}(u) n_{l,j,i}^{(\nu)}(u)\}
\end{aligned}
$$

$$= \sum_{k=0}^{N_s-1} \hat{\sigma}_{k,j,i}^2 \; + \; \sum_{\substack{k=0 \\ k \neq l}}^{N_s-1} \sum_{l=0}^{N_s-1} \tilde{\sigma}_{k,l,j,i}, \qquad (3.40)$$

where

$$\begin{aligned}
\hat{\sigma}_{k,j,i}^2 \; &\triangleq \; \mathbf{E}\{[n_{k,j,i}^{(\nu)}(u)]^2\} \\
&= \; \int_{-\infty}^{\infty} \int_{-\infty}^{\infty} p_{\phi(u)}(\varrho)\, p_{\Omega_k(u)}(\varphi) \\
&\qquad \left[\int_{-\infty}^{\infty} w(\rho - \varrho - \varphi)\, v_{k,j,i}(\rho)d\rho\right]^2 \; d\varrho d\varphi, \qquad (3.41)
\end{aligned}$$

and for $k \neq l$

$$\begin{aligned}
\tilde{\sigma}_{k,l,j,i} \; &\triangleq \; \mathbf{E}\{n_{k,j,i}^{(\nu)}(u)n_{l,j,i}^{(\nu)}(u)\} \\
&= \; \int_{-\infty}^{\infty} p_{\phi(u)}(\varrho) \\
&\qquad \left[\int_{-\infty}^{\infty} \int_{-\infty}^{\infty} w(\rho - \varrho - \varphi)\, v_{k,j,i}(\rho)d\rho\, p_{\Omega_k(u)}(\varphi)\, d\varphi\right] \\
&\qquad \left[\int_{-\infty}^{\infty} \int_{-\infty}^{\infty} w(\rho - \varrho - \psi)\, v_{l,j,i}(\rho)d\rho\, p_{\Omega_l(u)}(\psi)\, d\psi\right] \; d\varrho.
\end{aligned}$$

$$(3.42)$$

The calculation of this moments is conditioned on the time shift parameter $\Phi(u)$, but the results are independent of its value. These integrals can be evaluated numerically. To save computation, they can be simplified. Let's define

$$\hat{f}_k(\varsigma) \triangleq \int_{-\frac{\epsilon}{2}}^{\frac{\epsilon}{2}} w(\rho - \varsigma)\, v_{k,j,i}(\rho)\, d\rho. \qquad (3.43)$$

Notice that $\hat{f}_k(\varsigma)$ takes on significant values only for $|\varsigma| < \epsilon$. With a change of variables of integration, $\hat{\sigma}^2_{k,j,i}$ reduces to

$$\hat{\sigma}^2_{k,j,i} \;=\; \int_{-\infty}^{\infty} \hat{f}_k^2(\varsigma) \left[\underbrace{\int_{-\infty}^{\infty} p_{\phi(u)}(\varsigma - \varphi)\, p_{\Omega_k(u)}(\varphi)d\varphi}_{\text{p.d.f. of } \phi(u)+\Omega_k(u)}\right] d\varsigma\,. \tag{3.44}$$

The constraint in assumption (f) can be rewritten $\epsilon < \frac{T_f}{2} - N_h T_c$. With this constraint we can assume

$$\hat{f}_k(\varsigma) = 0 \text{ for } |\varsigma| \geq \frac{T_f}{2} - N_h T_c. \tag{3.45}$$

Also notice that, for $|\varsigma| < \frac{T_f}{2} - N_h T_c$, the probability density function of $\phi(u)+\Omega_k(u)$ reduces to

$$\int_{-\infty}^{\infty} p_{\phi(u)}(\varsigma - \varphi)\, p_{\Omega_k(u)}(\varphi)d\varphi \;=\; T_f^{-1} \int_{\varsigma - \frac{T_f}{2}}^{\varsigma + \frac{T_f}{2}} p_{\Omega_k(u)}(\varphi)d\varphi$$

$$=\; T_f^{-1} \underbrace{\int_{-N_h T_c}^{N_h T_c} p_{\Omega_k(u)}(\varphi)d\varphi}_{=1}, \tag{3.46}$$

since $(\varsigma + \frac{T_f}{2}) > N_h T_c$ and $(\varsigma - \frac{T_f}{2}) < -N_h T_c$. Therefore, the calculation of $\hat{\sigma}^2_{k,j,i}$ simplifies to

$$\hat{\sigma}^2_{k,j,i} \;=\; T_f^{-1} \int_{-\infty}^{\infty} \hat{f}_k^2(\varsigma)\, d\varsigma$$

$$=\; T_f^{-1} \int_{-\epsilon}^{\epsilon} \left[\int_{-\frac{\epsilon}{2}}^{\frac{\epsilon}{2}} w(\rho - \varsigma)\, v_{k,j,i}(\rho)\, d\rho\right]^2 d\varsigma$$

$$=\; \hat{\sigma}_w^2(\delta_j^k, \delta_i^k), \tag{3.47}$$

where

$$\hat{\sigma}_w^2(\theta, \eta) \;\stackrel{\triangle}{=}\; T_f^{-1} \int_{-\epsilon}^{\epsilon} m_w^2(\varsigma, \theta, \eta)\, d\varsigma, \tag{3.48}$$

and

$$m_w(\varsigma, \theta, \eta) \triangleq \int_{-\infty}^{\infty} w(\rho - \varsigma) \left[w(\rho - \theta) - w(\rho - \eta) \right] d\rho$$

$$= E_w \left[\gamma_w(\varsigma - \theta) - \gamma_w(\varsigma - \eta) \right]. \tag{3.49}$$

The function $m_w(\varsigma, \theta, \eta)$ and the parameters θ and η play an important role in determining the level of multiple-access interference.

The term $\tilde{\sigma}_{k,l,j,i}$, being a cross-correlation, might be expected to have a magnitude that is small with respect to $\hat{\sigma}_{k,j,i} \times \hat{\sigma}_{l,j,i}$, but this must be checked out, because there are $N_s(N_s - 1)$ cross-correlation terms, as opposed to N_s correlation terms (see (3.40)). Notice that we can write

$$\begin{aligned}
(\tilde{\sigma}_{k,l,j,i})^2 &= \left[T_f^{-1} \int_{-T_f/2}^{T_f/2} \left(\int_{-\infty}^{\infty} \hat{f}_k(\varrho + \varphi) \, p_{\Omega_k(u)}(\varphi) \, d\varphi \right) \right. \\
&\qquad \left. \left(\int_{-\infty}^{\infty} \hat{f}_l(\varrho + \psi) \, p_{\Omega_l(u)}(\psi) \, d\psi \right) d\varrho \right]^2 \\
&\leq \left[T_f^{-1} \int_{-T_f/2}^{T_f/2} \left(\int_{-\infty}^{\infty} \hat{f}_k(\varrho + \varphi) \, p_{\Omega_k(u)}(\varphi) \, d\varphi \right)^2 d\varrho \right] \\
&\qquad \left[T_f^{-1} \int_{-T_f/2}^{T_f/2} \left(\int_{-\infty}^{\infty} \hat{f}_l(\varrho\prime + \varphi\prime) \, p_{\Omega_l(u)}(\varphi\prime) \, d\varphi\prime \right)^2 d\varrho\prime \right]
\end{aligned}$$

$$\tag{3.50}$$

We now define

$$\begin{aligned}
\hat{g}_k(\varrho) &\triangleq \int_{-\infty}^{\infty} \hat{f}_k(\varrho + \varphi) \, p_{\Omega_k(u)}(\varphi) \, d\varphi \\
&= \int_{-\infty}^{\infty} \hat{f}_k(\varrho - \varphi) \, p_{\Omega_k(u)}(\varphi) \, d\varphi \\
&= \int_{-\infty}^{\infty} p_{\Omega_k(u)}(\varrho - \varphi) \, \hat{f}_k(\varphi) \, d\varphi \tag{3.51}
\end{aligned}$$

Since $\hat{f}_k(\varrho)$ takes significant values for $|\varrho| \leq \epsilon$ only, it is of short duration relative to $p_{\Omega_k(u)}(\varrho)$. If we omit the values $\varrho = 0$ and $\varrho = \pm N_h T_c$, the $p_{\Omega_k(u)}(\varrho)$ is sufficiently

smooth so that $p_{\Omega_k(u)}(\varrho - \varphi) \simeq p_{\Omega_k(u)}(\varrho)$ for $\varphi < \epsilon$. We can therefore apply the moment expansion [48] to write

$$\hat{g}_k(\varrho) \simeq p_{\Omega_k(u)}(\varrho) \int_{-\infty}^{\infty} \hat{f}_k(\varphi) \, d\varphi, \tag{3.52}$$

but notice that using (3.43) in (3.52) we get

$$\hat{g}_k(\varrho) \simeq p_{\Omega_k(u)}(\varrho) \int_{-\frac{\epsilon}{2}}^{\frac{\epsilon}{2}} \underbrace{\int_{-\infty}^{\infty} w(\rho - \varphi) \, d\varphi}_{=0} \, v_{k,j,i}(\rho) \, d\rho = 0 \tag{3.53}$$

by assumption (d). Therefore, using (3.50) through (3.53) as evidence we conclude that

$$|\tilde{\sigma}_{k,l,j,i}| \ll \hat{\sigma}_{k,j,i} \, \hat{\sigma}_{l,j,i}. \tag{3.54}$$

and approximate $\tilde{\sigma}_{k,l,j,i} \simeq 0$. Notice that the larger $N_h T_c$ is in comparison to the parameter ϵ (a function of the width of the impulse $w(t)$ and the time-shifts values used for data modulation), then the better the approximation in (3.52) is. Combining (3.40) and (3.47) and using $\tilde{\sigma}_{k,l,j,i} \simeq 0$, we get the following model for the total output noise variance

$$\sigma_{j,i}^2(N_u) = \sigma_{j,i}^2(1) + \sum_{\nu=2}^{N_u} (A^{(\nu)})^2 \sum_{k=0}^{N_s-1} \hat{\sigma}_w^2(\delta_j^k, \delta_i^k), \tag{3.55}$$

with $\hat{\sigma}_w^2(\delta_j^k, \delta_i^k)$ given by (3.48).

3.3   Single-user multiple-access performance

In this work the multiple-access performance of IR is analyzed in terms of the number of users supported by the system for a given bit error rate, bit transmission rate, and number of signals in the block waveform set. The substitution of the symbol signal-to-noise-ratio $\mathbf{SNR}_{\text{out}}^{(j,i)}(N_u)$ in (3.20) into the symbol error probability $\text{UBP}_e(N_u)$ in

(3.22) will provide the desired relation between error probability, number of users, transmission rate, and number of signals.

To calculate $\mathbf{SNR}_{\text{out}}^{(j,i)}(N_u)$, note that we can rewrite (3.15) as follows

$$
\begin{aligned}
m_{j,i} &= A^{(1)} E_s (1 - \alpha_{ji}) \\
&= A^{(1)} N_s E_w \left[1 - \frac{1}{N_s} \sum_{k=0}^{N_s - 1} \gamma_w (\delta_j^k - \delta_i^k) \right] \\
&= A^{(1)} \sum_{k=0}^{N_s - 1} m_w(\delta_j^k, \delta_j^k, \delta_i^k).
\end{aligned}
\tag{3.56}
$$

We substitute (3.55) and (3.56) in (3.20) to get

$$
\begin{aligned}
\mathbf{SNR}_{\text{out}}^{(j,i)}(N_u) &= \frac{m_{j,i}^2}{\sigma_{j,i}^2(N_u)} \\
&= \left[\left[\mathbf{SNR}_{\text{out}}^{(j,i)}(1) \right]^{-1} + \left[\frac{T_s}{T_w} \frac{T_w}{T_f} \frac{\beta(j,i)}{\sum_{\nu=2}^{N_u} \left(\frac{A^{(\nu)}}{A^{(1)}} \right)^2} \right]^{-1} \right]^{-1},
\end{aligned}
\tag{3.57}
$$

where

$$
\beta(j,i) \triangleq \frac{\left[\sum_{k=0}^{N_s - 1} m_w(\delta_j^k, \delta_j^k, \delta_i^k) \right]^2}{N_s \sum_{k=0}^{N_s - 1} \hat{\sigma}_w^2(\delta_j^k, \delta_i^k)}
\tag{3.58}
$$

is a normalized SNR parameter which is defined in terms of the pulse shape $w(t)$ and the data modulation times δ_j^k, δ_i^k, $k = 0, 1, \ldots, N_s - 1$. In (3.57) we have use the fact that the symbol transmission rate $R_s = \frac{1}{T_s} = \frac{1}{N_s T_f}$. The expression in 3.57 shows that the total symbol SNR is smaller than the smallest of $\mathbf{SNR}_{\text{out}}^{(j,i)}(1)$ and $\frac{T_s}{T_f} \frac{\beta(j,i)}{\sum_{\nu=2}^{N_u} \left(\frac{A^{(\nu)}}{A^{(1)}} \right)^2}$. The bit SNR can be found by substituting (3.57) in (3.21) to get

$$
\mathbf{SNRb}_{\text{out}}^{(j,i)}(N_u) = \left[\left[\mathbf{SNRb}_{\text{out}}^{(j,i)}(1) \right]^{-1} + \left[\frac{1}{R_b} \frac{1}{T_f} \frac{\beta(j,i)}{\sum_{\nu=2}^{N_u} \left(\frac{A^{(\nu)}}{A^{(1)}} \right)^2} \right]^{-1} \right]^{-1},
$$

where R_b is the bit transmission rate.

Note that (3.57) can be rewritten

$$\mathbf{SNR}_{\text{out}}^{(j,i)}(N_u) \;\; = \;\; \frac{(A^{(1)})^2 E_s(1 - \alpha_{ji})}{N_o + N_{MA}},$$

(3.60)

where

$$N_{MA} \;\; \triangleq \;\; \sum_{\nu=2}^{N_u} N_{MA}^{(\nu)}$$

(3.61)

is the *equivalent* power spectral density level of the total multiple-access interference, and

$$N_{MA}^{(\nu)} \;\; \triangleq \;\; (A^{(\nu)})^2 \; \frac{\sum_{k=0}^{N_s-1} \hat{\sigma}_{k,j,i}^2}{[E_s(1 - \alpha_{ji})]}$$

(3.62)

is the contribution corresponding to the νth user for $\nu = 2, 3, \ldots, N_u$.

In chapter 5 we will evaluate $\mathbf{SNR}_{\text{out}}^{(j,i)}(N_u)$ in (3.57) for the three types of M-ary signals discussed in chapter 4.

3.4   Multiple-access degradation factor

In order to simplify this analysis, let's assume that the signals are equally correlated with $\alpha_{ji} = \alpha$, $\beta(j,i) = \beta$, $\mathbf{SNRb}_{\text{out}}^{(j,i)}(1) = \mathbf{SNRb}_{\text{out}}(1)$ and $\mathbf{SNRb}_{\text{out}}^{(j,i)}(N_u) = \mathbf{SNRb}_{\text{out}}(N_u)$. Hence, we can write

$$\mathbf{SNRb}_{\text{out}}(N_u) \;\; = \;\; \left[[\mathbf{SNRb}_{\text{out}}(1)]^{-1} \; + \; \left[\frac{1}{R_b} \frac{\beta/T_f}{\sum_{\nu=2}^{N_u} \left(\frac{A^{(\nu)}}{A^{(1)}} \right)^2} \right]^{-1} \right]^{-1}.$$

(3.63)

Let's define $\mathbf{SNRb}_{\mathrm{spec}}$ to be the specified operating bit SNR to achieve the desired probability of error. Recall that $\mathbf{SNRb}_{\mathrm{out}}(1)$ is the bit SNR value when only user one is active, and that $\mathbf{SNRb}_{\mathrm{out}}(N_u) < \mathbf{SNRb}_{\mathrm{out}}(1)$ is the actual bit SNR when N_u users are active in the system. The $\mathbf{SNRb}_{\mathrm{rec}}(N_u) > \mathbf{SNRb}_{\mathrm{spec}}$ is the required value of $\mathbf{SNRb}_{\mathrm{out}}(1)$ that makes $\mathbf{SNRb}_{\mathrm{out}}(N_u) = \mathbf{SNRb}_{\mathrm{spec}}$, so user one can still meet the specified value of bit error probability even when N_u users are active. The value of $\mathbf{SNRb}_{\mathrm{rec}}(N_u)$ can be calculated solving

$$
\begin{aligned}
\mathbf{SNRb}_{\mathrm{out}}(Nu) &= \mathbf{SNRb}_{\mathrm{spec}} \\
&= \frac{\mathbf{SNRb}_{\mathrm{rec}}(N_u)}{1 + \mathbf{SNRb}_{\mathrm{rec}}(N_u)\left[\frac{1}{R_b}\frac{\beta/T_f}{\sum_{\nu=2}^{N_u}\left(\frac{A^{(\nu)}}{A^{(1)}}\right)^2}\right]^{-1}}
\end{aligned}
\tag{3.64}
$$

to get

$$
\mathbf{SNRb}_{\mathrm{rec}}(N_u) = \frac{\mathbf{SNRb}_{\mathrm{spec}}}{1 - \mathbf{SNRb}_{\mathrm{spec}}\left[\frac{1}{R_b}\frac{\beta/T_f}{\sum_{\nu=2}^{N_u}\left(\frac{A^{(\nu)}}{A^{(1)}}\right)^2}\right]^{-1}}
\tag{3.65}
$$

The ratio

$$
\mathrm{DF}(N_u) = \frac{\mathbf{SNRb}_{\mathrm{rec}}(N_u)}{\mathbf{SNRb}_{\mathrm{spec}}(1)}
\tag{3.66}
$$

is a degradation factor that measures the additional amount of SNR required by user one to overcome the negative effect of the multiple-access interference caused by the N_u users. Using (3.65) in (3.66) we get

$$
\mathrm{DF}(N_u) = \frac{1}{1 - \mathbf{SNRb}_{\mathrm{spec}}\left[\frac{1}{R_b}\frac{\beta/T_f}{\sum_{\nu=2}^{N_u}\left(\frac{A^{(\nu)}}{A^{(1)}}\right)^2}\right]^{-1}}.
\tag{3.67}
$$

It can be observed that, as N_u increases, $DF(N_u)$ also increases, meaning that $\mathbf{SNRb}_{rec}(N_u)$ must increase in order to keep constant the right hand side of (3.64). Ultimately, however, no amount of increase in $\mathbf{SNRb}_{rec}(N_u)$ can offset the increase in the other term. As a result, the number of users can be increased to a maximum number in which DF in (3.67) becomes infinity. On the other hand, note that $\mathbf{SNRb}_{rec}(N_u) \to \mathbf{SNRb}_{spec}$ as $N_u \to 1$, as would be expected with only one user active.

3.4.1 Degradation factor under ideal power control

When $A^{(\nu)} = A^{(1)}$ for $\nu = 2, 3, \ldots, N_u$, $DF(N_u)$ in (3.67) can be written

$$DF(N_u) = \frac{1}{1 - \mathbf{SNRb}_{spec} \left[\frac{1}{R_b} \frac{\beta/T_f}{(N_u - 1)} \right]^{-1}}. \tag{3.68}$$

The expression in (3.68) gives $DF(N_u)$ as a function of N_u. It is also possible to get an expression for $N_u(DF)$ as a function of DF as follows

$$N_u(DF) = \frac{1}{\mathbf{SNRb}_{spec}} \frac{1}{R_b} \frac{\beta}{T_f} (1 - \frac{1}{DF}) + 1. \tag{3.69}$$

The maximum number of users is

$$N_{max} \triangleq \lim_{DF \to \infty} N_u(DF) = \frac{1}{\mathbf{SNRb}_{spec}} \frac{1}{R_b} \frac{\beta}{T_f} + 1. \tag{3.70}$$

Similarly, it is also possible to get an expression for $R_b(DF)$ as a function of DF as follows

$$R_b(DF) = \frac{1}{\mathbf{SNRb}_{spec}} \frac{1}{N_u - 1} \frac{\beta}{T_f} (1 - \frac{1}{DF}) + 1. \tag{3.71}$$

The maximum bit transmission rate is

$$R_{\max} \triangleq \lim_{\mathrm{DF} \to \infty} R_b(\mathrm{DF}) = \frac{1}{\mathbf{SNRb}_{\mathrm{spec}}} \frac{1}{N_u - 1} \frac{\beta}{T_f} + 1. \qquad (3.72)$$

The values $N_{\max}$ and $R_{\max}$ are the largest values that N_u and R_b can attain, respectively, when the performance is determined by the amount of multiple-access interference produced by N_u active users, for a given value of $\mathbf{SNRb}_{\mathrm{spec}}$. Notice that there is a limit on how large $\mathbf{SNRb}_{\mathrm{spec}}$ can be for a given number of users N_u. This maximum value can be found if we let $\mathbf{SNRb}_{\mathrm{rec}}(N_u)$ take on large values in (3.64) to get

$$
\begin{aligned}
\mathbf{SNRb}_{\mathrm{spec-max}}(N_u) &\triangleq \lim_{\mathbf{SNRb}_{\mathrm{rec}}(N_u) \to \infty} \mathbf{SNRb}_{\mathrm{spec}} \\
&= \frac{1}{R_b} \frac{\beta/T_f}{(N_u - 1)}
\end{aligned}
\qquad (3.73)
$$

The limit on how small $\mathbf{SNRb}_{\mathrm{spec}}$ can be is investigated in the next section.

3.5 Multiple-access transmission capacity under ideal power control

In this section we perform an approximate analysis to estimate the total multiple-access capacity of IR in bits per second under ideal power control. To simplify the analysis, we again assume that the signals are equally correlated, with bit SNR given

by $\mathbf{SNRb}_{\text{spec}}$.[2] It is well known from communication theory that the M-ary symbol error probability PWE for equally correlated signals

$$\text{PWE} = 1 - \int_{-\infty}^{\infty} \left[1 - Q\left(\xi + \sqrt{2\,\mathbf{SNRb}_{\text{spec}}} \right) \right]^{M-1} \tag{3.74}$$

has the following limiting behavior [49]

$$\lim_{\text{M} \to \infty} \text{PWE} = \begin{cases} 1, & \text{if } \mathbf{SNRb}_{\text{spec}} < \log_e(2) \\ 0, & \text{if } \mathbf{SNRb}_{\text{spec}} > \log_e(2) \end{cases} \tag{3.75}$$

Hence $\mathbf{SNRb}_{\text{spec}-\text{lim}} \overset{\triangle}{=} \log_e(2)$ is the smallest value that $\mathbf{SNRb}_{\text{spec}}$ can be assigned when the performance is determined by the amount of multiple access interference produced by N_u active users. We can use the condition in (3.75) together with (3.70) to write

$$N_{\text{max}} < N_{\text{IR}} \overset{\triangle}{=} \frac{1}{\log_e(2)} \frac{1}{R_b} \frac{\beta}{T_f} + 1. \tag{3.76}$$

Hence, N_{IR} is attainable, in principle, using block waveforms signals with $M \to \infty$. Similarly, we can use the condition in (3.75) together with (3.72) to write

$$R_{\text{max}} < C_{\text{IR}}(N_u) \overset{\triangle}{=} \frac{1}{\log_e(2)} \frac{1}{N_u - 1} \frac{\beta}{T_f} + 1. \tag{3.77}$$

Hence, the term $C_{\text{IR}}(N_u)$ plays the role of *multiple-access channel capacity per user* of IR in bits per second. Another way to see this is by using Shannon's formula for channel capacity

$$C(B) = B \log_2(1 + \frac{1}{B} P(N_u)) \tag{3.78}$$

with bandwidth $B \overset{\triangle}{=} \frac{1}{T_w}$ in the order of Gigahertz, and

$$P(N_u) \overset{\triangle}{=} R_b\, \mathbf{SNRb}_{\text{spec}-\text{max}}(N_u) \tag{3.79}$$

---

[2]We have assumed that $\mathbf{SNRb}_{\text{out}}(1) = \mathbf{SNRb}_{\text{rec}}(N_u)$ so that the condition $\mathbf{SNRb}_{\text{out}}(N_u) = \mathbf{SNRb}_{\text{spec}}$ can be satisfied.

playing the role of *effective signal power to power noise density* ratio. Hence

$$
\begin{aligned}
C(B) &= B \, \log_2(1 \; + \; \frac{1}{B} \frac{\beta/T_f}{N_u - 1}) \\
&= \frac{B}{\log(2)} \sum_{k=1}^{\infty} \frac{(-1)^{k+1}}{k} \left(\frac{1}{B} \frac{\beta/T_f}{N_u - 1} \right)^k
\end{aligned}
\tag{3.80}
$$

With B in the order of Gigahertz, β on the order of hundreds and T_f in the order of hundreds of nanoseconds, it is clear that

$$
\left(\frac{1}{B} \frac{\beta/T_f}{N_u - 1} \right) \; < \; 0.01
\tag{3.81}
$$

and (3.80) can be approximated

$$
\begin{aligned}
C(B) &\simeq \frac{1}{\log(2)} \frac{\beta/T_f}{N_u - 1} \\
&= C_{\text{IR}}(N_u)
\end{aligned}
\tag{3.82}
$$

If C_{IR} is the multiple-access capacity per user of IR in bits per second, then

$$
\begin{aligned}
C_{\text{TOT}} &\triangleq N_{\lim} C_{\text{IR}} \\
&\simeq \frac{1}{\log(2)} \frac{\beta}{T_f}, \; N_u \; >> \; 1,
\end{aligned}
\tag{3.83}
$$

plays the role of *total multiple-access capacity* of IR in bits per second and gives an upper bound on the total combined bit transmission rate that can can be attained when the performance is determined by the amount of multiple-access interference with N_u users active.

In chapter 5 we will evaluate $N_u(\text{DF})$ in (3.69) and $C_{\text{IR}}(N_u)$ in (3.77) for the signals discussed in chapter 4.

Chapter 4

Block waveform encoding PPM signal sets

In this chapter we describe three signal sets with the PPM structure described in section 2.2.3. In each case the construction method is given, the correlation properties are discussed, the performance in AWGN is analyzed, and receiver simplification is discussed. Finally, a numerical example is given. In this example the performance in AWGN of the three sets of signals is calculated and compared.[1]

4.1 Orthogonal signals

4.1.1 Construction of orthogonal signals

Equation (4.1) defines the construction of orthogonal (OR) signals

$$S_i(t) = \sum_{k=0}^{N_s-1} w(t - kTf - [(k+i-1)_{\mathrm{mod}} M]T_{\mathrm{OR}}), \quad i = 1, 2, \ldots, M. \tag{4.1}$$

---

[1]As discussed in subsection 2.2.2, for the case under consideration ($N_u = 1$) the time hopping sequence $\{c_k^{(1)}\}$ and the delay $\tau^{(1)}$ have no effect in the correlation properties of the PPM signals, and they will be omitted in the analysis done in this chapter.

where $T_{\mathrm{OR}} > T_w$. For the OR PPM signals in (4.1) the normalized correlation coefficients are given by

$$\alpha_{ij} = \begin{cases} 1, & i = j \\ 0, & i \neq j \end{cases}, \tag{4.2}$$

and the normalized correlation matrix Λ_{OR} is the $M \times M$ identity matrix.

4.1.2 Selection of T_{OR}

For a fixed impulse waveform $w(t)$, N_s and T_f, the signal design in (4.1) depends only on T_{OR}. Clearly, in the presence of AWGN any $T_{\mathrm{OR}} > T_w$ will perform identically. We define $T_{\mathrm{OR}} \triangleq 2T_w$ in order to simplify the analysis when multiple-access interference is present (see section 5.1).

4.1.3 AWGN performance

For the OR PPM signals case, the bound on error probability in (3.22) (with $N_u = 1$) reduces to

$$\mathrm{UBP}_{\mathrm{e}}^{\mathrm{OR}}(1) \ \triangleq \ (M-1)Q\left(\sqrt{\mathbf{SNR}_{\mathrm{out}}^{\mathrm{OR}}(1)}\right), \tag{4.3}$$

where

$$\mathbf{SNR}_{\mathrm{out}}^{\mathrm{OR}}(1) \ = \ \frac{(A^{(1)})^2 E_s}{N_o}. \tag{4.4}$$

This symbol error probability can be converted to bit error probability as follows [49]

$$\mathrm{UBP}_{\mathrm{b}}^{\mathrm{OR}}(1) \ \triangleq \ \frac{M}{2} \int_{\sqrt{\mathbf{SNR}_{\mathrm{out}}^{\mathrm{OR}}(1)}}^{\infty} \frac{\exp(-\xi^2/2)}{\sqrt{2\pi}} \, d\xi. \tag{4.5}$$

4.1.4 Receiver simplification

To detect the M signals we will need to correlate the input signal with M reference signals. For large M this can result in a receiver of great complexity. We can take advantage of the structure of the OR PPM signals to simplify the construction of the receiver.

Let $x(t) = S_j(t - \tau^{(1)} - C_0^{(1)}(t - \tau^{(1)})) + n(t)$, where $S_j(t)$ is one of the signals in (4.1), $C_0^{(1)}(t)$ is the TH function defined in (2.6), and $n(t)$ is AWGN. Each of the M channel correlation outputs can be written

$$
\begin{aligned}
y_i &= \int_0^{N_s T_f} x(t)\, S_i(t - \tau^{(1)} - C_0^{(1)}(t - \tau^{(1)}))\, dt \\
&= \sum_{k=0}^{N_s-1} \sum_{q=0}^{M-1} \delta_{q,[(k+i-1)\bmod M]}\, z(k,q),
\end{aligned} \tag{4.6}
$$

where

$$
z(k,q) \triangleq \int_{kT_f+\tau^{(1)}+c_k^{(1)}T_c+qT_{\mathrm{OR}}}^{kT_f+\tau^{(1)}+c_k^{(1)}T_c+(q+1)T_{\mathrm{OR}}} x(t)\, w(t - kT_f - \tau^{(1)} - c_k^{(1)}T_c - qT_{\mathrm{OR}})\, dt \tag{4.7}
$$

and $\delta_{q,q'}$ is the Kronecker delta. From the expression for y_i, $i = 1, 2, \ldots, M$, it is clear that the receiver needs only one correlator and M store and sum circuits. The y_i can be calculated while $x(t)$ is received and no symbol delay occur. This is illustrated in figure 4.1.
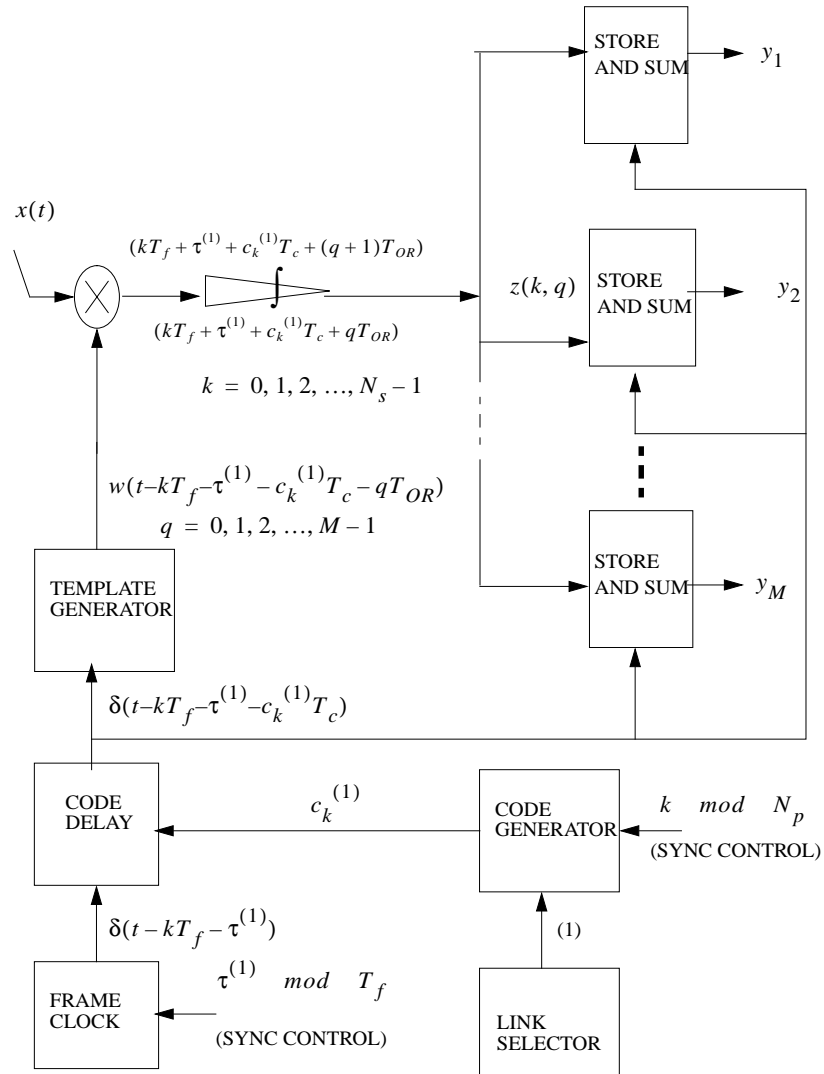
Figure 4.1: This diagram shows the single correlator and the M store and sum circuits that are needed in the simplified receiver for the OR PPM signals.

4.2 Equally correlated signals

4.2.1 Construction of equally correlated signals

One method for generating equally correlated (EC) signals $\{S_i(t)\}$ for $M \leq N_s$, where the value of N_s satisfies one of the following three conditions

$$(1)\ N_s = 2^m - 1, \quad m \geq 1, \text{ or}$$
$$(2)\ N_s = p, \quad\quad\quad p \text{ a prime, or}$$
$$(3)\ N_s = p(p+2), \quad p \text{ and } (p+2) \text{ form a twin prime},$$

consists in deleting the first column and the first row a $(N_s + 1) \times (N_s + 1)$ cyclic Hadamard matrix [41], and then use the i-th row of this modified matrix and the mapping $(+1) \rightarrow \tau_2$ and $(-1) \rightarrow \tau_1 = 0$ to produce the time shift pattern $\{\delta_i^k; k = 0, 1, 2, \ldots, N_s - 1\}$ defining the i-th signal. For example, the following modified Hadamard matrix with $M = N_s = 3$

$$\hat{H} = \begin{pmatrix} +1 & -1 & -1 \\ -1 & +1 & -1 \\ -1 & -1 & +1 \end{pmatrix} \tag{4.8}$$

results in the ensemble of signals represented by

$$\Delta_{EC} = \begin{bmatrix} \tau_2 & 0 & 0 \\ 0 & \tau_2 & 0 \\ 0 & 0 & \tau_2 \end{bmatrix}.$$

If in (4.8) we use the mapping $(+1) \rightarrow (+1)$ and $(-1) \rightarrow (0)$, then the matrix

$$\tilde{H} = \begin{bmatrix} a_1^1 & a_1^2 & a_1^3 \\ a_2^1 & a_2^2 & a_2^3 \\ a_3^1 & a_3^2 & a_3^3 \end{bmatrix} = \begin{bmatrix} 1 & 0 & 0 \\ 0 & 1 & 0 \\ 0 & 0 & 1 \end{bmatrix}$$

provides an alternate way to represent the set of signals Δ_{EC} as follows

$$\Delta_{EC} = \tau_2 \times \begin{bmatrix} a_1^1 & a_1^2 & a_1^3 \\ a_2^1 & a_2^2 & a_2^3 \\ a_3^1 & a_3^2 & a_3^3 \end{bmatrix}.$$

In general, $\tilde{H}$ is an $N_s \times N_s$ matrix where the i-th row $\{a_i^k, k = 0, 1, 2, \ldots, N_s - 1\}$ is an equivalent representation to the time shift pattern $\{\delta_i^k = a_i^k \tau_2; k = 0, 1, 2, \ldots, N_s - 1\}$ defining the i-th signal. Hence, the EC PPM signals can be written

$$S_i(t) = \sum_{k=0}^{N_s - 1} w(t - kTf - a_i^k \tau_2), \quad i = 1, 2, \ldots, M \tag{4.9}$$

For the EC PPM signals in 4.9 the correlation value is $\alpha_{ij} = \lambda, \ \forall i \neq j$, and the correlation matrix becomes

$$\Lambda_{\mathrm{EC}} = \begin{bmatrix} 1 & \lambda & \ldots & \lambda \\ \lambda & 1 & \ldots & \lambda \\ \vdots & \vdots & \ddots & \vdots \\ \lambda & \lambda & \ldots & 1 \end{bmatrix},$$

where

$$\begin{aligned} \lambda &= \frac{\frac{N_s - 1}{2} \gamma_w(0) + \frac{N_s + 1}{2} \gamma_w(\tau_2)}{N_s} \\ &\approx \frac{1 + \gamma_w(\tau_2)}{2} \text{ for } N_s \gg 1. \end{aligned} \tag{4.10}$$

4.2.2 Selection of τ_2

The signal design in (4.9) depends on $w(t)$ and τ_2. From (4.10) we can see that by using $\tau_2 = \tau_{\min}$ the minimum value of λ is

$$
\begin{aligned}
\lambda_{\min} &\triangleq \frac{\frac{N_s-1}{2}\gamma_w(0) + \frac{N_s+1}{2}\gamma_{\min}}{N_s} \\
&\approx \frac{1 + \gamma_{\min}}{2} \text{ for } N_s \gg 1.
\end{aligned}
\tag{4.11}
$$

The actual value of $\gamma_{\min}$ depends on the particular impulse $w(t)$ employed in the IR communication link. Figure 4.2 plots $\lambda_{\min}$ versus N_s for different hypothetical values of $\gamma_{\min}$. Note that $\lambda_{\min} \leq 0$ only for $N_s \leq \frac{1-\gamma_{\min}}{1+\gamma_{\min}}$, and that for $N_s \gg 1$ the $\lambda_{\min}$ value is strictly positive.
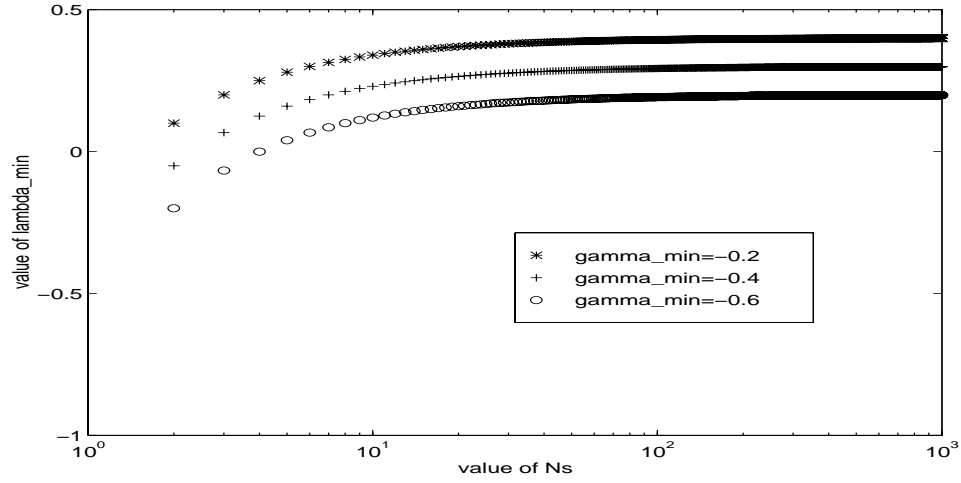
Figure 4.2: The value of $\lambda_{\min}$ versus N_s for different values of $\gamma_{\min}$.

4.2.3 AWGN performance

For equally correlated signals, the upper bound on error probability in (3.22) (with $N_u = 1$) reduces to

$$\text{UBP}_e^{EC}(1) \triangleq (M-1)Q\left(\sqrt{\mathbf{SNR}_{\text{out}}^{EC}(1)}\right), \tag{4.12}$$

where

$$\mathbf{SNR}_{\text{out}}^{EC}(1) = \frac{(A^{(1)})^2 E_s(1-\lambda)}{N_o}. \tag{4.13}$$

This symbol error probability can be converted to bit error probability as follows [49]

$$\text{UBP}_b^{EC}(1) \triangleq \frac{M}{2}\int_{\sqrt{\mathbf{SNR}_{\text{out}}^{EC}(1)}}^{\infty} \frac{\exp(-\xi^2/2)}{\sqrt{2\pi}}\,d\xi. \tag{4.14}$$

4.2.4 Receiver simplification

Let $x(t) = S_j(t - \tau^{(1)} - C_0^{(1)}(t - \tau^{(1)})) + n(t)$, where $S_j(t)$ is one of the signals in (4.9). Each of the M channel correlation outputs can be written

$$
\begin{aligned}
y_i &= \int_0^{N_s T_f} x(t)\,S_i(t - \tau^{(1)} - C_0^{(1)}(t - \tau^{(1)}))\,dt \\
&= \sum_{k=0}^{N_s-1}\sum_{m=1}^{2} \delta_{(m-1),a_i^k}\,z_m(k),
\end{aligned} \tag{4.15}
$$

where

$$z_m(k) \triangleq \int_{kT_f+\tau^{(1)}+c_k^{(1)}T_c+\tau_m}^{kT_f+\tau^{(1)}+c_k^{(1)}T_c+\tau_m+T_w} x(t)\,w(t - kT_f - \tau^{(1)} - c_k^{(1)}T_c - \tau_m)\,dt. \tag{4.16}$$

From the expression for y_i, $i = 1, 2, \ldots, M$, it is clear that the receiver needs only two correlators and M store and sum circuits. The y_i can be calculated while $x(t)$ is received and no symbol delay occurs. This is illustrated in figure 4.3.

4.3   N-Orthogonal signals

In this section we describe the construction of N-Orthogonal (NO) PPM signals.[2] A given NO signal set consists of $M = NL$ equal energy, equal time duration signals that have the following two properties: (1) The signal set may be divided into L disjoint subsets, each subset containing N signals, and (2) Signals from different subsets are orthogonal.

In [50] they give a construction of NO coded sets, when L is an integer power of N, using multiple phase-shift-keyed (MPSK) modulation with phase values $\theta_i = \frac{2\pi}{N}(i-1), i = 1, 2, \ldots, N$. The $NL \times NL$ matrix $\hat{\Lambda}_{\mathrm{NO}}$ containing the normalized signal correlation values can be partitioned in the following form

$$
\hat{\Lambda}_{\mathrm{NO}} = \begin{bmatrix} \Lambda_{\mathrm{MPSK}} & \mathbf{0} & \ldots & \mathbf{0} \\ \mathbf{0} & \Lambda_{\mathrm{MPSK}} & \ldots & \mathbf{0} \\ \vdots & \vdots & \ddots & \vdots \\ \mathbf{0} & \mathbf{0} & \ldots & \Lambda_{\mathrm{MPSK}} \end{bmatrix},
$$

where the $N \times N$ matrix Λ_{MPSK} is given by

$$
\Lambda_{\mathrm{MPSK}} = \begin{bmatrix} 1 & \cos(\theta_2 - \theta_1) & \ldots & \cos(\theta_N - \theta_1) \\ \cos(\theta_2 - \theta_1) & 1 & \ldots & \cos(\theta_N - \theta_2) \\ \vdots & \vdots & \ddots & \vdots \\ \cos(\theta_N - \theta_1) & \cos(\theta_N - \theta_2) & \ldots & 1 \end{bmatrix}.
$$

---

[2]N-Orthogonal phase-modulated coded signals are the generalization of bi-orthogonal signal sets and were first introduced by Reed and Scholtz [50], and later studied by Viterbi and Stiffler [51].
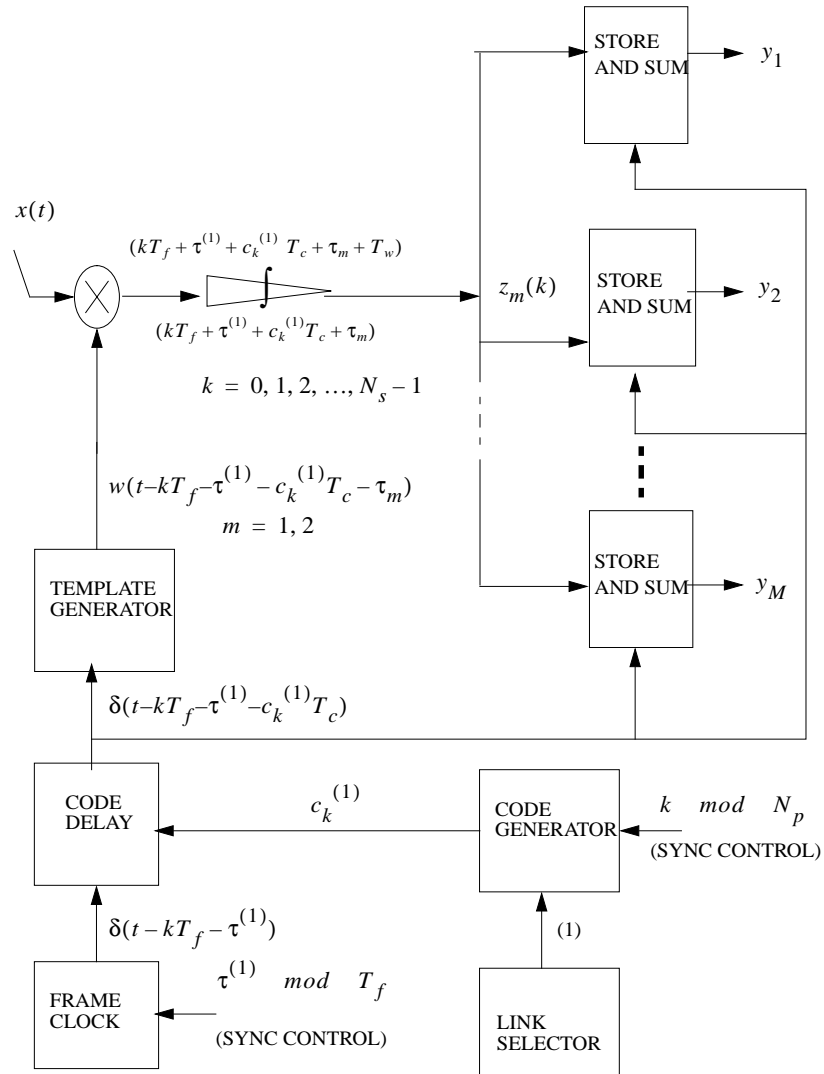
Figure 4.3: This diagram shows one of the two correlators and the M store and sum circuits that are needed in the simplified receiver for the EC PPM signals.

In this section we describe the construction of NO PPM sets, when L is a positive integer, using multiple time-shift-keyed (MTSK) modulation based on the set of N time shifts values

$$\tau_1 = 0, \tau_1 < \tau_2 \leq T_w, \ldots, \tau_{N-1} < \tau_N \leq (N-1)T_w. \tag{4.17}$$

The $NL \times NL$ matrix Λ_{NO} containing the normalized signal correlation values can be partitioned in the following form

$$\Lambda_{NO} = \begin{bmatrix} \Lambda_{MTSK} & \mathbf{0} & \ldots & \mathbf{O} \\ \mathbf{0} & \Lambda_{MTSK} & \ldots & \mathbf{0} \\ \vdots & \vdots & \ddots & \vdots \\ \mathbf{0} & \mathbf{0} & \ldots & \Lambda_{MTSK} \end{bmatrix}, \tag{4.18}$$

where the $N \times N$ matrix Λ_{MTSK} is given by

$$\Lambda_{MTSK} = \begin{bmatrix} 1 & \gamma_w(\tau_2 - \tau_1) & \ldots & \gamma_w(\tau_N - \tau_1) \\ \gamma_w(\tau_2 - \tau_1) & 1 & \ldots & \gamma_w(\tau_N - \tau_2) \\ \vdots & \vdots & \ddots & \vdots \\ \gamma_w(\tau_N - \tau_1) & \gamma_w(\tau_N - \tau_2) & \ldots & 1 \end{bmatrix}. \tag{4.19}$$

The matrix Λ_{MTSK} is the normalized correlation matrix for the set of N-ary signals $\{w(t - \tau_1), w(t - \tau_2), \ldots, w(t - \tau_N)\}$ defined by the pulse $w(t)$ and the time shift values in (4.17).

4.3.1   Construction of N-orthogonal signals

Equation (4.20) defines the construction of NO PPM sets

$$S_{m,l}(t) = \sum_{k=0}^{N_S-1} w(t - kT_f - \tau_m - [(k+l) \mod L]T_o), \tag{4.20}$$

$$m = 1, 2, \ldots, N, \quad l = 0, 1, 2, \ldots, L-1,$$

where $T_o \overset{\triangle}{=} \tau_{\mathrm{N}} + T_{\mathrm{OR}}$, and $LT_o < T_f$ (to avoid pulses overlapping between frames). The relation between the double index (m, l) and the index j is given by

$$
\begin{aligned}
j &= lN + m, & j &= 1, 2, \ldots, M, \\
l &= \lfloor \tfrac{j-1}{N} \rfloor, & l &= 0, 1, 2, \ldots, L-1, \\
m &= j - \lfloor \tfrac{j-1}{N} \rfloor N, & 1, &2, \ldots, N,
\end{aligned}
\tag{4.21}
$$

where $\lfloor z \rfloor$ denotes the integer part of z. It can be verified that for the signals in (4.20) the normalized correlation coefficients are given by

$$
\alpha_{ij} = \begin{cases}
0, & \lfloor \tfrac{i-1}{N} \rfloor \neq \lfloor \tfrac{j-1}{N} \rfloor \\
1, & i = j \\
\gamma_w(\tau_{ij}), & \lfloor \tfrac{i-1}{N} \rfloor = \lfloor \tfrac{j-1}{N} \rfloor
\end{cases} ,
\tag{4.22}
$$

where $\tau_{ij} \overset{\triangle}{=} \tau_{i - \lfloor \frac{i-1}{N} \rfloor N} - \tau_{j - \lfloor \frac{j-1}{N} \rfloor N}$. Hence, the set of M signals has correlation matrix Λ_{NO} given by (4.18), and every subset of N signals has correlation matrix Λ_{MTSK} given by (4.19).

4.3.2   Selection of $(\tau_1, \tau_2, \ldots, \tau_{\mathrm{N}})$

One criterion for selecting the time shift values $\boldsymbol{\tau} \overset{\triangle}{=} (\tau_1, \tau_2, \ldots, \tau_{\mathrm{N}})$ is to choose the values that minimize the probability of symbol error P_e in coherent communications using the N-ary signal set $\{w(t - \tau_1), w(t - \tau_2), \ldots, w(t - \tau_{\mathrm{N}})\}$. The $P_e \left(\frac{E_s}{N_o}, \Lambda \right)$ depends only on the symbol SNR value $\left(\frac{E_s}{N_o} \right)$ and the correlation properties Λ of the communications signal set.[3] Hence, we want to find $\boldsymbol{\tau}^{\mathrm{opt}} \overset{\triangle}{=} (\tau_1^{\mathrm{opt}}, \tau_2^{\mathrm{opt}}, \ldots, \tau_{\mathrm{N}}^{\mathrm{opt}})$ that

---

[3]The probability of error can be expressed as [52]

$$
P_e \left(\tfrac{E_s}{N_o}, \Lambda \right) = 1 - \frac{1}{M} \exp(-\tfrac{1}{2} \tfrac{E_s}{N_o}) \Phi \left(\sqrt{\tfrac{E_s}{N_o}}, \Lambda \right)
$$

where $\Phi(\sqrt{\tfrac{E_s}{N_o}}, \Lambda) = E_{\boldsymbol{\psi}} \left\{ \exp \sqrt{\tfrac{E_s}{N_o}} \max_i \psi_i \right\}$, $\boldsymbol{\psi}$ is a Gaussian random vector with probability density function $N(\mathbf{0}, \Lambda)$, and $E_{\boldsymbol{\psi}} \{\cdot\}$ is the expected value operator.

minimize $P_e\left(\frac{E_s}{N_o}, \Lambda_{\text{MTSK}}(\boldsymbol{\tau})\right)$. This is an optimization problem that can be stated as follows:

$$\underset{\boldsymbol{\tau} = (\tau_1, \tau_2, \ldots, \tau_N) \in \mathbf{P}}{\text{minimize}} \quad P_e\left(\frac{E_s}{N_o}, \Lambda_{\text{MTSK}}(\boldsymbol{\tau})\right) =$$

$$1 - \frac{1}{N} \exp\left(-\frac{E_s}{N_o}\right) \Phi\left(\sqrt{\frac{E_s}{N_o}}, \Lambda_{\text{MTSK}}(\boldsymbol{\tau})\right), \quad (4.23)$$

where $\mathbf{P}$ is the region defined by[4]

$$(0 < \tau_{12} \le T_w] \times (0 < \tau_{23} \le T_w] \times \ldots \times (0 < \tau_{(N-1)N} \le T_w]. \quad (4.24)$$

We can see that $\Lambda_{\text{MTSK}}(\boldsymbol{\tau}) \in \Upsilon$, where Υ is the class of admissible $\Lambda_{N \times N}$ defined by

1. $\Lambda = \Lambda^{\top}$,

2. $x\Lambda x^{\top} \ge 0, \forall x \in \Re^N$,

3. $\alpha_{i,i} = 1, i = 1, 2, \ldots, N$,

4. $\gamma_{\min} \le \alpha_{i,j} = \gamma_w(\tau_i - \tau_j) \le 1, \ i \ne j, \ i,j = 1, 2, \ldots, N$,

where $\Re$ is the set of real numbers. For $N = 2$ it can be shown that the optimal solution is $\boldsymbol{\tau}^{\text{opt}} = (0, \tau_{\min})$, and the corresponding correlation matrix is

$$\Lambda_{\text{MTSK}}(\boldsymbol{\tau}^{\text{opt}}) = \begin{bmatrix} 1 & \gamma_{\min} \\ \gamma_{\min} & 1 \end{bmatrix}. \quad (4.25)$$

For $N > 2$, the optimal solution $\boldsymbol{\tau}^{\text{opt}}$ might depend on the $\left(\frac{E_s}{N_o}\right)$ value, and the corresponding $N \times N$ correlation matrix has the form

$$\Lambda_{\text{MTSK}}(\boldsymbol{\tau}^{\text{opt}}(\tfrac{E_s}{N_o})) = \begin{bmatrix} 1 & \alpha_{21}^{opt}(\frac{E_s}{N_o}) & \ldots & \alpha_{N1}^{opt}(\frac{E_s}{N_o}) \\ \alpha_{21}^{opt}(\frac{E_s}{N_o}) & 1 & \ldots & \alpha_{2N}^{opt}(\frac{E_s}{N_o}) \\ \vdots & \vdots & \ddots & \vdots \\ \alpha_{N1}^{opt}(\frac{E_s}{N_o}) & \alpha_{N2}^{opt}(\frac{E_s}{N_o}) & \ldots & 1 \end{bmatrix}, \quad (4.26)$$

---

[4]Since $\gamma_w(\tau_{ij}) = 0$ for $\tau_{ij} \ge T_w$, we need to consider only $0 < \tau_{ij} \le T_w$.

where

$$\alpha_{ij}^{\mathrm{opt}}\left(\tfrac{E_s}{N_o}\right) = \gamma_w\left(\tau_i^{\mathrm{opt}}\left(\tfrac{E_s}{N_o}\right) - \tau_j^{\mathrm{opt}}\left(\tfrac{E_s}{N_o}\right)\right). \qquad (4.27)$$

Note that the time-shift values are interrelated. For example $\tau_{14} = \tau_{12} + \tau_{23} + \tau_{34}$.

For any given pulse $w(t)$, this optimization problem is difficult to solve both by analytic methods and by computer search. For intermediate and high values of $\left(\tfrac{E_s}{N_o}\right)$, an approximate solution to the problem in (4.23) is given by substituting $P_e\left(\tfrac{E_s}{N_o}, \Lambda_{\mathrm{MTSK}}(\boldsymbol{\tau})\right)$ by the union bound on the probability of error $\mathrm{UBP}_e\left(\tfrac{E_s}{N_o}, \Lambda_{\mathrm{MTSK}}(\boldsymbol{\tau})\right)$, and find by computer search the time shift values $\hat{\boldsymbol{\tau}}^{\mathrm{opt}} \triangleq \left(\hat{\tau}_1^{\mathrm{opt}}, \hat{\tau}_2^{\mathrm{opt}}, \ldots, \hat{\tau}_N^{\mathrm{opt}}\right)$ that minimize $\mathrm{UBP}_e\left(\tfrac{E_s}{N_o}, \Lambda_{\mathrm{MTSK}}(\boldsymbol{\tau})\right)$.[5] The corresponding optimization problem is

$$\underset{\boldsymbol{\tau}=(\tau_1,\tau_2,\ldots,\tau_N)\in\mathbf{P}}{\mathrm{minimize}} \quad \frac{1}{N}\sum_{i=1}^{N}\sum_{\substack{j=1\\i\neq j}}^{N} Q\left(\sqrt{\tfrac{E_s}{N_o}(1-\gamma_w(\tau_{ij}))}\right). \qquad (4.28)$$

To find the solution in (4.28) for high $\left(\tfrac{E_s}{N_o}\right)$ values,[6] the calculation in (4.28) can be approximated by

$$
\begin{aligned}
\underset{\boldsymbol{\tau}=(\tau_1,\tau_2,\ldots,\tau_N)\in\mathbf{P}}{\mathrm{minimize}} \quad \max(\quad &\gamma_w(\tau_{12}), \gamma_w(\tau_{13}), \ldots, \gamma_w(\tau_{1N}),\\
&\gamma_w(\tau_{23}), \gamma_w(\tau_{24}), \ldots, \gamma_w(\tau_{2N}),\\
&\vdots\\
&\gamma_w(\tau_{(N-2)(N-1)}), \gamma_w(\tau_{(N-2)N}),,\\
&\gamma_w(\tau_{(N-1)N}) \quad).
\end{aligned}
\qquad (4.29)
$$

---

[5] Both functions $\mathrm{UBP}_e\left(\tfrac{E_s}{N_o}, \Lambda\right)$ and $P_e\left(\tfrac{E_s}{N_o}, \Lambda\right)$ are not only close at high $\left(\tfrac{E_s}{N_o}\right)$ values, but also both $P_e\left(\tfrac{E_s}{N_o}, \Lambda\right)$ (weak simplex conjecture, see [52]) and $\mathrm{UBP}_e\left(\tfrac{E_s}{N_o}, \Lambda\right)$ (see [53]) are minimized by the regular simplex set at all $\left(\tfrac{E_s}{N_o}\right)$ values. Hence, we conjecture that both functions are minimized by $\Lambda_{\mathrm{MTSK}}(\boldsymbol{\tau}^{\mathrm{opt}}(\tfrac{E_s}{N_o}))$ at high $\left(\tfrac{E_s}{N_o}\right)$ values.

[6] At high $\left(\tfrac{E_s}{N_o}\right)$ values the signals of the set that are closest together in the signal space (i.e., have maximum correlation value) determines the performance bound.

4.3.3 AWGN performance

For NO PPM signals, the upper bound on error probability in (3.22) (with $N_u = 1$) reduces to

$$\mathrm{UBP}_\mathrm{e}^\mathrm{NO}(1) \quad \triangleq \quad \frac{1}{N}\sum_{\substack{i=1 \\ i \neq j}}^{N}\sum_{j=1}^{N} Q\left(\sqrt{\mathbf{SNR}_\mathrm{out}^{\mathrm{MTSK}(j,i)}(1)}\right) \; + \; (NL-N)\,Q\left(\sqrt{\mathbf{SNR}_\mathrm{out}^{\mathrm{OR}}(1)}\right),$$

$$(4.30)$$

where

$$\mathbf{SNR}_\mathrm{out}^\mathrm{OR}(1) \quad = \quad \frac{(A^{(1)})^2 E_s}{N_o}, \tag{4.31}$$

and

$$\mathbf{SNR}_\mathrm{out}^{\mathrm{MTSK}(j,i)}(1) \quad = \quad \frac{(A^{(1)})^2 E_s[1 - \gamma_w(\tau_{ji})]}{N_o}. \tag{4.32}$$

For $N = 2$ notice that we have $L - 1$ orthogonal tests and one "quasi antipodal" test[7] for determining the bound. Hence

$$\mathrm{UBP}_\mathrm{e}^\mathrm{NO}(1) \quad = \quad Q\left(\sqrt{\mathbf{SNR}_\mathrm{out}^{\mathrm{MTSK}(1,2)}(1)}\right) \; + \; (2L-2)Q\left(\sqrt{\mathbf{SNR}_\mathrm{out}^\mathrm{OR}(1)}\right) \quad (4.33)$$

is the union bound for the symbol error probability, where

$$\mathbf{SNR}_\mathrm{out}^{\mathrm{MTSK}(1,2)}(1) \quad = \quad \frac{(A^{(1)})^2 E_s(1 - \gamma_\mathrm{min})}{N_o}. \tag{4.34}$$

For $N = 2$ the union bound for the bit error probability $\mathrm{UBP}_\mathrm{b}^\mathrm{NO}(1)$ can be calculated assuming that complementary binary patterns representing data symbols are encoded using a pair of signals consisting of the signal and the pseudo-antipodal version of it. If the decoder decides correctly the orthogonal dimension but errs in

---

[7]Recall that the signals $w(t)\,and\,w(t - \tau_\mathrm{min})$ can not be antipodal since $\gamma_\mathrm{min} > -1$.

the pseudo-antipodal test, every bit of the word is incorrect. If the decoder decides the wrong orthogonal dimension, bit errors are equally distributed. The probability of a given bit being in error is obtained by averaging over the probability of each of these types of error. Hence

$$
\begin{aligned}
\text{UBP}_b^{\text{NO}}(1) \quad &= \quad \int_{\sqrt{\mathbf{SNR}_{\text{out}}^{\text{MTSK}(1,2)}(1)}}^{\infty} \frac{\exp(-\xi^2/2)}{\sqrt{2\pi}} \, d\xi \; + \\
&\qquad \frac{(2L-2)}{2} \int_{\sqrt{\mathbf{SNR}_{\text{out}}^{\text{OR}}(1)}}^{\infty} \frac{\exp(-\xi^2/2)}{\sqrt{2\pi}} \, d\xi.
\end{aligned}
\tag{4.35}
$$

4.3.4 Receiver simplification

We can take advantage of the structure of the NO PPM signals to simplify the construction of the receiver.

Let $x(t) = S_j(t - \tau^{(1)} - C_0^{(1)}(t - \tau^{(1)})) + n(t)$, where $S_j(t)$ is one of the signals in (4.20). Each of the M channel correlation output can be written

$$
\begin{aligned}
y_{m,l} \quad &= \quad \int_0^{N_s T_f} x(t) S_{m,l}(t - \tau^{(1)} - C_0^{(1)}(t - \tau^{(1)})) dt \\
&= \quad \sum_{k=0}^{N_s-1} \sum_{q=0}^{L-1} \delta_{q,[(k+l) \bmod L]} z_m(k,q),
\end{aligned}
\tag{4.36}
$$

where

$$
z_m(k,q) \triangleq \int_{kT_f + \tau^{(1)} + c_k^{(1)} T_c + qT_o}^{kT_f + \tau^{(1)} + c_k^{(1)} T_c + (q+1)T_o} x(t) \, w(t - kT_f - \tau^{(1)} - c_k^{(1)} T_c - \tau_m - qT_o) \, dt.
\tag{4.37}
$$

From the expression for $y_{m,l}$, it is clear that the receiver needs only N correlators and $M = NL$ store and sum circuits. The $y_{m,l}$ can be calculated while $x(t)$ is received and no symbol delay occur. This is illustrated in figure 4.4.
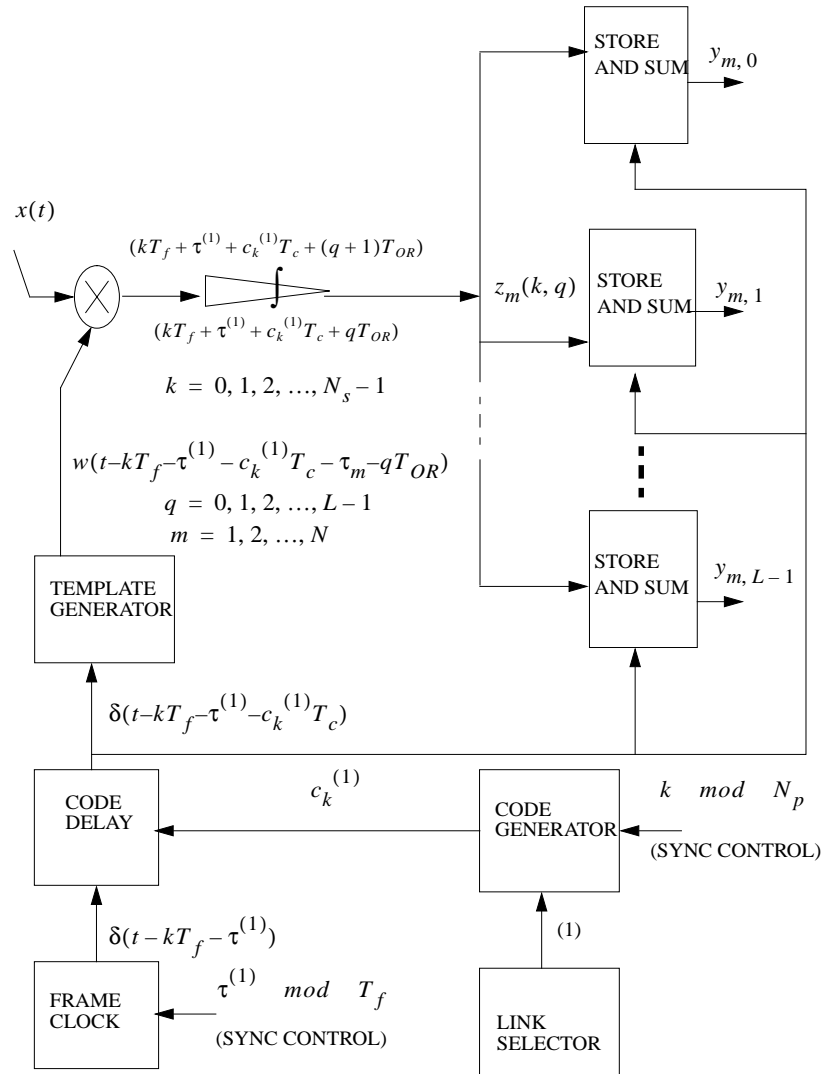
Figure 4.4: This diagram shows one of the N correlators and L of the $M = NL$ store and sum circuits that are needed in the simplified receiver for NO PPM signals.

4.4   Numerical example

In this section we calculate the symbol error probability in AWGN for $M = 8$ for the three types of signals just discussed. In IR modulation, the UWB received pulse $w(t)$ can be modeled by

$$w(t) = \left[1 - 4\pi \left[\frac{t}{t_n}\right]^2\right] \exp\left(-2\pi \left[\frac{t}{t_n}\right]^2\right), \tag{4.38}$$

where the value $t_n = 0.4472$ ns was used to fit the model $w(t)$ to the measured waveform $w_T(t)$. The UWB pulse $w_T(t)$ is a unit-energy template with duration $T_w = 1.0$ ns that was taken from a multipath-free and noise-free measurement in a particular IR link. The signal correlation function corresponding to $w(t)$ is

$$\gamma_w(\tau) = \left[1 - 4\pi \left[\frac{\tau}{t_n}\right]^2 + \frac{4\pi^2}{3} \left[\frac{\tau}{t_n}\right]^4\right] \exp\left(-\pi \left[\frac{\tau}{t_n}\right]^2\right). \tag{4.39}$$

In this case $\tau_{\min} = 0.2419$ ns and $\gamma_{\min} = -0.6183$. Both $w(t - \frac{T_w}{2})$ and $\gamma_w(\tau)$ are shown in figure 4.5. Using this $w(t)$ we can calculate

$$F_w(f) = \sqrt{2} t_n \left[\frac{\pi (f t_n)^2}{2}\right] \exp -\frac{\pi (f t_n)^2}{2} \tag{4.40}$$

which has a maximum at $f = \frac{1}{t_n}\sqrt{\frac{2}{\pi}} = 1.7842$ Gigahertz. Figure 4.6 shows a a normalized plot of $F_w(f)$ calculated using $t_n = 0.4472$ ns.

To calculate the performance bound for OR PPM signals, notice that (4.3) can be rewritten

$$\text{UBP}_e^{\text{OR}}(1) = \text{UBP}_e\left(\frac{E_s}{N_o}, \Lambda_{\text{OR}}\right) \tag{4.41}$$
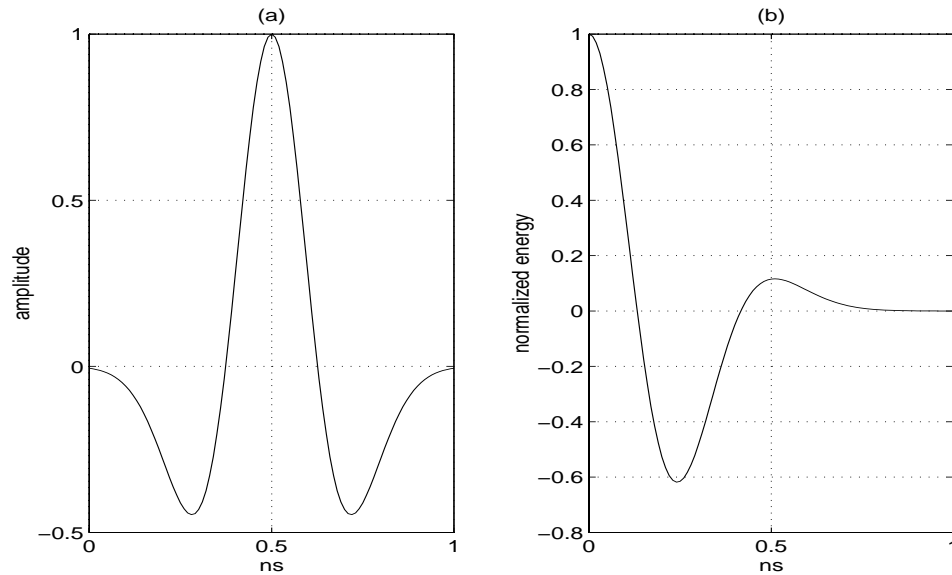
Figure 4.5: (a) The pulse $w(t - \frac{T_w}{2})$ as a function of time t. (b) The signal autocorrelation $\gamma_w(\tau)$ as a function of time shift τ.
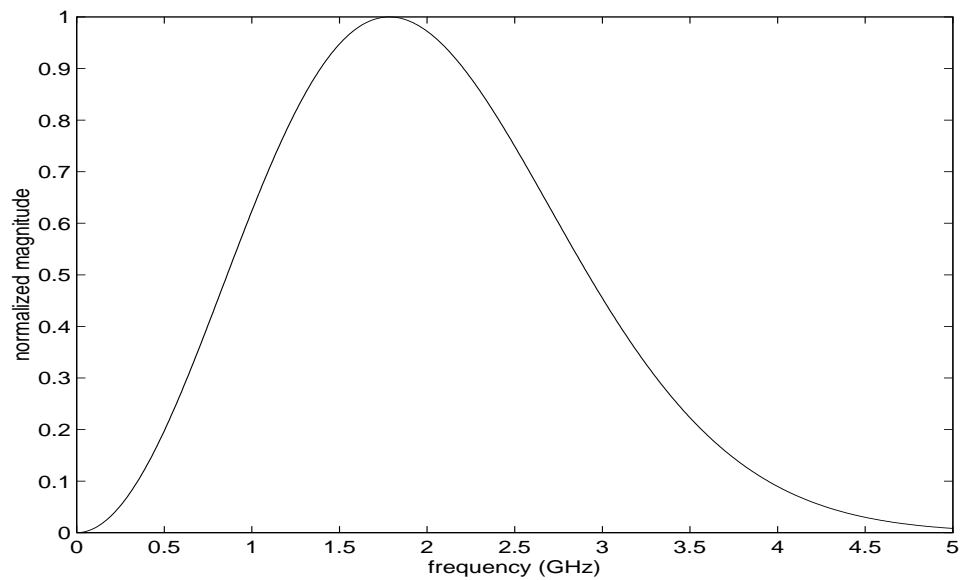
Figure 4.6: Fourier transform $F_w(f)$ of the pulse $w(t)$.

and we just need to evaluate (4.41) for different values of $\left(\frac{E_s}{N_o}\right)$. To calculate the performance for EC PPM signals, notice that (4.12) can be rewritten

$$
\begin{aligned}
\mathrm{UBP}_{\mathrm{e}}^{\mathrm{EC}}(1) &= \mathrm{UBP}_{\mathrm{e}}\left(\tfrac{E_s}{N_o},\Lambda_{\mathrm{EC}}\right) \\
&= \mathrm{UBP}_{\mathrm{e}}\left(\tfrac{E_s}{N_o}(1-\lambda),\Lambda_{\mathrm{OR}}\right).
\end{aligned}
\tag{4.42}
$$

To calculate the performance for NO PPM signals, notice that (4.30) can be rewritten

$$
\begin{aligned}
\mathrm{UBP}_{\mathrm{e}}^{\mathrm{NO}}(1) &= \mathrm{UBP}_{\mathrm{e}}\left(\tfrac{E_s}{N_o},\Lambda_{\mathrm{NO}}\right) \\
&= \mathrm{UBP}_{\mathrm{e}}\left(\tfrac{E_s}{N_o},\Lambda_{\mathrm{OR}}\right) - \mathrm{DUBP}_{\mathrm{e}}\left(\tfrac{E_s}{N_o},\Lambda_{\mathrm{MTSK}},\bar{\Lambda}_{\mathrm{OR}}\right),
\end{aligned}
\tag{4.43}
$$

where $\mathrm{DUBP}_{\mathrm{e}}\left(\frac{E_s}{N_o},\Lambda_{\mathrm{MTSK}},\bar{\Lambda}_{\mathrm{OR}}\right)$ is the difference in performance between the NO PPM signal set and the OR PPM signal set for the same value of M, and is given by

$$
\begin{aligned}
\mathrm{DUBP}_{\mathrm{e}}\left(\tfrac{E_s}{N_o},\Lambda_{\mathrm{MTSK}},\bar{\Lambda}_{\mathrm{OR}}\right) &\triangleq \mathrm{UBP}_{\mathrm{e}}\left(\tfrac{E_s}{N_o},\Lambda_{\mathrm{OR}}\right) - \mathrm{UBP}_{\mathrm{e}}\left(\tfrac{E_s}{N_o},\Lambda_{\mathrm{NO}}\right) \\
&= (NL-1)Q\left(\sqrt{\tfrac{E_s}{N_o}}\right) - \mathrm{UBP}_{\mathrm{e}}\left(\tfrac{E_s}{N_o},\Lambda_{\mathrm{MTSK}}\right) - \\
&\qquad (NL-N)Q\left(\sqrt{\tfrac{E_s}{N_o}}\right) \\
&= (N-1)Q\left(\sqrt{\tfrac{E_s}{N_o}}\right) - \mathrm{UBP}_{\mathrm{e}}\left(\tfrac{E_s}{N_o},\Lambda_{\mathrm{MTSK}}\right) \\
&= \mathrm{UBP}_{\mathrm{e}}\left(\tfrac{E_s}{N_o},\bar{\Lambda}_{\mathrm{OR}}\right) - \mathrm{UBP}_{\mathrm{e}}\left(\tfrac{E_s}{N_o},\Lambda_{\mathrm{MTSK}}\right),
\end{aligned}
\tag{4.44}
$$

where $\bar{\Lambda}_{\mathrm{OR}}$ is an $N \times N$ identity matrix corresponding to a set of N orthogonal signals. Hence, the difference in performance $\mathrm{DUBP}_{\mathrm{e}}\left(\frac{E_s}{N_o},\Lambda_{\mathrm{MTSK}},\bar{\Lambda}_{\mathrm{OR}}\right)$ is dictated by N and is independent of L.

In this example we evaluate (4.43) for $M = 8$ with $L = 2$. This requires the calculation of $\hat{\boldsymbol{\tau}}^{\mathrm{opt}}\left(\frac{E_s}{N_o}\right)$ in (4.28) for $N = 4$ and different values of $\left(\frac{E_s}{N_o}\right)$. For each value of $\left(\frac{E_s}{N_o}\right)$ considered, the minimization is carried in two steps. In the first step a coarse approximation to $\hat{\boldsymbol{\tau}}^{\mathrm{opt}} = \left(\hat{\tau}_1^{\mathrm{opt}}, \hat{\tau}_2^{\mathrm{opt}}, \hat{\tau}_3^{\mathrm{opt}}, \hat{\tau}_4^{\mathrm{opt}}\right)$ is found by exhaustive search in the region $\mathbf{P}$ defined in (4.24) with an incremental step of 0.01 nanoseconds. In

the second step this coarse value is used as a starting point of a simplex search method [54]. This provided a more precise value of $\hat{\boldsymbol{\tau}}^{\text{opt}} = \left(\hat{\tau}_1^{\text{opt}}, \hat{\tau}_2^{\text{opt}}, \hat{\tau}_3^{\text{opt}}, \hat{\tau}_4^{\text{opt}}\right)$. Table 4.1 shows $\hat{\boldsymbol{\tau}}^{\text{opt}}\left(\frac{E_s}{N_o}\right)$ for different values of $\left(\frac{E_s}{N_o}\right)$. Table 4.2 shows the corresponding values of $\text{UBP}_{\text{e}}\left(\frac{E_s}{N_o},\Lambda_{\text{MTSK}}(\hat{\boldsymbol{\tau}}^{\text{opt}}(\frac{E_s}{N_o}))\right)$ and $\text{DUBP}_{\text{e}}\left(\frac{E_s}{N_o},\Lambda_{\text{MTSK}}(\hat{\boldsymbol{\tau}}^{\text{opt}}(\frac{E_s}{N_o})),\bar{\Lambda}_{\text{OR}}\right)$.

$\left(\frac{E_s}{N_o}\right)$ (dB)	$\hat{\boldsymbol{\tau}}^{\text{opt}} = \left(\hat{\tau}_1^{\text{opt}}, \hat{\tau}_2^{\text{opt}}, \hat{\tau}_3^{\text{opt}}, \hat{\tau}_4^{\text{opt}}\right)$ (ns)
2	$(0.0, 0.19381752, 0.35302358, 0.54683541)$
4	$(0.0, 0.19068768, 0.35045188, 0.54113714)$
6	$(0.0, 0.18725300, 0.34807298, 0.53531977)$
8	$(0.0, 0.18460247, 0.34689223, 0.53149639)$
10	$(0.0, 0.19072413, 0.35430263, 0.54500740)$
12	$(0.0, 0.15057900, 0.30033943, 0.45092310)$
14	$(0.0, 0.14558436, 0.29101003, 0.43657833)$
16	$(0.0, 0.14279746, 0.28555227, 0.42832342)$
18	$(0.0, 0.14095107, 0.28180320, 0.42274070)$

Table 4.1: Values $\hat{\boldsymbol{\tau}}^{\text{opt}}\left(\frac{E_s}{N_o}\right)$ for N=4 calculated using the pulse in (4.38) to solve the minimization problem in (4.28).

Figure 4.7 shows $\text{UBP}_{\text{e}}\left(\frac{E_s}{N_o},\Lambda_{\text{OR}}\right)$, $\text{UBP}_{\text{e}}\left(\frac{E_s}{N_o},\Lambda_{EC}\right)$ and $\text{UBP}_{\text{e}}\left(\frac{E_s}{N_o},\Lambda_{\text{NO}}\right)$ for $N = 4$, $L = 2$, $M = 8$.

4.5   Conclusion

This section described the construction of orthogonal, equally correlated and N-orthogonal block waveform PPM signals for ultra-wideband impulse radio modulation. The construction uses a set of time-shift-keyed signals to construct the PPM signals. In the N-orthogonal PPM case the signal design depends on the SNR value at which the communications link is operated, since in this case the *optimum* set of time-shift-keyed signals is a function of the SNR value.

$\left(\frac{E_s}{N_o}\right)$ (dB)	$\mathrm{UBP_e}\left(\frac{E_s}{N_o},\Lambda_{\mathrm{MTSK}}\right)$ (prob. of error)	$\mathrm{UBP_e}\left(\frac{E_s}{N_o},\bar{\lambda}_{O}\right)$ (prob. of error)	$\mathrm{DUBP_e}\left(\frac{E_s}{N_o},\Lambda_{\mathrm{MTSK}},\bar{\lambda}_{\mathrm{OR}}\right)$
2	$2.4003952E^{-1}$	$3.1208591E^{-1}$	$7.2046391E^{-2}$
4	$1.1726925E^{-1}$	$1.6948590E^{-1}$	$5.2216648E^{-2}$
6	$4.1460574E^{-2}$	$6.9021416E^{-2}$	$2.7560842E^{-2}$
8	$9.1811626E^{-3}$	$1.8013159E^{-2}$	$8.8319966E^{-2}$
10	$1.0597741E^{-3}$	$2.3481033E^{-3}$	$1.2883292E^{-3}$
12	$4.4588128E^{-5}$	$1.0290787E^{-4}$	$5.8319742E^{-5}$
14	$3.2869771E^{-7}$	$8.0854443E^{-7}$	$4.7984672E^{-7}$
16	1.55400285^{-10}	$4.1970834E^{-10}$	$2.6430805E^{-10}$
18	$9.3470225E^{-16}$	$2.9535000E^{-15}$	$2.0187984E^{-15}$

Table 4.2: Values $\mathrm{UBP_e}\left(\frac{E_s}{N_o},\Lambda_{\mathrm{MTSK}}\right)$, $\mathrm{UBP_e}\left(\frac{E_s}{N_o},\bar{\lambda}_{\mathrm{OR}}\right)$ and $\mathrm{DUBP_e}\left(\frac{E_s}{N_o},\Lambda_{\mathrm{MTSK}},\bar{\lambda}_{\mathrm{OR}}\right)$ corresponding to $\hat{\tau}^{\mathrm{opt}}\left(\frac{E_s}{N_o}\right)$ in table 4.1.
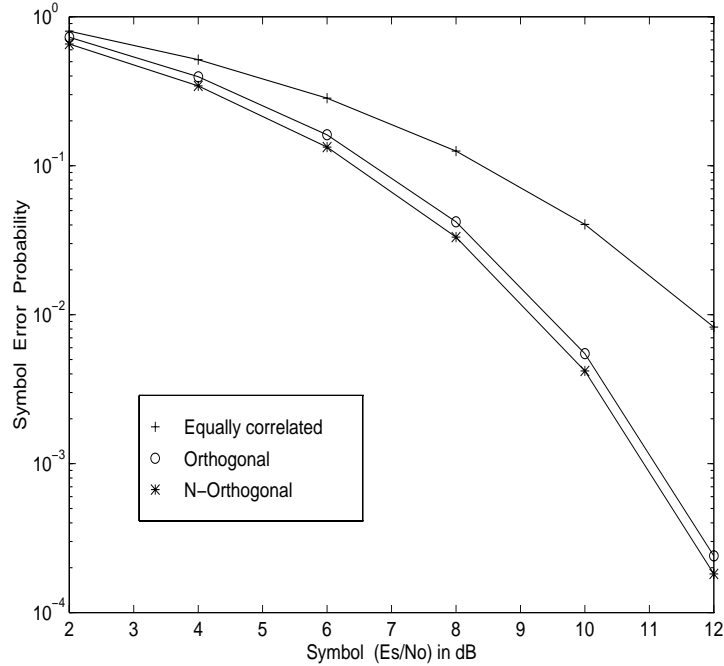
Figure 4.7: The $\mathrm{UBP_e}\left(\frac{E_s}{N_o},\Lambda_{EC}\right)$, $\mathrm{UBP_e}\left(\frac{E_s}{N_o},\Lambda_{\mathrm{OR}}\right)$ and $\mathrm{UBP_e}\left(\frac{E_s}{N_o},\Lambda_{\mathrm{NO}}\right)$ for $N=4$, $L=2$, $M=8$.

Since the PPM signals are linearly independent, it is not possible to reduce the dimensionality M of the signal set. Nevertheless, we can take advantage of the structure of the PPM signals to reduce the complexity of the receiver and use less than M correlators combined with M store and sum circuits without introducing a symbol delay.

Chapter 5

Multiple-access performance using block waveform encoding TH PPM signals

In this chapter we evaluate $\mathbf{SNR}_{\text{out}}^{(j,i)}(N_u)$ in (3.57) for the three types of block waveform encoding PPM signal sets presented in chapter 4. Once $\mathbf{SNR}_{\text{out}}^{(j,i)}(N_u)$ is known, we can use the corresponding expressions for symbol error probability derived in chapter 4 to analyze the multiple-access performance of these signals.

5.1   Performance using orthogonal signals

For the orthogonal signals in section 4.1 we have that

$$\delta_j^k = [(k+j-1) \bmod M]T_{\text{OR}} \tag{5.1}$$

for $1 \leq j \leq M$ and $k = 0, 1, 2, \ldots, N_s - 1$. Hence

$$v_{k,j,i}(\rho) = w(\rho - [(k+j-1) \bmod M]T_{\text{OR}}) - w(\rho - [(k+i-1) \bmod M]T_{\text{OR}}) \tag{5.2}$$

for $k = 0, 1, 2, \ldots, N_s - 1$ and $j \neq i$, $j, i = 1, 2, \ldots, M$. Using (5.2) in (3.47) we get

$$\hat{\sigma}_{\text{OR}}^2 \quad \stackrel{\triangle}{=} \quad \hat{\sigma}_{k,j,i}^2$$

$$
\begin{aligned}
&= \hat{\sigma}_w^2([(k+j-1) \bmod M]T_{\mathrm{OR}}, [(k+i-1) \bmod M]T_{\mathrm{OR}}) \\
&= \frac{1}{T_f} \int_\epsilon^\epsilon m_w^2(\varsigma, [(k+j-1) \bmod M]T_{\mathrm{OR}}, [(k+i-1) \bmod M]T_{\mathrm{OR}})\, d\varsigma \\
&= \frac{E_w^2}{T_f} \int_{-\epsilon}^\epsilon [\gamma_w(\varsigma - [(k+j-1) \bmod M]T_{\mathrm{OR}}) - \gamma_w(\varsigma - [(k+i-1) \bmod M]T_{\mathrm{OR}})]^2\, d\varsigma \\
&\overset{(i)}{=} \frac{E_w^2}{T_f} \int_{-\epsilon}^\epsilon [\gamma_w(\varsigma - 0) - \gamma_w(\varsigma - T_{\mathrm{OR}})]^2\, d\varsigma \quad \text{for all } i \neq j \\
&= \frac{1}{T_f} \int_{-\epsilon}^\epsilon m_w^2(\varsigma, 0, T_{\mathrm{OR}})\, d\varsigma \\
&= \hat{\sigma}_w^2(0, T_{\mathrm{OR}}),
\end{aligned}
$$

$$(5.3)$$

where $\epsilon = 2(T_w + (M-1)T_{\mathrm{OR}})(see(2.28))$.[1] Notice that step (i) is possible because $|\delta_j^k - \delta_i^k| \geq T_{\mathrm{OR}}$, i.e., in the range of integration $[-\epsilon, \epsilon]$ the functions $\gamma_w(\varsigma - [(k+j-1) \bmod M]T_{\mathrm{OR}})$ and $\gamma_w(\varsigma - [(k+i-1) \bmod M]T_{\mathrm{OR}})$ do not overlap for $j \neq i$. Hence

$$
\begin{aligned}
\sum_{k=0}^{N_s-1} \hat{\sigma}_{k,j,i}^2 &= N_s\, \hat{\sigma}_{\mathrm{OR}}^2 \\
&= N_s\, \hat{\sigma}_w^2(0, T_{\mathrm{OR}}), \quad \epsilon = 2(T_w + (M-1)T_{\mathrm{OR}}). \tag{5.4}
\end{aligned}
$$

Similarly, it can be shown that

$$
\begin{aligned}
m_{\mathrm{OR}} &\overset{\triangle}{=} m_w(\delta_j^k, \delta_j^k, \delta_i^k) \\
&= m_w([(k+j-1) \bmod M]T_{\mathrm{OR}}, [(k+j-1) \bmod M]T_{\mathrm{OR}}, [(k+i-1) \bmod M]T_{\mathrm{OR}}) \\
&= m_w(0, 0, T_{\mathrm{OR}}). \tag{5.5}
\end{aligned}
$$

Hence

$$
\begin{aligned}
\sum_{k=0}^{N_s-1} m_w(\delta_j^k, \delta_j^k, \delta_i^k) &= N_s\, m_{\mathrm{OR}} \\
&= N_s\, m_w(0, 0, T_{\mathrm{OR}}), \quad \epsilon = 2(T_w + (M-1)T_{\mathrm{OR}}). \tag{5.6}
\end{aligned}
$$

---

[1]Note that for this type of orthogonal signals the parameter ϵ grows with M, therefore for large values of M the assumption in (e) and the assumption $\tilde{\sigma}_{k,l,j,i} \simeq 0$ both will need to be revised.

The value in (5.6) corresponds to m_{ji} in (3.56) with $\alpha_{ji} = 0$. Substituting (5.4) and (5.6) in (3.58) we get

$$
\begin{aligned}
\beta_{\mathrm{OR}} &\triangleq \frac{\left[\sum_{k=0}^{N_s-1} m_w(\delta_j^k, \delta_j^k, \delta_i^k)\right]^2}{N_s \sum_{k=0}^{N_s-1} \hat{\sigma}_{k,j,i}^2} \\
&= \frac{m_{\mathrm{OR}}^2}{\hat{\sigma}_{\mathrm{OR}}^2} \\
&= \frac{m_w^2(0,0,T_{\mathrm{OR}})}{\hat{\sigma}_w^2(0,T_{\mathrm{OR}})}, \quad \epsilon = 2(T_w + (M-1)T_{\mathrm{OR}}),
\end{aligned}
\tag{5.7}
$$

and the expression for the symbol SNR in the case of orthogonal signals is

$$
\mathbf{SNR}_{\mathrm{out}}^{\mathrm{OR}}(N_u) \triangleq \left[\left[\frac{(A^{(1)})^2 E_s}{N_o}\right]^{-1} + \left[\frac{T_s}{T_w}\frac{T_w}{T_f}\frac{\beta_{\mathrm{OR}}}{\sum_{\nu=2}^{N_u}\left(\frac{A^{(\nu)}}{A^{(1)}}\right)^2}\right]^{-1}\right]^{-1}.
\tag{5.8}
$$

Note that (5.8) can be rewritten as in (3.60) to give

$$
\mathbf{SNR}_{\mathrm{out}}^{\mathrm{OR}}(N_u) = \frac{(A^{(1)})^2 E_s}{N_o + N_{\mathrm{OR}}},
\tag{5.9}
$$

where

$$
N_{\mathrm{OR}} \triangleq \sum_{\nu=2}^{N_u} N_{\mathrm{OR}}^{(\nu)}
\tag{5.10}
$$

and

$$
N_{\mathrm{OR}}^{(\nu)} \triangleq (A^{(\nu)})^2 \frac{E_w}{T_f} \int_{-(T_w+T_{\mathrm{OR}})}^{(T_w+T_{\mathrm{OR}})} \frac{\left[\gamma_w(\varsigma) - \gamma_w(\varsigma - T_{\mathrm{OR}})\right]^2}{\left[\gamma_w(0) - \gamma_w(T_{\mathrm{OR}})\right]} \, d\varsigma
\tag{5.11}
$$

for $\nu = 2, 3, \ldots, N_u$.

The expression in (5.8) gives the symbol SNR value for use in the expression for bit error probability in (4.5) for N_u greater than one.

5.2   Performance using equally correlated signals

For the equally correlated signals described in section 4.2 we have that

$$\delta_j^k \in \{\tau_1 = 0, 0 < \tau_2 < T_w\} \tag{5.12}$$

for $k = 0, 1, 2, \ldots, N_s - 1$, and

$$v_{k,j,i}(\rho) = \begin{cases} \left\{ \begin{array}{c} w(\rho - \tau_1) - w(\rho - \tau_2) \neq 0 \\ \text{or} \\ w(\rho - \tau_2) - w(\rho - \tau_1) \neq 0 \end{array} \right\}, & \text{for } \frac{N_s+1}{2} \text{ hops} \\ \left\{ \begin{array}{c} w(\rho - \tau_1) - w(\rho - \tau_1) = 0 \\ \text{or} \\ w(\rho - \tau_2) - w(\rho - \tau_2) = 0 \end{array} \right\}, & \text{for } \frac{N_s-1}{2} \text{ hops} \end{cases} \tag{5.13}$$

Using (5.13) in (3.47) we notice that, for the $\frac{N_s-1}{2}$ hops in which $v_{k,j,i}(\rho) = 0$, $\hat{\sigma}_{k,j,i}^2 = 0$, and for the $\frac{N_s+1}{2}$ hops in which $v_{k,j,i}(\rho) \neq 0$,

$$\begin{aligned} \hat{\sigma}_{k,j,i}^2 &= T_f^{-1} \int_{-\epsilon}^{\epsilon} \left(\int_{-\infty}^{\infty} w(\rho - \varsigma) \left\{ \begin{array}{c} w(\rho - \tau_1) - w(\rho - \tau_2) \\ \text{or} \\ w(\rho - \tau_2) - w(\rho - \tau_1) \end{array} \right\} d\rho \right)^2 d\varsigma \\ &= \frac{E_w^2}{T_f} \int_{-\epsilon}^{\epsilon} \left(\left\{ \begin{array}{c} \gamma_w(\varsigma) - \gamma_w(\varsigma - \tau_2) \\ \text{or} \\ \gamma_w(\varsigma - \tau_2) - \gamma_w(\varsigma) \end{array} \right\} \right)^2 d\varsigma \\ &= \frac{E_w^2}{T_f} \int_{-\epsilon}^{\epsilon} \left(\gamma_w(\varsigma) - \gamma_w(\varsigma - \tau_2) \right)^2 d\varsigma \\ &= T_f^{-1} \int_{-\epsilon}^{\epsilon} m_w^2(\varsigma, 0, \tau_2) \, d\varsigma \\ &= \hat{\sigma}_w^2(0, \tau_2), \end{aligned} \tag{5.14}$$

where $\epsilon = 2(T_w + \tau_2)$. If we define

$$\hat{\sigma}^2_{\text{EC}} \;\triangleq\; \frac{2}{T_f} \int_{-\epsilon}^{\epsilon} m_w^2(\varsigma, 0, \tau_2)\, d\varsigma$$

$$= \; 2\, \hat{\sigma}_w^2(0, \tau_2), \tag{5.15}$$

we can write

$$\hat{\sigma}^2_{k,j,i} = \begin{cases} \frac{1}{2}\hat{\sigma}^2_{\text{EC}}, & \text{for } \frac{N_s+1}{2} \text{ hops} \\ 0, & \text{for } \frac{N_s-1}{2} \text{ hops} \end{cases}. \tag{5.16}$$

Hence

$$\sum_{k=0}^{N_s-1} \hat{\sigma}^2_{k,j,i} \;=\; \frac{N_s + 1}{2}\, \frac{\hat{\sigma}^2_{\text{EC}}}{2}$$

$$\simeq \; \frac{N_s}{4}\, \hat{\sigma}^2_{\text{EC}} \quad \text{for } N_s \gg 1. \tag{5.17}$$

Similarly, we can write

$$m_w(\delta_j^k, \delta_j^k, \delta_i^k) = \begin{cases} \left\{ \begin{array}{c} m_w(\tau_1, \tau_1, \tau_2) \\ \text{or} \\ m_w(\tau_2, \tau_2, \tau_1) = m_w(\tau_1, \tau_1, \tau_2) \end{array} \right\}, & \text{for } \frac{N_s+1}{2} \text{ hops} \\ \left\{ \begin{array}{c} m_w(\tau_1, \tau_1, \tau_1) = 0 \\ \text{or} \\ m_w(\tau_2, \tau_2.\tau_2) = 0 \end{array} \right\}, & \text{for } \frac{N_s-1}{2} \text{ hops} \end{cases}. \tag{5.18}$$

If we define

$$m_{\text{EC}} \;\triangleq\; m_w(0, 0, \tau_2) \tag{5.19}$$

we can write

$$\sum_{k=0}^{N_s-1} m_w(\delta_j^k, \delta_j^k, \delta_i^k) \;=\; \frac{N_s + 1}{2}\, m_{\text{EC}}$$

$$\simeq \; \frac{N_s}{2}\, m_{\text{EC}}, \; N_s \gg 1,$$

$$= \; \frac{N_s}{2}\, m_w(0, 0, \tau_2), \; \epsilon = 2(T_w + \tau_2) \tag{5.20}$$

63

The value in (5.20) corresponds to m_{ji} in (3.56) with $\alpha_{ji} = \lambda$. Substituting (5.17) and (5.20) in (3.58) we get

$$\beta_{\mathrm{EC}} \quad \triangleq \quad \frac{m_{\mathrm{EC}}^2}{\hat{\sigma}_{\mathrm{EC}}^2}$$
$$= \quad \frac{m_w^2(0,0,\tau_2)}{2\,\hat{\sigma}_w^2(0,\tau_2)}, \;\; \epsilon = 2(T_w + \tau_2), \tag{5.21}$$

and the expression for the symbol SNR in the case of equally correlated signals is

$$\mathbf{SNR}_{\mathrm{out}}^{\mathrm{EC}}(N_u) \quad \triangleq \quad \left[\left[\frac{(A^{(1)})^2 E_s (1-\lambda)}{N_o} \right]^{-1} + \left[\frac{T_s}{T_w} \frac{T_w}{T_f} \frac{\beta_{\mathrm{EC}}}{\sum_{\nu=2}^{N_u} \left(\frac{A^{(\nu)}}{A^{(1)}} \right)^2} \right]^{-1} \right]^{-1}. \tag{5.22}$$

Note that (5.22) can be rewritten as in (3.60) to give

$$\mathbf{SNR}_{\mathrm{out}}^{\mathrm{EC}}(N_u) \quad = \quad \frac{(A^{(1)})^2 E_s (1-\lambda)}{N_o + N_{\mathrm{EC}}} \tag{5.23}$$

where

$$N_{\mathrm{EC}} \quad \triangleq \quad \sum_{\nu=2}^{N_u} N_{\mathrm{EC}}^{(\nu)} \tag{5.24}$$

and

$$N_{\mathrm{EC}}^{(\nu)} \quad \triangleq \quad (A^{(\nu)})^2 \frac{E_w}{T_f} \int_{-(T_w+\tau_2)}^{(T_w+\tau_2)} \frac{[\gamma_w(\varsigma) - \gamma_w(\varsigma - \tau_2)]^2}{[\gamma_w(0) - \gamma_w(\tau_2)]} d\varsigma \tag{5.25}$$

for $\nu = 2, 3, \ldots, N_u$.

The expression in (5.22) gives the symbol SNR value for use in the expression for bit error probability in (4.14) for N_u greater than one.

5.3 Performance using N-orthogonal signals

For the N-orthogonal signals in section 4.3 we have that

$$\delta_j^k \in \{\tau_J + [(k+l) \bmod L] T_o\} \tag{5.26}$$

for $j = 1, 2, \ldots, M$, $J \stackrel{\triangle}{=} j - \lfloor \frac{j-1}{N} \rfloor N = 1, 2, \ldots, N$, and $l = \lfloor \frac{j-1}{N} \rfloor = 0, 1, 2, \ldots, L-1$. Hence

$$v_{k,j,i}(\rho) = w(\rho - \delta_j^k) - w(\rho - \delta_i^k) \tag{5.27}$$

for $k = 0, 1, 2, \ldots, N_s - 1$ and $j \neq i$, $j, i = 1, 2, \ldots, M$. Using (5.27) in (3.47) we get

$$
\begin{aligned}
\hat{\sigma}_{k,j,i}^2 &= T_f^{-1} \int_{-\epsilon}^{\epsilon} \left(\int_{-\infty}^{\infty} w(\rho - \varsigma) \; \left[w(\rho - \delta_j^k) - w(\rho - \delta_i^k) \right] \, d\rho \right)^2 d\varsigma \\
&= \frac{E_w^2}{T_f} \int_{-\epsilon}^{\epsilon} \left[\gamma_w(\varsigma - \delta_j^k) - \gamma_w(\varsigma - \delta_i^k) \right]^2 d\varsigma \\
&= \hat{\sigma}_w^2(\delta_j^k, \delta_i^k),
\end{aligned}
\tag{5.28}
$$

where $\epsilon = 2(T_w + \tau_N + (L-1)T_o)$.[2]. When the pair of signals (j, i) each one belongs to distinct disjoint (orthogonal) subsets (i.e. $\lfloor \frac{j-1}{N} \rfloor \neq \lfloor \frac{i-1}{N} \rfloor$), we have that

$$|\delta_j^k - \delta_i^k| \geq T_o. \tag{5.29}$$

In this case, we can use a procedure similar to the one used in orthogonal signals to show that

$$\sum_{k=0}^{N_s-1} \hat{\sigma}_{k,j,i}^2 = N_s \hat{\sigma}_{\mathrm{OR}}^2 \tag{5.30}$$

and

$$\sum_{k=0}^{N_s-1} m_w(\delta_j^k, \delta_j^k, \delta_i^k) = N_s m_{\mathrm{OR}}. \tag{5.31}$$

---

[2]Note that for this type of N-orthogonal signals the parameter ϵ grows with L, therefore for large values of L (i.e., large values of $M = NL$ for N fixed) the assumption in (e) and the assumption $\tilde{\sigma}_{k,l,j,i} \simeq 0$ both will need to be revised.

When the pair of signals (j, i) both belong to one of the L subsets containing N signals (i.e. $\lfloor \frac{j-1}{N} \rfloor = \lfloor \frac{i-1}{N} \rfloor$), we have that

$$\delta_j^k - \delta_i^k = \tau_J - \tau_I \tag{5.32}$$

for $k = 0, 1, 2, \ldots, N_s - 1$. Hence, in the range of integration $[-\epsilon, \epsilon]$ we can write

$$\int_{-\epsilon}^{\epsilon} \left[\gamma_w(\varsigma - \delta_j^k) - \gamma_w(\varsigma - \delta_i^k) \right]^2 d\varsigma = \int_{-\epsilon}^{\epsilon} \left[\gamma_w(\varsigma - \tau_J) - \gamma_w(\varsigma - \tau_I) \right]^2 d\varsigma \tag{5.33}$$

therefore

$$
\begin{aligned}
\hat{\sigma}_{\text{MTSK}(j,i)}^2 & \triangleq \hat{\sigma}_{k,j,i}^2 \\
& = \frac{E_w^2}{T_f} \int_{-\epsilon}^{\epsilon} \left[\gamma_w(\varsigma - \tau_J) - \gamma_w(\varsigma - \tau_I) \right]^2 d\varsigma \\
& = \frac{1}{T_f} \int_{-\epsilon}^{\epsilon} m_w^2(\varsigma, \tau_J, \tau_I) \, d\varsigma \\
& = \hat{\sigma}_w^2(\tau_J, \tau_I).
\end{aligned} \tag{5.34}
$$

Hence

$$
\begin{aligned}
\sum_{k=0}^{N_s-1} \hat{\sigma}_{k,j,i}^2 & = N_s \, \hat{\sigma}_{\text{MTSK}(j,i)}^2 \\
& = N_s \, \hat{\sigma}_w^2(\tau_J, \tau_I), \ \epsilon = 2(T_w + \tau_N + (L-1)T_o).
\end{aligned} \tag{5.35}
$$

Similarly, it can be shown that

$$
\begin{aligned}
m_{\text{MTSK}(j,i)} & \triangleq m_w(\delta_j^k, \delta_j^k, \delta_i^k) \\
& = m_w(\tau_J, \tau_J, \tau_I).
\end{aligned} \tag{5.36}
$$

Hence

$$\sum_{k=0}^{N_s-1} m_w(\delta_j^k, \delta_j^k, \delta_i^k) = N_s\, m_{\mathrm{MTSK}(j,i)}$$

$$= N_s\, m_w(\tau_J, \tau_J, \tau_I), \tag{5.37}$$

$$\epsilon = 2(T_w + \tau_N + (L-1)T_o),$$

$$J = j - \lfloor \frac{j-1}{N} \rfloor N,\ 1 \le j \le M.$$

The value in (5.37) corresponds to m_{ji} in (3.56) with $\alpha_{ji} = \gamma_w(\tau_J - \tau_I)$. Putting the two cases together, we can write

$$\sum_{k=0}^{N_s-1} \hat{\sigma}_{k,j,i}^2 = \begin{cases} N_s\hat{\sigma}_{\mathrm{OR}}^2, & \text{for } \lfloor \frac{j-1}{N} \rfloor \ne \lfloor \frac{i-1}{N} \rfloor \\ N_s\hat{\sigma}_{\mathrm{MTSK}(j,i)}^2, & \text{for } \lfloor \frac{j-1}{N} \rfloor = \lfloor \frac{i-1}{N} \rfloor \end{cases} \tag{5.38}$$

and

$$\sum_{k=0}^{N_s-1} m_w(\delta_j^k, \delta_j^k, \delta_i^k) = \begin{cases} N_s m_{\mathrm{OR}}, & \text{for } \lfloor \frac{j-1}{N} \rfloor \ne \lfloor \frac{i-1}{N} \rfloor \\ N_s m_{\mathrm{MTSK}(j,i)}, & \text{for } \lfloor \frac{j-1}{N} \rfloor = \lfloor \frac{i-1}{N} \rfloor \end{cases}. \tag{5.39}$$

Hence, the expression for the symbol SNR is

$$\mathbf{SNR}_{\mathrm{out}}^{\mathrm{NO}(j,i)}(N_u) = \begin{cases} \mathbf{SNR}_{\mathrm{out}}^{\mathrm{OR}}(N_u), & \text{for } \lfloor \frac{j-1}{N} \rfloor \ne \lfloor \frac{i-1}{N} \rfloor \\ \\ \mathbf{SNR}_{\mathrm{out}}^{\mathrm{MTSK}(j,i)}(N_u), & \text{for } \lfloor \frac{j-1}{N} \rfloor = \lfloor \frac{i-1}{N} \rfloor \end{cases}, \tag{5.40}$$

where $\mathbf{SNR}_{\mathrm{out}}^{\mathrm{OR}}(N_u)$ was calculated in (5.8) and

$$\mathbf{SNR}_{\mathrm{out}}^{\mathrm{MTSK}(j,i)}(N_u) \triangleq \left[\left[\frac{(A^{(1)})^2 E_s(1-\alpha_{ji})}{N_o} \right]^{-1} + \left[\frac{T_s}{T_w} \frac{T_w}{T_f} \frac{\beta_{\mathrm{MTSK}(j,i)}}{\sum_{\nu=2}^{N_u} \left(\frac{A^{(\nu)}}{A^{(1)}} \right)^2} \right]^{-1} \right]^{-1}, \tag{5.41}$$

where

$$\beta_{\mathrm{MTSK}(j,i)} \triangleq \frac{m_{\mathrm{MTSK}(j,i)}^2}{\hat{\sigma}_{\mathrm{MTSK}(j,i)}^2}$$

$$= \frac{m_w^2(\tau_J, \tau_J, \tau_I)}{\hat{\sigma}_w^2(\tau_J, \tau_I)}, \tag{5.42}$$

$$\epsilon = 2(T_w + \tau_N + (L-1)T_o), \; J = j - \lfloor \frac{j-1}{N} \rfloor N$$

was calculated by substituting (5.35) and (5.37) in (3.58). Note that (5.41) can be rewritten as in (3.60) to give

$$\mathbf{SNR}_{\text{out}}^{\text{MTSK}(j,i)}(N_u) = \frac{(A^{(1)})^2 E_s (1 - \alpha_{ji})}{N_o + N_{\text{MTSK}(j,i)}} \tag{5.43}$$

where

$$N_{\text{MTSK}(j,i)} \overset{\triangle}{=} \sum_{\nu=2}^{N_u} N_{\text{MTSK}(j,i)}^{(\nu)} \tag{5.44}$$

and

$$N_{\text{MTSK}(j,i)}^{(\nu)} \overset{\triangle}{=} (A^{(\nu)})^2 \frac{E_w}{T_f} \int_{-2(T_w+\tau_N)}^{2(T_w+\tau_N)} \frac{[\gamma_w(\varsigma - \tau_J) - \gamma_w(\varsigma - \tau_I)]^2}{[\gamma_w(\tau_J - \tau_J) - \gamma_w(\tau_J - \tau_I)]} d\varsigma \tag{5.45}$$

for $\nu = 2, 3, \ldots, N_u$.

The expression in (5.40) gives the symbol SNR values for use in the expression for bit error probability in (4.35) for N_u greater than one.

5.4 Numerical results under ideal power control

In this section we make numerical calculations of the multiple-access performance, degradation factor and capacity for the three types of signals just discussed. The

pulse shape $w(t)$ and the signal correlation $\gamma_w(\tau)$ are the same used in the example in section 4.4, and are reproduced here for convenience

$$w(t) = \left[1 - 4\pi \left[\frac{t}{t_n}\right]^2\right] \exp\left(-2\pi \left[\frac{t}{t_n}\right]^2\right) \tag{5.46}$$

and

$$\gamma_w(\tau) = \left[1 - 4\pi \left[\frac{\tau}{t_n}\right]^2 + \frac{4\pi^2}{3}\left[\frac{\tau}{t_n}\right]^4\right] \exp\left(-\pi \left[\frac{\tau}{t_n}\right]^2\right). \tag{5.47}$$

Note that, given the pulse $w(t)$, β_{OR} depends on T_{OR}, β_{EC} depends on τ_2, and, for $N = 2$, $\beta_{\mathrm{MTSK}(j,i)}$ depends on $\hat{\tau}_2^{opt}$. In general, T_{OR}, τ_2 and $\hat{\tau}_2^{opt}$ can be chosen either to maximize the corresponding β or to maximize the corresponding $\mathbf{SNR}_{\mathrm{out}}(1)$. The first situation is desirable when the multiple-access interference dominates, while the second situation is desirable when the AWGN dominates. In the present analysis the values of τ_2 and $\hat{\tau}_2^{opt}$ were chosen to maximize $\mathbf{SNR}_{\mathrm{out}}^{\mathrm{EC}}(1)$ and $\mathbf{SNR}_{\mathrm{out}}^{\mathrm{MTSK}(j,i)}(1)$, respectively. The value of $T_{\mathrm{OR}} > T_w$ does not affect directly the value of $\mathbf{SNR}_{\mathrm{out}}^{\mathrm{OR}}(1)$, and was chosen to simplify the analysis in the presence of multiple-access interference.

Table 5.1 shows the parameters necessary to calculate the three SNR values $\mathbf{SNRb}_{\mathrm{out}}^{\mathrm{OR}}(N_u)$, $\mathbf{SNRb}_{\mathrm{out}}^{\mathrm{EC}}(N_u)$ and $\mathbf{SNRb}_{\mathrm{out}}^{\mathrm{MTSK}(1,2)}(N_u)$ for three different pulse widths. Using set 1 of the parameters in table 5.1, figures 5.1 to 5.9 and 5.11 to 5.16 were calculated.

Figures 5.1, 5.2 and 5.3 show the multiple-access performance of IR for the EC PPM, OR PPM and NO PPM signal sets, respectively, using $R_b = 9.6$ Kbps for each user. These curves represent the base 10 logarithm of the probability of bit error, as a function of number of simultaneous users N_u for different values of M (with $N = 2$ for the NO PPM sets) under perfect power control conditions. The bit $\left(\frac{E_b}{N_o}\right)$ was set to 11.40 dB. This resulted in a one-user bit SNR of $\mathbf{SNRb}_{\mathrm{out}}^{\mathrm{EC}}(1) = 10.48$

dB, $\mathbf{SNRb}_{\text{out}}^{\text{OR}}(1) = 11.40$ dB, and $\mathbf{SNRb}_{\text{out}}^{\text{MTSK}(1,2)}(1) = 13.49$ dB, corresponding to a one-user bit error probability of $\text{UBP}_{\text{b}}^{\text{EC}}(1) \simeq 4.04 \times 10^{-4}$, $\text{UBP}_{\text{b}}^{\text{OR}}(1) \simeq 1.01 \times 10^{-4}$, and $\text{UBP}_{\text{b}}^{\text{NO}}(1) \simeq 1.08 \times 10^{-6}$, respectively, with $M = 2$.

Figures 5.4, 5.5 and 5.6 show the multiple-access performance of IR for the EC PPM, OR PPM and NO PPM signal sets, respectively. The curves show performance for the pairs $(R_b = 38.4 \text{ Kbps}, M = 2)$, $(R_b = 19.2 \text{ Kbps}, M = 2)$, $(R_b = 9.6 \text{ Kbps}, M = 2)$, $(R_b = 19.2 \text{ Kbps}, M = 4)$, and $(R_b = 38.4 \text{ Kbps}, M = 16)$.

Figures 5.7, 5.8 and 5.9 show the multiple-access performance of IR for the EC PPM, OR PPM and NO PPM signal sets, respectively, using $R_b = 1048$ Kbps for each user. The bit $(\frac{E_b}{N_o})$ was set to 14.30 dB. This resulted in a one-user bit SNR of $\mathbf{SNRb}_{\text{out}}^{\text{EC}}(1) = 13.39$ dB, $\mathbf{SNRb}_{\text{out}}^{\text{OR}}(1) = 14.30$ dB, and $\mathbf{SNRb}_{\text{out}}^{\text{MTSK}(1,2)}(1) = 16.40$ dB, corresponding to a one-user bit error probability of $\text{UBP}_{\text{b}}^{\text{EC}}(1) \simeq 1.9 \times 10^{-6}$, $\text{UBP}_{\text{b}}^{\text{OR}}(1) \simeq 1.0 \times 10^{-7}$, and $\text{UBP}_{\text{b}}^{\text{NO}}(1) \simeq 2.5 \times 10^{-11}$, respectively, with $M = 2$.

Figure 5.10 show the multiple-access capacity of IR $C_{\text{IR}}(N_u)$ in bits per second defined in section 3.5 for EC signals, corresponding to the sets $1, 2, 3$ of parameters in table 5.1.

Figures 5.11 and 5.12 show the number of users $N_u(\text{DF})$ as a function of the degradation factor DF for the EC PPM and OR PPM signal sets, respectively, using $R_b = 9.6$ Kbps per user. These curves represent $N_u(\text{DF})$ for different values of M under perfect power control conditions. For every value of M considered, the one-user bit SNR $\mathbf{SNRb}_{\text{out}}^{\text{EC}}(1)$ and $\mathbf{SNRb}_{\text{out}}^{\text{OR}}(1)$ were set to get a one-user bit error probability of $\text{UBP}_{\text{b}}^{\text{EC}}(1) \simeq 10^{-3}$ and $\text{UBP}_{\text{b}}^{\text{OR}}(1) \simeq 10^{-3}$, respectively.

Figure 5.13 shows $N_u(\text{DF})$ for the OR PPM signal set, using $R_b = 9.6$ Kbps per user. The curves are calculated for the pairs $(M = 8, P_e = 10^{-5})$, $(M = 4, P_e =$

10^{-4}), ($M = 2, P_e = 10^{-3}$), ($M = 2, P_e = 10^{-4}$) and ($M = 2, P_e = 10^{-5}$) with $P_e = \mathrm{UBP}_{\mathrm{b}}^{\mathrm{OR}}(1)$.

Figure 5.14 shows $N_u(\mathrm{DF})$ for the EC PPM signal set, using $R_b = 9.6$ Kbps per user. The curves are calculated using $2 \leq M \leq 1024$ with $\mathrm{UBP}_{\mathrm{b}}^{\mathrm{EC}}(1) \simeq 10^{-3}$. Also shown is the value of $N_u(\mathrm{DF}) \to N_{\mathrm{IR}}$ for large values of both DF and M.

Figures 5.15 and 5.16 shows $N_U(\mathrm{DF})$ for the EC PPM and OR PPM signal sets, respectively, using $R_b = 1048$ Kbps per user. These curves represent $N_u(\mathrm{DF})$ for different values of M under perfect power control conditions. For every value of M considered, the one-user bit SNR $\mathbf{SNRb}_{\mathrm{out}}^{\mathrm{EC}}(1)$ and $\mathbf{SNRb}_{\mathrm{out}}^{\mathrm{OR}}(1)$ were set to get a one-user bit error probability of $\mathrm{UBP}_{\mathrm{b}}^{\mathrm{EC}}(1) \simeq 1E - 7$ and $\mathrm{UBP}_{\mathrm{b}}^{\mathrm{OR}}(1) \simeq 1E - 7$, respectively.

5.5   Discussion of results

From figures 5.1, 5.2 and 5.3, the benefits of using block waveform modulation are evident. By using higher values of M other than 2, it is possible either to increase the number of users for a fixed probability of error, or to improve the probability of detection for a fixed number of users N_u, without increasing each user's signal power. It can be seen that the benefit in going from one value of M to the next value actually decreases as M increases, a behavior similar to the performance of block waveforms in AWGN. It is also clear that NO PPM ranks first, OR PPM ranks second, and EC PPM ranks third in terms of multiple-access performance. This is to be expected because NO PPM ranks first, OR PPM ranks second, and EC PPM ranks third in terms of "good" correlation properties. This behavior is similar to the performance of block waveforms in AWGN.

set 1 of parameters	set 2 of parameters	set 3 of parameters
$t_n = 0.2877$ ns	$t_n = 0.4472$ ns	$t_n = 0.7531$ ns
$T_w = 0.75$ ns	$T_w = 1.2$ ns	$T_w = 2.0$ ns
$\tau_{\min} = 0.1556$ ns	$\tau_{\min} = 0.2419$ ns	$\tau_{\min} = 0.4073$ ns
$\hat{\sigma}^2_{\mathrm{EC}} = 0.000121$	$\hat{\sigma}^2_{\mathrm{EC}} = 0.000454$	$\hat{\sigma}^2_{\mathrm{EC}} = 0.002167$
$m^2_{\mathrm{EC}} = 0.0305$	$m^2_{\mathrm{EC}} = 0.0737$	$m^2_{\mathrm{EC}} = 0.2089$
$\beta_{\mathrm{EC}} = 253.42$	$\beta_{\mathrm{EC}} = 162.28$	$\beta_{\mathrm{EC}} = 96.37$
$\hat{\sigma}^2_{\mathrm{OR}} = 0.000035$	$\hat{\sigma}^2_{\mathrm{OR}} = 0.000130$	$\hat{\sigma}^2_{\mathrm{OR}} = 0.000619$
$m^2_{\mathrm{OR}} = 0.0116$	$m^2_{\mathrm{OR}} = 0.0281$	$m^2_{\mathrm{OR}} = 0.0798$
$\beta_{\mathrm{OR}} = 337.04$	$\beta_{\mathrm{OR}} = 216.83$	$\beta_{\mathrm{OR}} = 128.87$
$\hat{\sigma}^2_{\mathrm{MTSK(1,2)}} = 0.000060$	$\hat{\sigma}^2_{\mathrm{MTSK(1,2)}} = 0.000227$	$\hat{\sigma}^2_{\mathrm{MTSK(1,2)}} = 0.001084$
$m^2_{\mathrm{MTSK(1,2)}} = 0.0305$	$m^2_{\mathrm{MTSK(1,2)}} = 0.0737$	$m^2_{\mathrm{MTSK(1,2)}} = 0.2089$
$\beta_{\mathrm{MTSK(1,2)}} = 504.54$	$\beta_{\mathrm{MTSK(1,2)}} = 324.57$	$\beta_{\mathrm{MTSK(1,2)}} = 192.72$
$C_{\mathrm{TOT}} = 3.3964$ Gigabits	$C_{\mathrm{TOT}} = 2.3412$ Gigabits	$C_{\mathrm{TOT}} = 1.3903$ Gigabits

Table 5.1: Parameters calculated using $\tau_2 = \tau_{\min}$, $T_{\mathrm{OR}} = 2T_w$, $\hat{\tau}_1^{\mathrm{opt}} = 0$, $\hat{\tau}_2^{\mathrm{opt}} = \tau_{\min}$ and $T_f = 100$ ns.

The values of M used in figures 5.1, 5.2 and 5.3 are consistent with the assumption (2.28) in (e) and the assumption $\tilde{\sigma}_{k,l,j,i} \simeq 0$, which impose a limit on the size of M for both OR PPM and NO PPM signals. For the EC PPM signals there is no restriction on how far M can go.[3] These curves show that, under relatively ideal conditions, IR modulation with block waveform PPM signals using moderated values of M is potentially able to support thousands of users, each transmitting at a rate about ten Kbps at bit error rates of 10^{-4}.

From figures 5.4, 5.5 and 5.6 we see another advantage in using $M > 2$. We observe that for a fixed N_u, the multiple-access performance degrades as R_b is increased for $M = 2$ fixed. Also, we observe that for fixed N_u, the multiple-access performance can be maintained or even increased as R_b is increased when $M > 2$ is used. In both cases the $\mathbf{SNRb}_{\mathrm{out}}(N_u)$ is kept constant as R_b changes.

Figures 5.7, 5.8 and 5.9 repeats the calculation shown in figures 5.1, 5.2 and 5.3, but now using a high bit data rate and lower bit error probability. Theses curves show that, under relatively ideal conditions, IR modulation with block waveform PPM signals using moderate M is potentially able to support hundreds of users, each transmitting at a rate over a Megabit per second, with error rates as low as 10^{-8}.

In both low data rate (figures 5.1, 5.2 and 5.3) and high data rate (figures 5.7, 5.8 and 5.9) cases, the combined transmission rates give a transmission capacity of over 500 Megabits per second using receivers of moderate complexity.

From figure 5.10 it is clear that the multiple-access capacity per user of IR in bps $C_{\mathrm{IR}}(N_u) = 3.3964$ Gigabits using set 1 is higher than $C_{\mathrm{IR}}(N_u) = 2.3412$ Gigabits

---

[3]Of course, there are other factors such as decoding delay, minimum symbol SNR for acquisition and tracking, and increased sensitivity to mismatched system parameters, that will eventually limit the maximum value of M to be used in practice.

using set 2, which in turn is higher than $C_{\text{IR}}(N_u) = 1.3903$ Gigabits using the set 3 of parameters in table 5.1. Similarly, from table 5.1 we see that the total multiple-access capacity of IR in bps C_{TOT} using set 1 is higher than C_{TOT} using set 2, which in turn is higher than C_{TOT} using the set 3 of parameters. This is to be expected since the set 1 corresponds to "more impulsive" signals, which means that the TH PPM signals corresponding to different users are less likely to suffer collisions among them. Another point of view is that a narrower pulse implies more spreading gain in the frequency domain.

Figures 5.11 and 5.12 show how by using higher values of M other than 2, it is possible to increase the number of users N_u as a function of additional amount of SNR required (i.e., degradation factor DF), for a fixed probability of bit error. Figure 5.13 shows the same effect when the probability of error is decreased. Again, it can be seen that the benefit in going from one value of M to the next value actually decreases as M increases. This is more evident in figure 5.14, where the number of users $N_u(\text{DF})$ is shown to reach a maximum N_{IR} no matter how large both DF and M become.

Figures 5.15 and 5.16 repeat the calculation shown in figures 5.11 and 5.12, but now using a high data bit rate and lower bit error probability.

It can be observed that, for a fixed $\textbf{SNRb}_{\text{out}}(1)$ and R_b, the $N_u(\text{DF})$ curves have a threshold effect, i.e, the number of users grows significantly only in specific regions defined by DF. This threshold effect is also observed when M is varied.

All these curves provides valuable guidelines to design a system in applications that require low R_b and moderate bit error rate, as well as applications in which high values of R_b and low values of bit error rate are required. In both applications, it is convenient to choose system parameters values in those regions where the number of

users grows rapidly as additional SNR is provided, as well as in those regions where the multiple-access performance suffer gradual degradation as the number of users is increased.
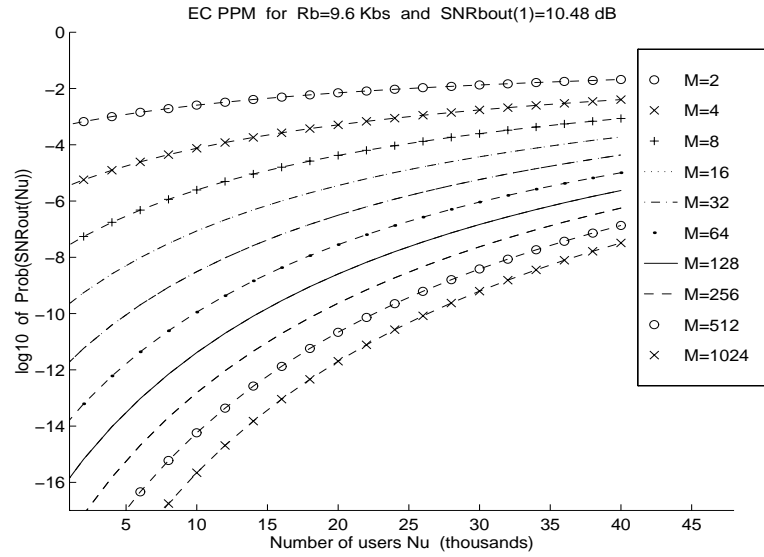

Figure 5.1: The base 10 logarithm of the probability of bit error for EC PPM signals, as a function of the number of simultaneous users N_u for different values of M, using $R_b = 9.6$ Kbps, $\mathbf{SNRb}_{\text{out}}^{\text{EC}}(1) = 10.48$ dB and set 1 of parameters in table 5.1.
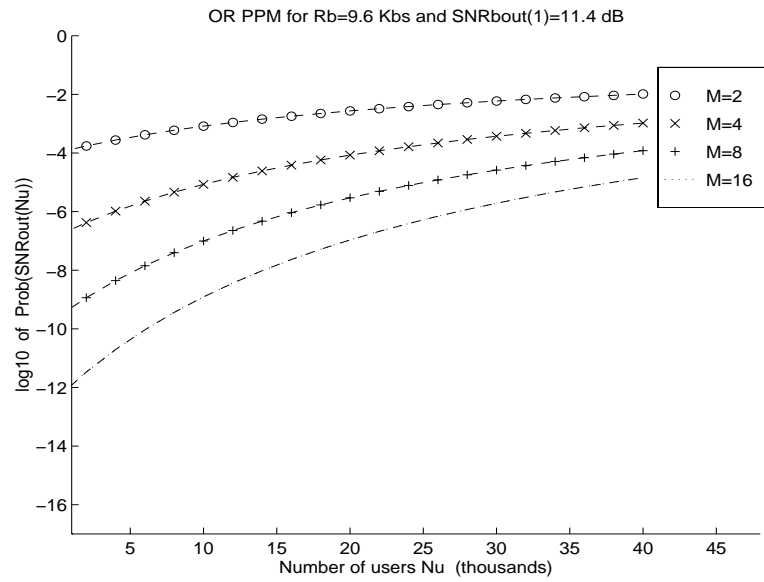
OR PPM for Rb=9.6 Kbs and SNRbout(1)=11.4 dB

Figure 5.2: The base 10 logarithm of the probability of bit error for OR PPM signals, as a function of N_u for different values of M, using $R_b = 9.6$ Kbps, $\mathbf{SNRb}_{\mathrm{out}}^{\mathrm{OR}}(1) = 11.40$ dB and set 1 of parameters in table 5.1.
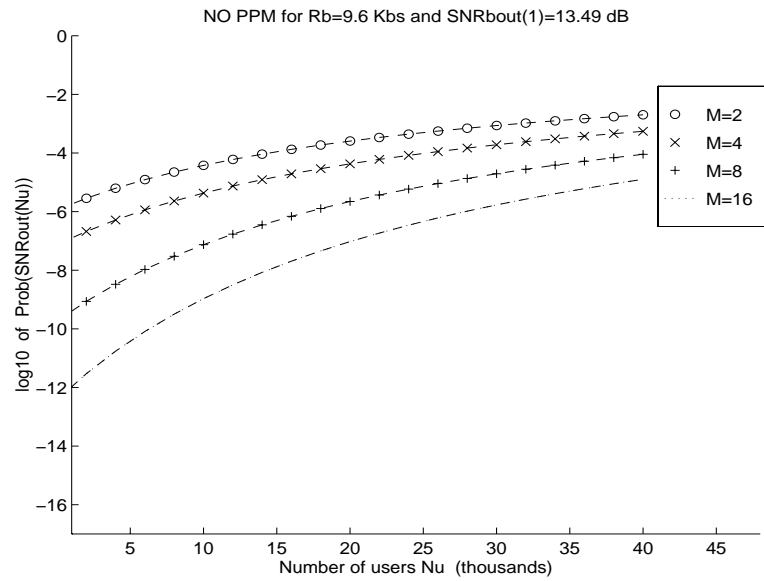
Figure 5.3: The base 10 logarithm of the probability of bit error for NO PPM signals, as a function of N_u for different values of M, using $R_b = 9.6$ Kbps, $\mathbf{SNRb}_{\text{out}}^{\text{MTSK}(1,2)}(1) = 13.49$ dB, $\mathbf{SNRb}_{\text{out}}^{\text{OR}}(1) = 11.40$ dB and set 1 of parameters in table 5.1.

EC PPM for SNRbout(1)=10.48 dB
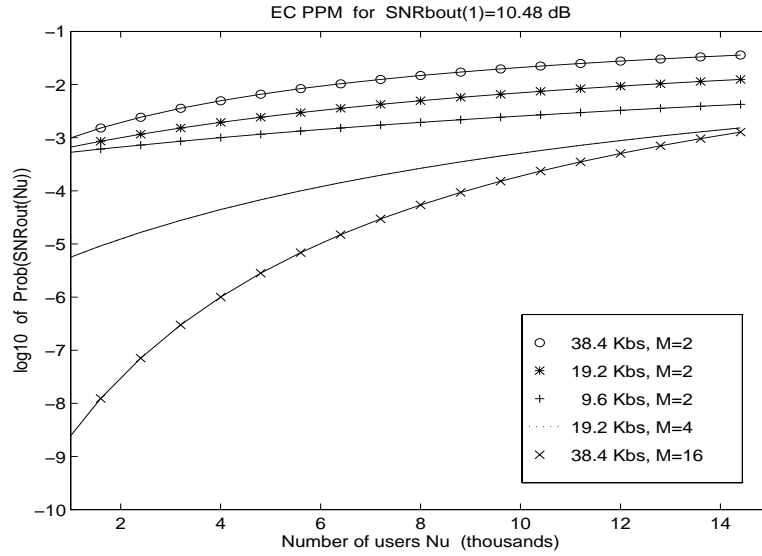
Figure 5.4: The base 10 logarithm of the probability of bit error for EC PPM signals, as a function of N_u for different pairs (R_b, M), using $\mathbf{SNRb}_{\mathrm{out}}^{\mathrm{EC}}(1) = 10.48$ dB and set 1 of parameters in table 5.1.

OR PPM for SNRbout(1)=11.4 dB

Figure 5.5: The base 10 logarithm of the probability of bit error for OR PPM signals, as a function of N_u for different pairs (R_b, M), using $\mathbf{SNRb}_{\mathrm{out}}^{\mathrm{OR}}(1) = 11.40$ dB and set 1 of parameters in table 5.1.

NO PPM for SNRbout(1)=13.49 dB

Figure 5.6: The base 10 logarithm of the probability of bit error for NO PPM signals, as a function of N_u for different pairs (R_b, M), using the value of $\mathbf{SNRb}_{\text{out}}^{\text{MTSK}(1,2)}(1) = 13.49$ dB, $\mathbf{SNRb}_{\text{out}}^{\text{OR}}(1) = 10.40$ dB and set 1 of parameters in table 5.1.
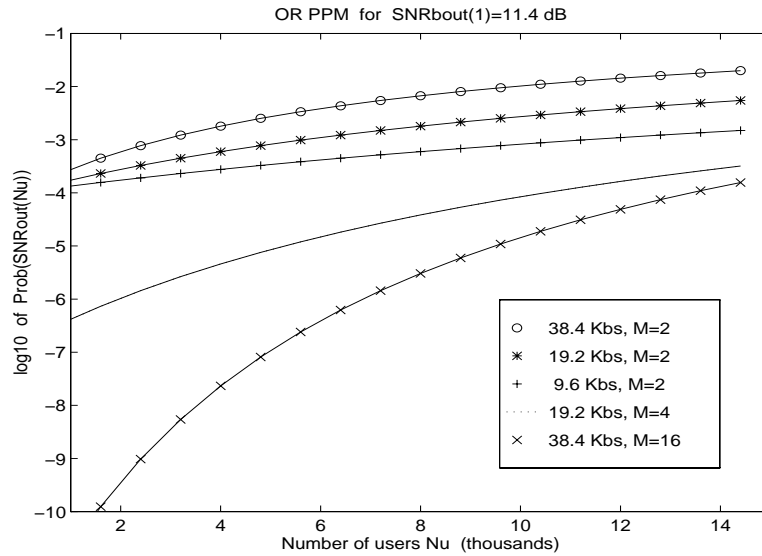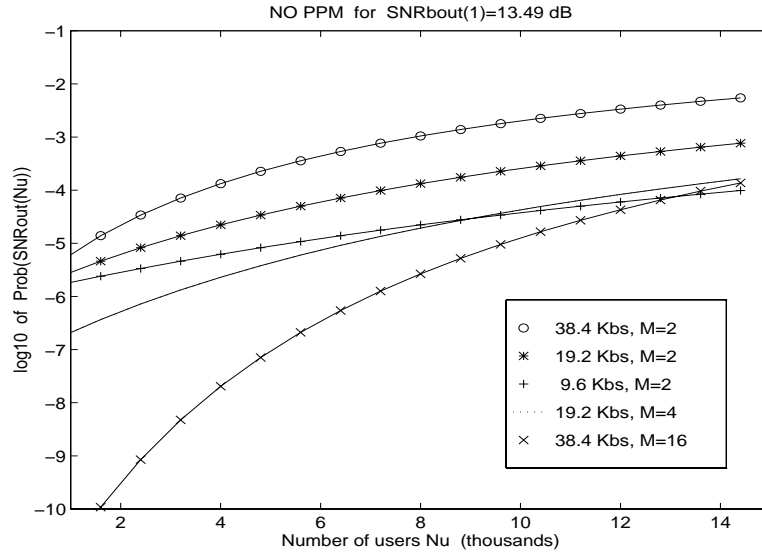

EC PPM for Rb=1048 Kbs and SNRbout(1)=13.39 dB

Figure 5.7: The base 10 logarithm of the probability of bit error for EC PPM signals, as a function of the number of simultaneous users N_u for different values of M, using $R_b = 1048$ Kbps, $\mathbf{SNRb}_{\text{out}}^{\text{EC}}(1) = 13.39$ dB and set 1 of parameters in table 5.1.
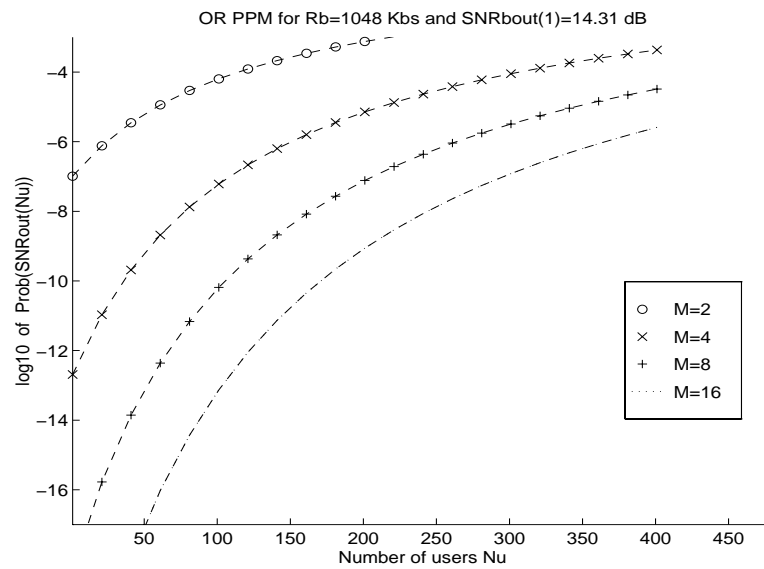
Figure 5.8: The base 10 logarithm of the probability of bit error for OR PPM signals, as a function of N_u for different values of M, using $R_b = 1048$ Kbps, $\mathbf{SNRb}_{\mathrm{out}}^{\mathrm{OR}}(1) = 14.30$ dB and set 1 of parameters in table 5.1.
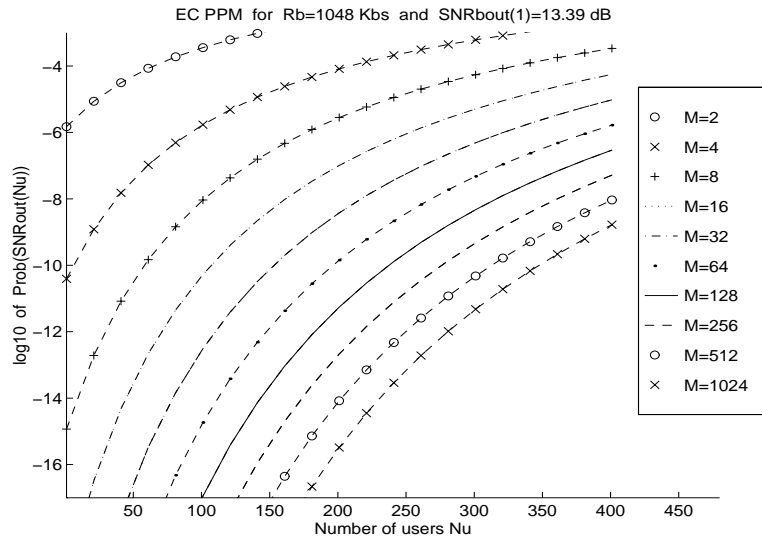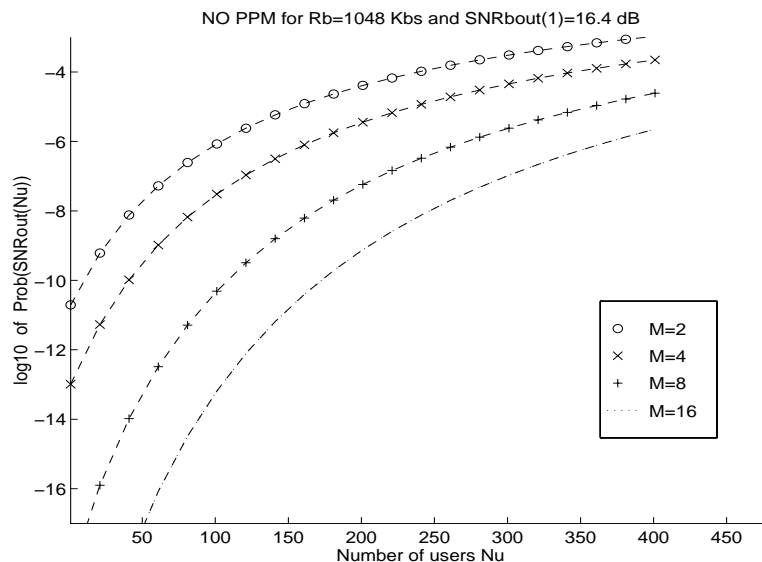
Figure 5.9: The base 10 logarithm of the probability of bit error for NO PPM signals, as a function of N_u for different values of M, using $R_b = 1048$ Kbps, $\mathbf{SNRb}_{\mathrm{out}}^{\mathrm{MTSK}(1,2)}(1) = 16.40$ dB, $\mathbf{SNRb}_{\mathrm{out}}^{\mathrm{OR}}(1) = 14.30$ dB and set 1 of parameters in table 5.1.
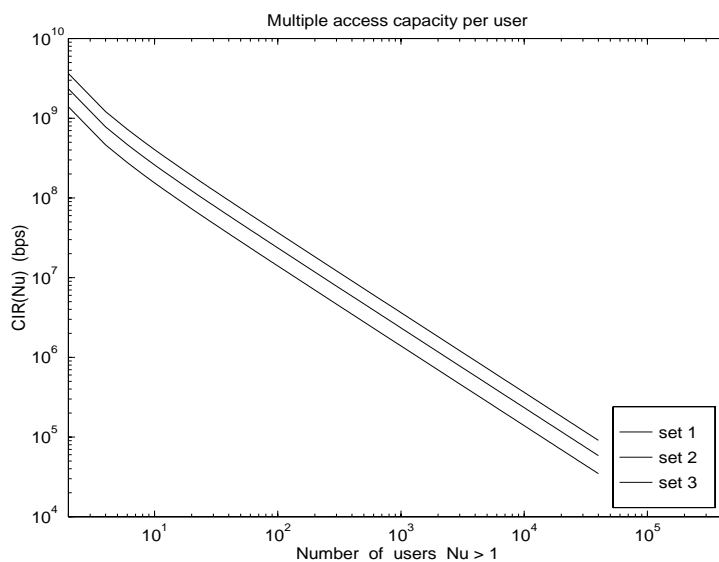
Figure 5.10: The multiple-access capacity per user $C_{\mathrm{IR}}(N_u)$ in bps as a function of N_u, calculated using the sets $1, 2, 3$ of parameters in table 5.1.
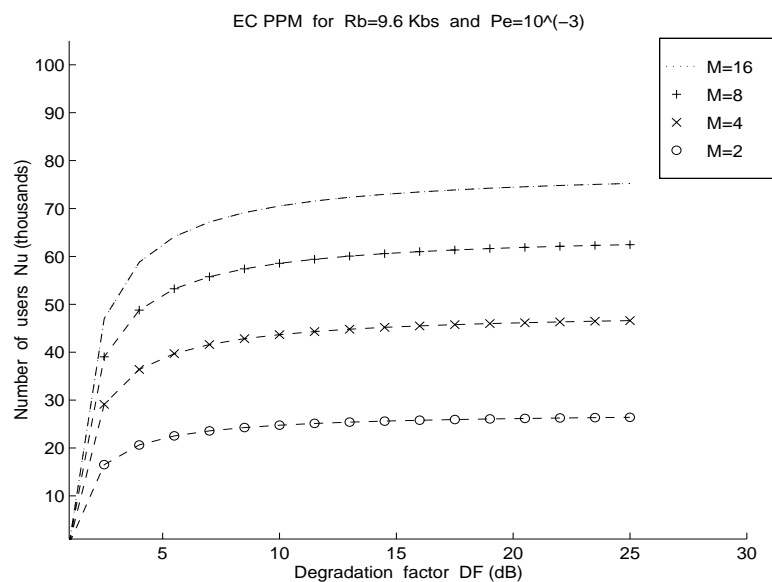
Figure 5.11: The number of users $N_u(\mathrm{DF})$ as a function of the degradation factor DF for EC PPM signals, calculated for different values of M under perfect power control conditions using $R_b = 9.6$ Kbps, $P_e = \mathrm{UBP}_{\mathrm{b}}^{\mathrm{EC}}(1) \simeq 10^{-3}$ and set 1 of parameters in table 5.1.

Figure 5.12: The number of users $N_u(\mathrm{DF})$ for OR PPM signals, calculated for different values of M under perfect power control conditions using $R_b = 9.6$ Kbps, $P_e = \mathrm{UBP}_{\mathrm{b}}^{\mathrm{OR}}(1) \simeq 10^{-3}$ and set 1 of parameters in table 5.1.
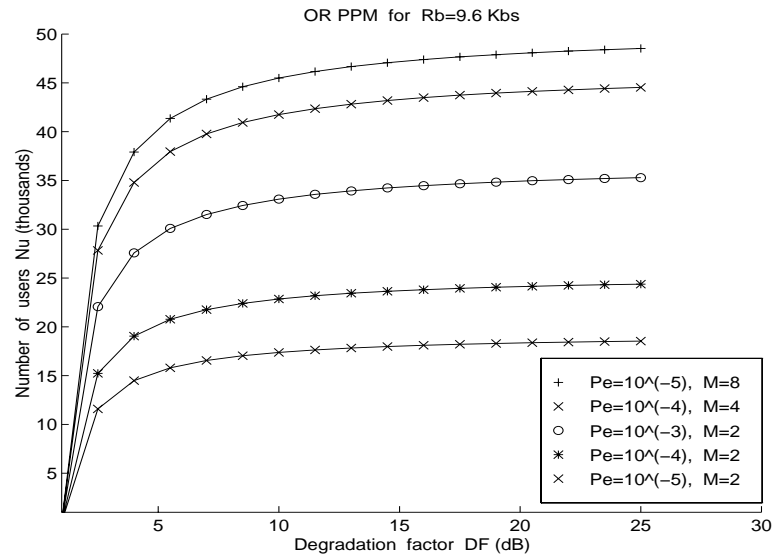
Figure 5.13: The number of users $N_u(\mathrm{DF})$ for OR PPM signals calculated for different pairs (M, P_e), with $P_e = \mathrm{UBP}_{\mathrm{b}}^{\mathrm{OR}}(1)$. The curves were calculated using $R_b = 9.6$ Kbps and set 1 of parameters in table 5.1.
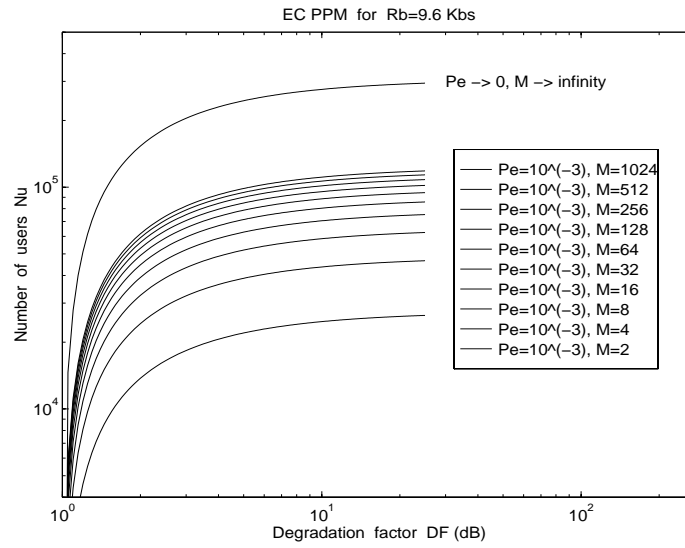
Figure 5.14: The number of users $N_u(\mathrm{DF})$ for EC PPM signals, calculated using $2 \le M \le 1024$ with $P_e = \mathrm{UBP}_{\mathrm{b}}^{\mathrm{EC}}(1) \simeq 10^{-3}$. Also shown is the value of $N_u(\mathrm{DF}) \rightarrow N_{\mathrm{IR}}$ for large values of both DF and M. The curves were calculated using $R_b = 9.6$ Kbps and set 1 of parameters in table 5.1.
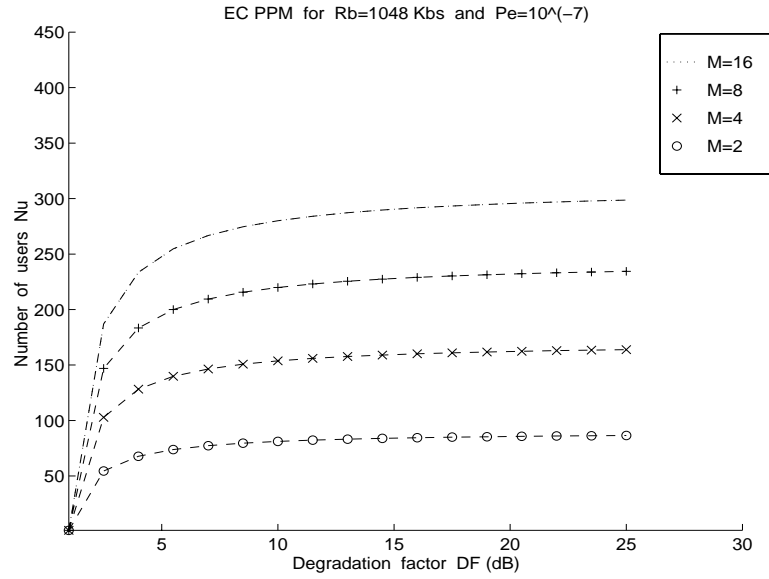
Figure 5.15: The number of users $N_u(\mathrm{DF})$ for EC PPM signals, calculated for different values of M under perfect power control conditions using $R_b = 1048$ Kbps, $\mathrm{UBP}_{\mathrm{b}}^{\mathrm{EC}}(1) \simeq 10^{-7}$ and set 1 of parameters in table 5.1.
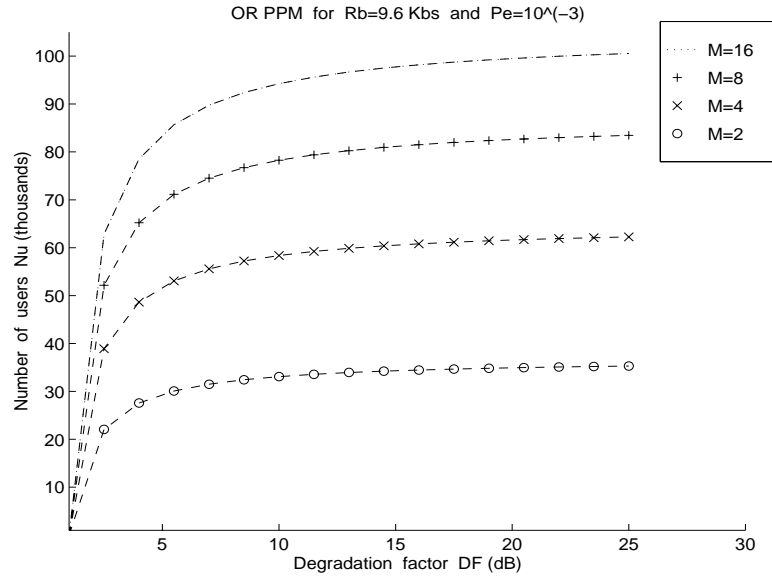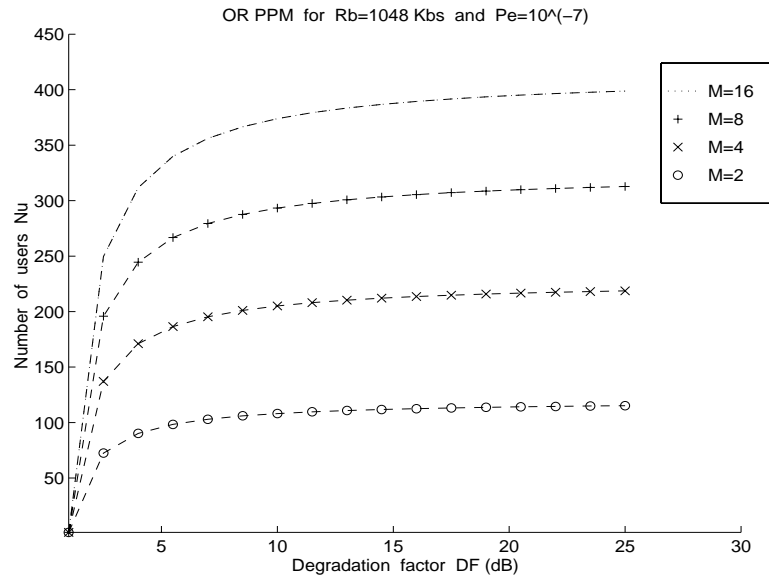

Figure 5.16: The number of users $N_u(\mathrm{DF})$ for OR PPM signals, calculated for different values of M under perfect power control conditions using $R_b = 1048$ Kbps, $\mathrm{UBP}_{\mathrm{b}}^{\mathrm{OR}}(1) \simeq 10^{-7}$ and set 1 of parameters in table 5.1.

Chapter 6

Performance of IR in the presence of dense multipath

In this chapter we make an assessment of the performance of non-binary IR modulation in an indoor multipath environment with detection using a Rake receiver. For a particular set of $M = 4$ signals and symbol error probability of 10^{-3}, the performance in the presence of multipath using a mismatched Rake receiver with $K = 10$ fingers is shown to be, on average, just 3 dB worse than performance in the absence of multipath using a correlation receiver.

6.1 Channel and signal models

6.1.1 Channel models

In this analysis we consider two types of channels. (1) IR-AWGN: Wireless IR channel with free space propagation conditions and AWGN. This model was described in section 2.1. (2) IR-MP: Wireless indoor IR multipath channel. In this model the transmitted signal is $\sqrt{E_s} w_{tx}(t)$ and the received signal is $\sqrt{E_a} \tilde{w}(u, t) + n(t)$. The pulse $\sqrt{E_a} \tilde{w}(u, t)$ is a time spreaded version of $\sqrt{E_s} w(t)$, with duration $T_m >> T_w$

and average energy E_a. The u indexes an event taking place in the sample space of a certain random experiment. The random experiment is a measurement experiment performed in an office building where $\tilde{w}(u,t)|_{u=u_o=(R_o, I_o, J_o)}$ denotes the IR-MP channel pulse response measured in the absence of noise at position (I_o, J_o) inside room R_o. For performance analysis purpose, it will be assumed that the IR-MP channel can be characterized by the ensemble of pulses responses

$$\{\tilde{w}(u_o, t)\}, \; u_o = 1, 2, \ldots, u_*. \tag{6.1}$$

6.1.2 Signal models

In the present analysis we assume one user and perfect synchronization. Under these circumstances, the spread spectrum time-hopping sequence modulation has no effect on the correlation properties of the communication signals, and will be omitted in the expressions defining the signals and their correlation values. Analysis is further simplified by noting that the set of communication signals, each one consisting of a train of N_s time-shifted subnanosecond pulses of the form

$$\sum_{k=0}^{N_s-1} \sqrt{E_s} w(t - \tau_j - kT_f), \quad j = 1, 2, \ldots, M, \tag{6.2}$$

and the set of time-shift-keyed (TSK) communication signals

$$\sqrt{E_s} w(t - \tau_j), \quad j = 1, 2, \ldots, M, \tag{6.3}$$

both have the same set of normalized correlation matrix Λ_{TSK} for

$$\tau_1 = 0, \; \tau_1 \; < \; \tau_2 \; \leq \; T_w, \; \ldots, \; \tau_{M-1} \; < \; \tau_M \; \leq \; (M-1)T_w \; < \; T_f \tag{6.4}$$

where T_f is the frame period of the pulse train in (6.2). The energy in a signal in (6.2) is N_s times the energy in a signal in (6.3). We will assume that the same statement is true for communication signals used in the IR-MP channel, i.e., the set of communication signals

$$\sum_{k=0}^{N_s-1} \sqrt{E_a}\tilde{w}(u, t - \tau_j - kT_f), \quad j = 1, 2, \ldots, M, \tag{6.5}$$

and the set of communication signals

$$\sqrt{E_a}\tilde{w}(u, t - \tau_j), \quad j = 1, 2, \ldots, M, \tag{6.6}$$

both have the same set of normalized correlation matrix $\tilde{\Lambda}_{\mathrm{TSK}}(u)$ for the time shifts in (6.4) and $\tau_M + T_m < T_f$. The average energy in a signal in (6.5) is N_s times the average energy in a signal in (6.6).

6.2 Receiver signal processing and performance in a multipath channel

6.2.1 Receiver signal processing

In the IR-AWGN model, the impulse response of the channel is (slowly) time-invariant and deterministic. When the communication signal $\sqrt{E_s}w_{tx}(t - \tau_j)$ is transmitted, the received signal consists of the signal $\sqrt{E_s}w(t - \tau_j)$ plus AWGN. Therefore, the detection problem becomes the coherent detection of M signals in the presence of Gaussian noise, and the optimum receiver is the correlation receiver (CRcvr), i.e, a bank of filters matched to the M signals used to convey information.

In the IR-MP model, the impulse response of the channel is time-variant and random. When the signal $\sqrt{E_s}w_{tx}(t - \tau_j)$ is transmitted, the received signal consists

of the communication signal $\sqrt{E_a}\tilde{w}(u, t - \tau_j)$ (modified by the channel in some random form) plus AWGN. In order to be able to derive the optimum receiver, a precise statistical characterization of the channel is required. Mathematical models of real-world channels are usually derived making not quite realistic assumptions in order to make the model analytically tractable. In this sense, the optimum receiver derived using those channel models is not optimum for the real-world channel. This is specially true for UWB signal propagation, where the UWB signals suffer frequency distortions as they propagate through walls and other obstacles. A different approach that bypasses this modeling problem and permits performance characterization of a realizable receiver is explained here.

Conditioned on the random event $u = u_o$, the impulse response of the channel is time-invariant and deterministic. In this case the received signal consists of the communication signal $\sqrt{E_a}\tilde{w}(u_o, t - \tau_j)$ plus AWGN (of course, for different u_o, the sets of received signals are different). For every $u = u_o$, the theory of the CRcvr can be applied, i.e, the *optimum* receiver is a bank of filters matched to the M signals $\sqrt{E_a}\tilde{w}(u_o, t - \tau_j)$, $j = 1, 2, \ldots, M$. The problem is that this receiver must be able to match the random variations in the received signal for every $u = u_o$. With this motivation, we introduce the *perfect* Rake (PRake) receiver, a super Rake receiver that has an unlimited number of correlation resources and is able to construct a reference signal $\sqrt{E_a}\tilde{w}(u_o, -(t - \tau_j))$ that is perfectly matched to the signal received $\sqrt{E_a}\tilde{w}(u_o, t - \tau_j)$ over the multipath channel. For every $u = u_o$, performance analysis using the PRake receiver can be calculated, and the average performance can be obtained by averaging over all values of u.

The PRake receiver provides the best performance attainable. But the PRake receiver is difficult (if not impossible) to build. We only can build a simpler *sub-optimum* but viable receiver to demodulate the signals. With this motivation, we

introduce the *mismatched Rake* (MRake) receiver, a receiver analogous to the conventional Rake receiver [5] that has a limited number K of correlators or *fingers* and is able to construct a reference signal $\sqrt{E_a^{(K)}}\tilde{w}^{(K)}(u_o, -(t - \tau_j))$ that is only a mismatched version of the signal $\sqrt{E_a}\tilde{w}(u_o, t - \tau_j)$ received over the multipath channel. The part of the received signal that is not matched in the MRake receiver, denoted $\sqrt{E_a^{(K)}}\tilde{w}_c^{(K)}(u_o, t - \tau_j)$, will act as some form of interference that must be taken into account, especially for small values of K. Again, for every $u = u_o$, the theory of the CRcvr can be applied, and performance analysis using the MRake receiver can be calculated. The average performance can be obtained by averaging over all values of u.

To make this idea work, we need a good representation for all possible received signals $\sqrt{E_a}\tilde{w}(u_o, t - \tau_j)$. One way to get a very accurate representation is to use a pool of noise-free measured signal responses of the channel under study (Of course, these signals must be the actual signals used for communications over the multipath channel). As the size of this pool gets larger and larger, the performance curves will be more representative of the performance attainable in that particular channel. These ideas are explained more in detail in the following sections.

6.2.2 Receiver reference signals

Assume $\sqrt{E_s}w_{tx}(t - \tau_j)$ is transmitted over the IR channel in the absence of noise. The signals received in the IR-AWGN and IR-MP channels are $\sqrt{E_s}w(t - \tau_j)$ and

$\sqrt{E_a}\tilde{w}(u, t - \tau_j)$, respectively. The reference signals used by the receiver in the demodulation process are

$$\sqrt{E_s}w\big(-(t - \tau_j)\big) \qquad \text{(IR-AWGN CRcvr)},$$

$$\sqrt{E_a}\tilde{w}\big(u, -(t - \tau_j)\big) \qquad \text{(IR-MP PRake)}, \qquad (6.7)$$

$$\sqrt{E_a^{(K)}}\tilde{w}^{(K)}\big(u, -(t - \tau_j)\big) \quad \text{(IR-MP MRake)},$$

where $\sqrt{E_a^{(K)}}\tilde{w}^{(K)}(u, t - \tau_j)$ is the "K-paths mismatched version" of $\sqrt{E_a}\tilde{w}(u, t - \tau_j)$ given by

$$\sqrt{E_a^{(K)}}\tilde{w}^{(K)}(u, t - \tau_j) \quad \triangleq \quad \sum_{k=1}^{K} a_k(u)\, w(t - \tau_k(u)). \qquad (6.8)$$

The values of $\{a_k(u)\}$ and $\{\tau_k(u)\}$ are calculated finding the K strongest peaks in the envelope of the filtered signal $\tilde{w}(u, t) * w(-t)/\sqrt{E_w}$, where $*$ denotes the convolution operation. The signal

$$\sqrt{E_a^{(K)}}\tilde{w}_c^{(K)}(u, t - \tau_j) \quad \triangleq \quad \sqrt{E_a}\tilde{w}(u, t - \tau_j) - \sqrt{E_a^{(K)}}\tilde{w}^{(K)}(u, t - \tau_j), \qquad (6.9)$$

is the "complement" of $\sqrt{E_a^{(K)}}\tilde{w}^{(K)}(u, t - \tau_j)$, i.e., the part of $\sqrt{E_a}\tilde{w}(u, t - \tau_j)$ that is not matched by the MRake receiver. In the following lines we will describe the correlation properties of these reference signals.

6.2.2.1 The CRcvr reference signals

The correlation function of $\sqrt{E_s}w(t)$ is

$$R(\tau) \quad \triangleq \quad \int_{-\infty}^{\infty} \sqrt{E_s}w(t)\, \sqrt{E_s}w(t - \tau)\, dt. \qquad (6.10)$$

The normalized signal correlation function is defined by

$$\gamma_w(\tau) \triangleq \frac{R(\tau)}{R(0)}. \tag{6.11}$$

The energy of the signal $\sqrt{E_s}w(t)$ is

$$E_{\overline{w}} = R(0) = E_s. \tag{6.12}$$

The normalized correlation value between $\sqrt{E_s}w(t - \tau_i)$ and $\sqrt{E_s}w(t - \tau_j)$ is given by

$$\alpha_{ij} \triangleq \gamma_w(\tau_i - \tau_j). \tag{6.13}$$

The correlation matrix containing the α_{ij} values is denoted Λ_{TSK}.

6.2.2.2 The PRake reference signals

The correlation function of $\sqrt{E_a}\tilde{w}(u, t)$ is

$$\begin{aligned}
R_{\mathrm{MP}}(u, \tau) &\triangleq \int_{-\infty}^{\infty} \sqrt{E_a}\tilde{w}(u, t)\sqrt{E_a}\tilde{w}(u, t - \tau)\, dt \\
&\triangleq E_a\, r_{\mathrm{MP}}(u, \tau).
\end{aligned} \tag{6.14}$$

The normalized signal correlation function is defined by

$$\gamma_{\mathrm{MP}}(u, \tau) \triangleq \frac{R_{\mathrm{MP}}(u, \tau)}{R_{\mathrm{MP}}(u, 0)}. \tag{6.15}$$

The energy of the signal $\sqrt{E_a}\tilde{w}(u, t)$ is

$$E_{\tilde{w}}(u) = R_{\mathrm{MP}}(u, 0) = E_a\, r_{\mathrm{MP}}(u, 0), \tag{6.16}$$

where $r_{\mathrm{MP}}(u, 0)$ is the *"IR-MP channel multipath gain"*.

The normalized correlation value between $\sqrt{E_a}\tilde{w}(u, t - \tau_i)$ and $\sqrt{E_a}\tilde{w}(u, t - \tau_j)$ is given by

$$\tilde{\alpha}_{ij}(u) \triangleq \gamma_{\mathrm{MP}}(u, \tau_i - \tau_j). \tag{6.17}$$

The correlation matrix containing the $\tilde{\alpha}_{ij}(u)$ values is denoted $\tilde{\Lambda}_{\mathrm{TSK}}(u)$.

6.2.2.3   The MRake reference signals

The correlation function of $\sqrt{E_a^{(K)}}\tilde{w}^{(K)}(u, t)$ is

$$
\begin{aligned}
R_{\mathrm{MP}}^{(K)}(u, \tau) &\triangleq \int_{-\infty}^{\infty} \sqrt{E_a^{(K)}}\tilde{w}^{(K)}(u, t) \sqrt{E_a^{(K)}}\tilde{w}^{(K)}(u, t - \tau)\, dt \\
&\triangleq E_a^{(K)}\, r_{\mathrm{MP}}^{(K)}(u, \tau).
\end{aligned} \tag{6.18}
$$

The normalized signal correlation function is defined by

$$\gamma_{\mathrm{MP}}^{(K)}(u, \tau) \triangleq \frac{R_{\mathrm{MP}}^{(K)}(u, \tau)}{R_{\mathrm{MP}}^{(K)}(u, 0)}. \tag{6.19}$$

The energy of the signal $\sqrt{E_a^{(K)}}\tilde{w}^{(K)}(u, t)$ is

$$E_{\tilde{w}}^{(K)}(u) = R_{\mathrm{MP}}^{(K)}(u, 0) = E_a^{(K)}\, r_{\mathrm{MP}}^{(K)}(u, 0), \tag{6.20}$$

where $r_{\mathrm{MP}}^{(K)}(u, 0)$ is the *"K-mismatched IR-MP channel multipath gain"*.

The normalized correlation value between $\sqrt{E_a^{(K)}}\tilde{w}^{(K)}(u, t - \tau_i)$ and $\sqrt{E_a^{(K)}}\tilde{w}^{(K)}(u, t - \tau_j)$ is given by

$$\tilde{\alpha}_{ij}^{(K)}(u) \triangleq \gamma_{\mathrm{MP}}^{(K)}(u, \tau_i - \tau_j). \tag{6.21}$$

The correlation matrix containing the $\tilde{\alpha}_{ij}^{(K)}(u)$ values is denoted $\tilde{\Lambda}_{\mathrm{TSK}}^{(K)}(u)$. The signal cross correlation function between $\sqrt{E_a^{(K)}}\tilde{w}^{(K)}(u, t)$ and $\sqrt{E_a^{(K)}}\tilde{w}_c^{(K)}(u, t)$ is defined by

$$C_{\mathrm{MP}}^{(K)}(u, \tau) \triangleq \int_{-\infty}^{\infty} \sqrt{E_a^{(K)}}\tilde{w}_c^{(K)}(u, t) \sqrt{E_a^{(K)}}\tilde{w}^{(K)}(u, t - \tau)\, dt$$

$$\overset{\triangle}{=} \quad E_a^{(K)} \, c_{\mathrm{MP}}^{(K)}(u, \tau). \tag{6.22}$$

6.2.3 Receiver Performance

The union bound on the symbol error probability in coherent detection using a CRcvr is given by

$$\mathrm{UBP}_e = \frac{1}{M} {\sum_{i=1}^{M}}_{i \neq j} \sum_{j=1}^{M} \, Q\left(\sqrt{\frac{m_y^2(i|j)}{\sigma_y^2(i,j)}}\right) \tag{6.23}$$

where $\left(\frac{m_y^2(i|j)}{\sigma_y^2(i,j)}\right)$ is the SNR value involved in the decision between the pair of signals (i,j), and

$$m_y(i|j) \quad = \quad E_s\left[1 - \alpha_{ij}\right] \tag{6.24}$$

and

$$\sigma_y^2(i,j) \quad = \quad N_o E_s\left[1 - \alpha_{ij}\right] \tag{6.25}$$

are the mean and variance of the Gaussian decision variables $y_{i|j}$, respectively. Hence,

$$\left(\frac{m_y^2(i|j)}{\sigma_y^2(i,j)}\right) = \frac{E_s}{N_o}\left[1 - \alpha_{ij}\right]. \tag{6.26}$$

Hence, UBP_e is a function of the received signal-to-noise-ratio (SNR) $\left(\frac{E_s}{N_o}\right)$ and the correlation properties Λ_{TSK} of the communication signal set [52]. Conditioned on $u = u_o$, this result is also valid for the PRake and MRake receivers. For the PRake receiver, the union bound is given by

$$\mathrm{UBP}_e(u_o) = \frac{1}{M} {\sum_{i=1}^{M}}_{i \neq j} \sum_{j=1}^{M} \, Q\left(\sqrt{\frac{m_{\tilde{y}}^2(i|j)}{\sigma_{\tilde{y}}^2(i,j)}}\right) \tag{6.27}$$

where $\left(\frac{m_{\tilde{y}}^2(i|j)}{\sigma_{\tilde{y}}^2(i,j)}\right)$ is the SNR value involved in the decision between the pair of signals (i,j), and

$$m_{\tilde{y}}(i|j) \;=\; E_s r_{MP}(u_o,0)\left[1-\tilde{\alpha}_{ij}(u_o)\right] \tag{6.28}$$

and

$$\sigma_{\tilde{y}}^2(i,j) \;=\; N_o E_s r_{MP}(u_o,0)\left[1-\tilde{\alpha}_{ij}(u_o)\right] \tag{6.29}$$

are the mean and variance of the (conditioned) Gaussian decision variables $\tilde{y}_{i|j}$, respectively. Hence,

$$\left(\frac{m_{\tilde{y}}^2(i|j)}{\sigma_{\tilde{y}}^2(i,j)}\right) = \frac{E_a r_{\mathrm{MP}}(u_o,0)}{N_o}\left[1-\tilde{\alpha}_{ij}(u_o)\right] \tag{6.30}$$

Similarly, for the MRake receiver the union bound is given by

$$\mathrm{UBP}_e^{(K)}(u_o) \;=\; \frac{1}{M}\sum_{\substack{j=1 \\ i\neq j}}^{M}\sum_{i=1}^{M} Q\left(\sqrt{\frac{(m_{\hat{y}}^{(K)}(i|j))^2}{(\sigma_{tot}^{(K)}(i,j))^2}}\right) \tag{6.31}$$

where $\left(\frac{(m_{\hat{y}}^{(K)}(i|j))^2}{(\sigma_{tot}^{(K)}(i,j))^2}\right)$ is the SNR value involved in the decision between the pair of signals (i,j), and $m_{\hat{y}}^{(K)}(i|j)$ and $(\sigma_{tot}^{(K)}(i,j))^2$ are the mean and variance of the (conditioned) Gaussian decision variables $\hat{y}_{i|j}$, respectively, and are given by

$$m_{\hat{y}}^{(K)}(i|j) \;=\; E_a^{(K)} r_{MP}^{(K)}(u_o,0)\left[1-\tilde{\alpha}_{ij}^{(K)}(u_o)\right] \tag{6.32}$$

and

$$(\sigma_{tot}^{(K)}(i,j))^2 \;=\; (\sigma_{\hat{y}}^{(K)}(i,j))^2 + (\sigma_{c}^{(K)}(i,j))^2, \tag{6.33}$$

where

$$(\sigma_{\hat{y}}^{(K)}(i,j))^2 = N_o E_a^{(K)} r_{MP}^{(K)}(u_o, 0) \left[1 - \tilde{\alpha}_{ij}^{(K)}(u_o) \right] \tag{6.34}$$

is the term that accounts for the presence of the AWGN, and

$$(\sigma_c^{(K)}(i,j))^2 = (E_a^{(K)})^2 \left[c_{MP}^{(K)}(u_o, 0) - c_{MP}^{(K)}(u_o, \tau_j - \tau_i) \right]^2 \tag{6.35}$$

is the term that accounts for the presence of the signal-dependent *self-noise* in (6.9) that is not matched by the MRake.[1] Hence,

$$\left(\frac{(m_{\hat{y}}^{(K)}(i|j))^2}{(\sigma_{tot}^{(K)}(i,j))^2} \right) = \frac{(m_{\hat{y}}^{(K)}(i|j))^2}{(\sigma_{\hat{y}}^{(K)}(i,j))^2 + (\sigma_c^{(K)}(i,j))^2}$$

$$= \left[\left(\frac{(m_{\hat{y}}^{(K)}(i|j))^2}{(\sigma_{\hat{y}}^{(K)}(i,j))^2} \right)^{-1} + \left(\frac{(m_{\hat{y}}^{(K)}(i|j))^2}{(\sigma_c^{(K)}(i,j))^2} \right)^{-1} \right]^{-1}. \tag{6.36}$$

The expressions in (6.27) and (6.31) are conditioned on the event $u = u_o$. The average probability of error can be obtained by taking the expected value $\mathbf{E}\{\cdot\}$ with respect to u to get

$$\overline{\text{UBP}}_e = \mathbf{E}_u\{\text{UBP}_e(u)\} \tag{6.37}$$

and

$$\overline{\text{UBP}}_e^{(K)} = \mathbf{E}_u\{\text{UBP}_e^{(K)}(u)\}. \tag{6.38}$$

Note that $\overline{\text{UBP}}_e$ is a function of

$$\left(\frac{E_a}{N_o} \right)(i,j) \triangleq \mathbf{E}_u \left\{ \frac{m_{\hat{y}}^2(i|j)}{\sigma_{\hat{y}}^2(i,j)} \right\} \tag{6.39}$$

---

[1] In this analysis the self-noise is considered to be zero-mean Gaussian with power equal to its variance.

and that $\overline{\mathrm{UBP}}_e^{(K)}$ is a function of

$$\left(\frac{E_a^{(K)}}{N_o + N_{ji}}\right)(i,j) \triangleq \mathbf{E}_u\left\{\frac{(m_{\hat{y}}^{(K)}(i|j))^2}{(\sigma_{tot}^{(K)}(i,j))^2}\right\} \tag{6.40}$$

for $i \neq j$, $i,j = 1,2,\ldots,M$. The expressions in (6.39) and (6.40) are the average received symbol SNR for the PRake and MRake receivers, respectively.

The expected values in (6.37) and (6.38) can be approximated by the sample mean values

$$\overline{\mathrm{UBP}}_e \approx \frac{1}{u_*}\sum_{u_o=1}^{u_*}\mathrm{UBP}_e(u_o) \tag{6.41}$$

and

$$\overline{\mathrm{UBP}}_e^{(K)} \approx \frac{1}{u_*}\sum_{u_o=1}^{u_*}\mathrm{UBP}_e^{(K)}(u_o) \tag{6.42}$$

calculated over the ensemble in (6.1).

6.2.4 Communications signal sets

Figure 6.1 shows the four MTSK signal sets under study. Each signal set has the form in (6.3) with $M = 4$ signals defined by the time shift values

$$
\begin{aligned}
&(a) \quad (\tau_1 = \hat{\tau}_1^{opt} = 0,\ \tau_2 = \hat{\tau}_2^{opt},\ \tau_3 = \hat{\tau}_3^{opt},\ \tau_4 = \hat{\tau}_4^{opt}). \\
&(b) \quad (\tau_1 = 0,\ \tau_2 = \tau_{\min},\ \tau_3 = T_w + \tau_{\min}, \tau_4 = T_w + 2\tau_{\min}), \\
&(c) \quad (\tau_1 = 0,\ \tau_2 = 0.55\tau_{\min},\ \tau_3 = T_w + 0.55\tau_{\min}, \tau_4 = T_w + 1.10\tau_{\min}), \\
&(d) \quad (\tau_1 = 0,\ \tau_2 = Tw,\ \tau_3 = 2T_w,\ \tau_4 = 3T_w)
\end{aligned}
\tag{6.43}
$$

The correlation matrices corresponding to these signal sets, calculated using the
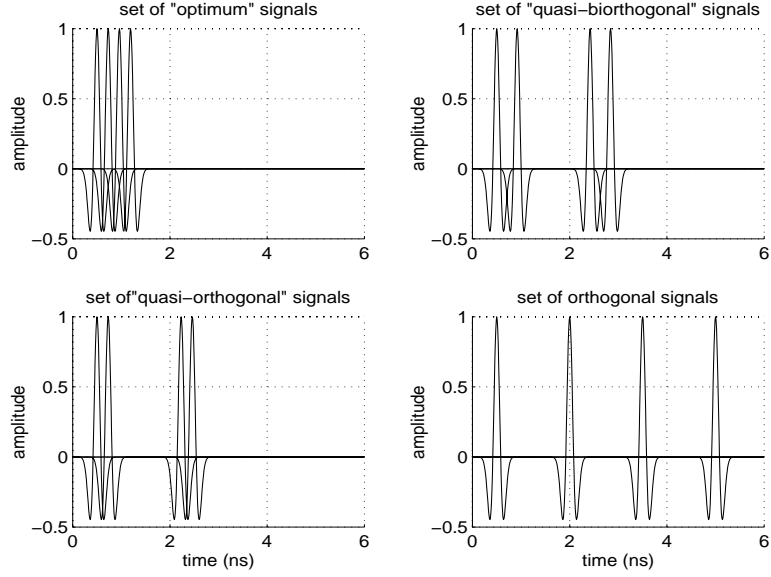
Figure 6.1: The four sets of quaternary PPM data signals under study. (a) Optimum. (b) Quasi-biorthogonal. (c) Quasi-orthogonal. (d) Orthogonal.

pulse $w(t)$ described in the next section, are given in the equations below.

$$
\Lambda_{\mathrm{TSK}}^{(a)} = \begin{pmatrix}
+1.00 & -0.04 & -0.57 & -0.02 \\
-0.04 & +1.00 & -0.04 & -0.57 \\
-0.57 & -0.04 & +1.00 & -0.04 \\
-0.02 & -0.57 & -0.04 & +1.00
\end{pmatrix}
\tag{6.44}
$$

$$
\Lambda_{\mathrm{TSK}}^{(b)} = \begin{pmatrix}
+1.00 & -0.61 & 0.00 & 0.00 \\
-0.61 & +1.00 & 0.00 & 0.00 \\
0.00 & 0.00 & +1.00 & -0.61 \\
0.00 & 0.00 & -0.61 & +1.00
\end{pmatrix}
\tag{6.45}
$$

$$
\Lambda_{\mathrm{TSK}}^{(c)} = \begin{pmatrix}
+1.00 & -0.04 & 0.00 & 0.00 \\
-0.04 & +1.00 & 0.00 & 0.00 \\
0.00 & 0.00 & +1.00 & -0.04 \\
0.00 & 0.00 & -0.04 & +1.00
\end{pmatrix}
\tag{6.46}
$$

$$
\Lambda_{\mathrm{TSK}}^{(d)} = \begin{pmatrix} +1.00 & 0.00 & 0.00 & 0.00 \\ 0.00 & +1.00 & 0.00 & 0.00 \\ 0.00 & 0.00 & +1.00 & 0.00 \\ 0.00 & 0.00 & 0.00 & +1.00 \end{pmatrix} \tag{6.47}
$$

Signal set (b) corresponds to an N-Orthogonal signal set with $N = 2$, $L = 2$, $\tau_1 = 0$, $\tau_2 = \tau_{\min}$ and $T_o = \tau_{\min} + T_w$. The signal set (c) corresponds to an orthogonal signal set with $M = 4$ that takes advantage of the first zero crossing in the signal correlation function. The signal set (d) corresponds to an orthogonal signal set with $M = 4$ and $T_{\mathrm{OR}} = T_w$. The signal set (a) corresponds to an N-Orthogonal signal set with $N = 4$, $L = 1$, $\tau_1 = \hat{\tau}_1^{opt}$, $\tau_2 = \hat{\tau}_2^{opt}$, $\tau_3 = \hat{\tau}_3^{opt}$ and $\tau_4 = \hat{\tau}_4^{opt}$, with the time shift values calculated by solving the optimization problem in (4.29).[2]

6.3   Numerical results

The pulse shape $w(t)$ and the signal correlation $\gamma_w(\tau)$ are the same used in the example in section 4.4, and are reproduced here for convenience

$$
w(t) = \left[1 - 4\pi \left[\frac{t}{t_n} \right]^2 \right] \exp \left(-2\pi \left[\frac{t}{t_n} \right]^2 \right), \tag{6.48}
$$

and

$$
\gamma_w(\tau) = \left[1 - 4\pi \left[\frac{\tau}{t_n} \right]^2 + \frac{4\pi^2}{3} \left[\frac{\tau}{t_n} \right]^4 \right] \exp \left(-\pi \left[\frac{\tau}{t_n} \right]^2 \right). \tag{6.49}
$$

The value $t_n = 0.7531$ ns was used to fit the model $w(t)$ to the measured waveform $w_{\mathrm{T}}(t)$. The UWB pulse $w_{\mathrm{T}}(t)$ is a unit-energy template with duration $T_w = 1.5$ ns that was taken from a multipath-free and noise-free measurement in a particular IR link. The signal correlation function of $w_{\mathrm{T}}(t)$ is denoted $\gamma_{w_{\mathrm{T}}}(\tau)$. The signal

---

[2] The signal set (a) is *optimum* in the sense that it minimizes the union bound of probability of error at high SNR values.

correlation function $\gamma_w(\tau)$ has a minimum $\gamma_{\min} = -0.6183$ at the time shift value $\tau_{\min} = 0.408$ ns.

The symbol error probabilities in (6.41) and (6.42) where calculated using the ensemble in (6.1) with $u_* = 352$. The 352 pulse responses $\tilde{w}(u_o, t)$ were taken from signal propagation data recorded in an UWB propagation measurements experiment [13]. In this experiment, multipath profiles were measured in different rooms and hallways. In each room, $T_m = 300$ nanosecond-long windows of multipath measurements were recorded at 49 different locations arranged spatially in a 7x7 square grid with 6 inch spacing, with the transmitter, the receiver and the environment kept stationary. The 352 normalized correlation functions $\gamma_{\mathrm{MP}}(u_o, \tau)$ were calculated from measured signals received in eight different rooms. Due to the multipath effects, the signal correlations at each point are different from each other. They are the sample functions of $\gamma_{\mathrm{MP}}(u_o, \tau)$ as described before. Figure 6.2 show the signal correlation functions involved in this example. The distortion in $\gamma_{\mathrm{MP}}(u_o, \tau)$ caused by multipath is evident.

Figures 6.3 compares UBP_e and $\overline{\mathrm{UBP}}_e$ for all the signal sets. Figures 6.4, 6.5, 6.6, 6.7, show UBP_e, $\overline{\mathrm{UBP}}_e$ and $\overline{\mathrm{UBP}}_e^{(K)}$ for the sets of signals (a), (b), (c) and (d), respectively.

6.4   Discussion of results

The use of time-shift-keyed signals with $M = 4$ allows to double the data transmission rate without increasing the transmission bandwidth. With respect to performance, from figures 6.4, 6.5, 6.6 and 6.7 we can see that, in the IR-AWGN channel, signal set (a) has the best performance, but in the IR-MP channel, signal (b) has the best performance. This is attributed to the fact that signal design (b) is designed
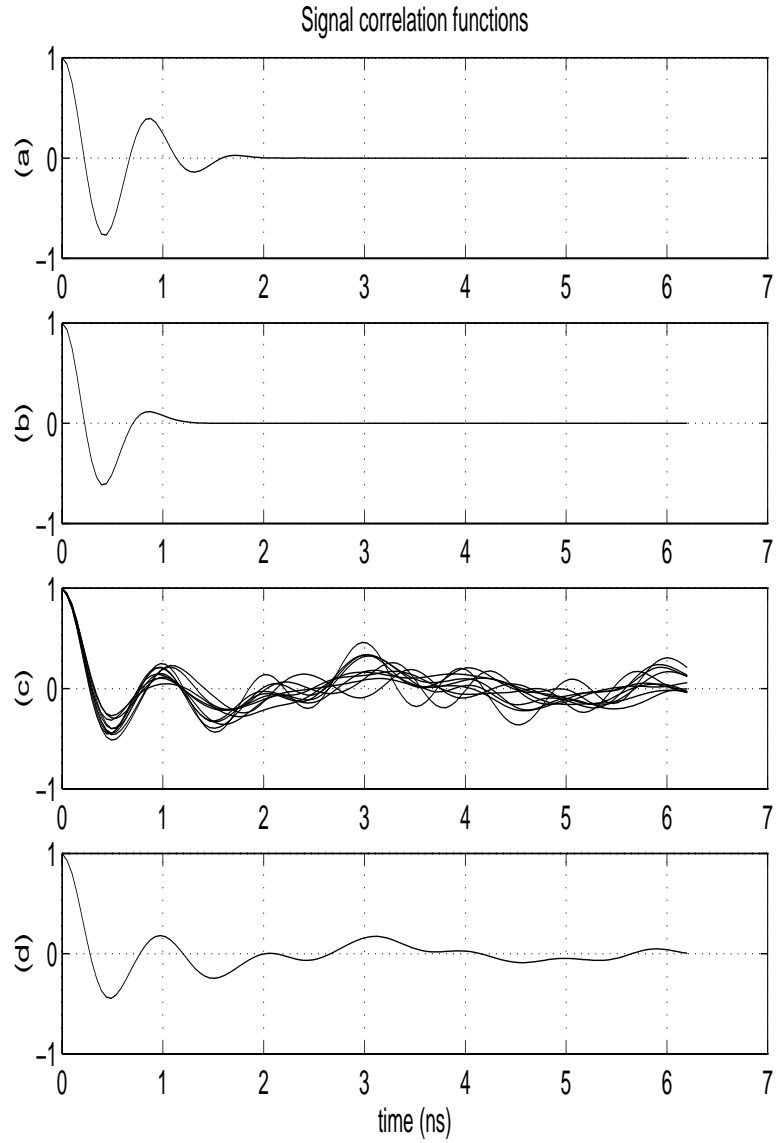
Figure 6.2: Signal correlation functions : (a) $\gamma_{w_{\mathrm{T}}}(\tau)$, (b) $\gamma_w(\tau)$, (c) $\gamma_{\mathrm{MP}}(u_o, \tau)$ for a few different values of u_o, and (d) The average of $\gamma_{\mathrm{MP}}(u_o, \tau)$ taken over the realizations in (c).
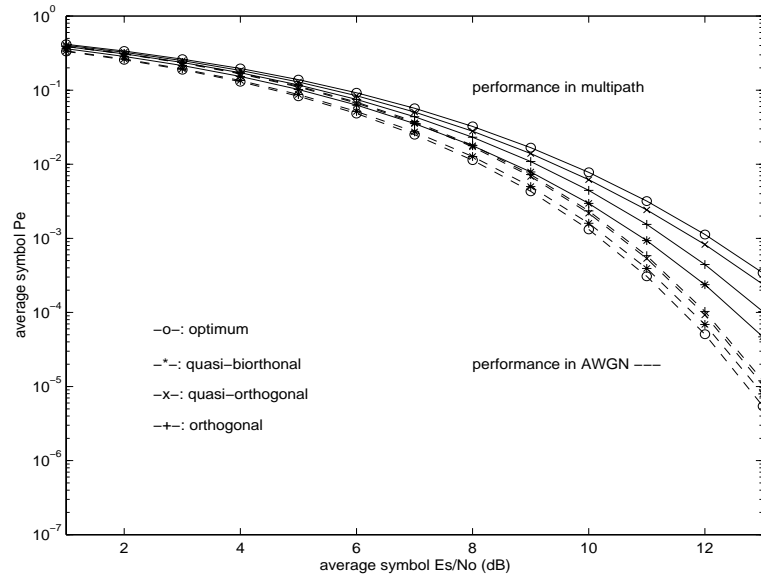
Figure 6.3: The curves for UBP_e and $\overline{UBP}_e$, calculated using signal sets (a), (b), (c) and (d).
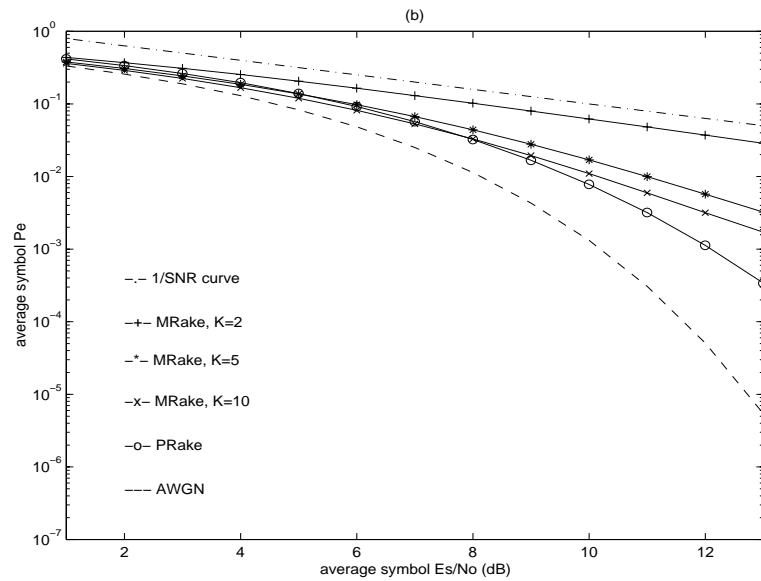

Figure 6.4: The curves for UBP_e, $\overline{\mathrm{UBP}}_e$ and $\overline{\mathrm{UBP}}_e^{(K)}$ for $K = 2, 5, 10$, calculated using signal set (a).

Figure 6.5: The curves for UBP_e, $\overline{\text{UBP}}_e$ and $\overline{\text{UBP}}_e^{(K)}$ for $K = 2, 5, 10$, calculated using signal set (b).
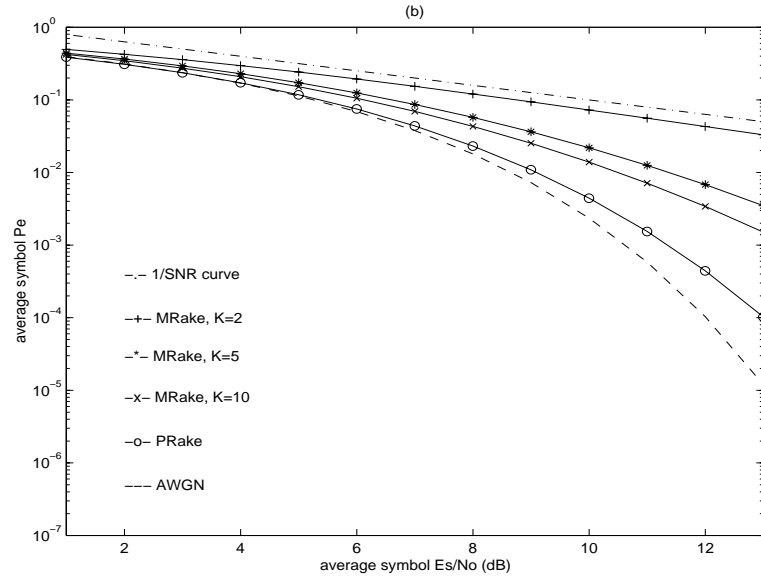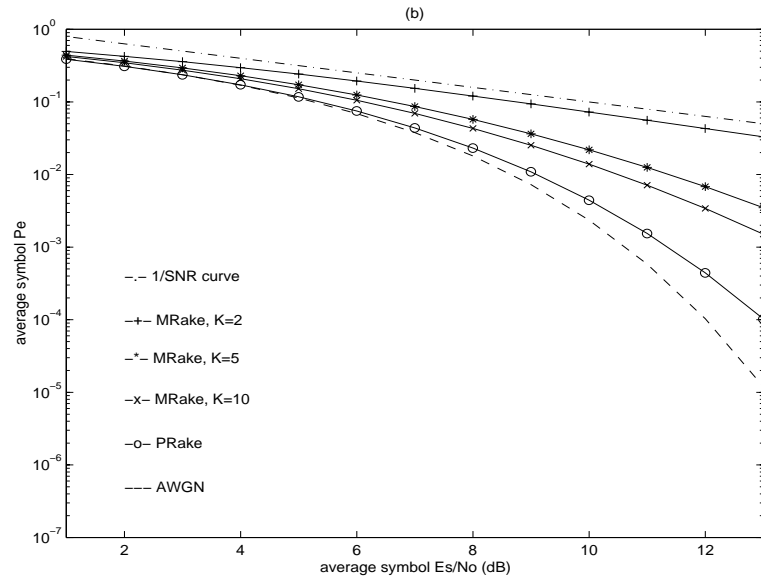

Figure 6.6: The curves for UBP_e, $\overline{\text{UBP}}_e$ and $\overline{\text{UBP}}_e^{(K)}$ for $K = 2, 5, 10$, calculated using signal set (c).
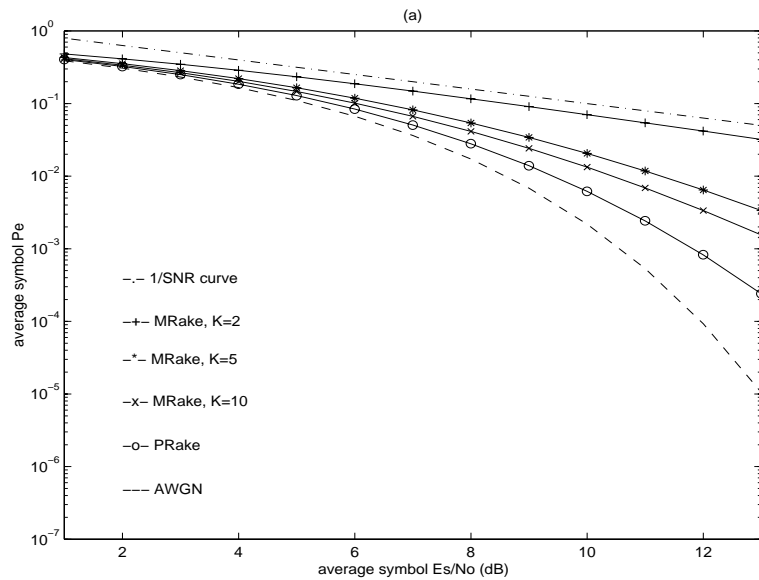
Figure 6.7: The curves for $\mathrm{UBP_e}$, $\overline{\mathrm{UBP}}_{\mathrm{e}}$ and $\overline{\mathrm{UBP}}_{\mathrm{e}}^{(K)}$ for $K = 2, 5, 10$, calculated using signal set (d).

using the values $\tau_{\min}$ and is less susceptible to variations in the signal correlation function [19].

From figure 6.5 we can see that a mismatched Rake receiver with $K = 2$ has performance close to the 1/SNR curve. This degradation is attributed to the presence of both multipath and a considerable self-noise component. Also from figure 6.5 we see that, for a symbol error probability of 10^{-3}, performance in multipath using a mismatched Rake with $K = 10$ is about 2 dB worse than performance in multipath using a perfect Rake, and this performance is in turn about 1 dB worse than performance in AWGN using a correlation receiver.

This analysis shows that for a symbol error probability of 10^{-3}, the performance of impulse radio modulation in the presence of dense multipath is, on average, 3 dB worse than performance in the absence of multipath. It is also shown that

this performance is potentially achievable by using a mismatched Rake receiver of moderate complexity and $M = 4$ communication signals.

Chapter 7

CONCLUSIONS AND FUTURE RESEARCH

This chapter provides conclusions and comments about this research work, and a few guidelines for future research.

7.1   Conclusions

This work has contributed to understand the capabilities of IR using block-waveform PPM signals. The numerical examples given in chapter 5 for a free space propagation channel show that for applications requiring high data rate (1024 Kbps) combined with low probability of bit error (10^{-8}), IR modulation is potentially able to support hundreds of users. Similarly , for applications requiring low data rate (9.6 Kbps) and moderate probability of error (10^{-4}), IR is potentially able to support thousands of users. In either case, the combined transmission rates give a transmission capacity of over 500 Megabits per second using receivers of moderate complexity.

The real payoff of IR will be in wireless transmission in multipath channels. The numerical examples in chapter 6 show that for a one-user case and symbol error probability of 10^{-3}, the performance in the presence of multipath using non-binary TSK modulation with $M = 4$ signals and a mismatched Rake receiver with $K = 10$

fingers is, on average, just 3 dB worse than performance in the absence of multipath using a correlation receiver.

These results support the conclusion that IR will have good multiple-access performance even in dense multipath channels. Hence, IR modulation, together with technological advances in communication circuits and systems, will allow us to build relatively simple and low-cost, low-power transceivers that can be used for short range, high speed reliable multiple-access communications over multipath wireless channels.

7.2   Future research

Although a prototype has been built that is able to operate at about 150 Kbps in a single user link, there are a few basic problems that need to be solved before the potential of IR can be really exploited. One of them is to develop a circuit that can provide fast acquisition and tracking of the TH sequence. Another is to be able to include in a small set of chips a moderate number of correlators.

In relation with this research work, it would be worthwhile to study the following issues. In this analysis we assumed a continuous random TH sequence. What would be the impact of using a discrete pseudorandom TH sequence? The sensitivity to mismatched system parameters definitely grows with the number of signals M. How can this sensitivity be quantified? In this analysis we assume that the mismatched Rake receiver always perfectly locks to the K strongest paths in quasi static conditions. What is the effect of loosing track of some of theses paths as the receiver moves?

Reference List

[1] N. Morinaga, M. Nakagawa and. R. Kohono, *"New Concepts and Technologies for Achieving Highly Reliable and High-Capacity Multimedia Wireless Communications Systems,"* IEEE Communications magazine, January 1997, pp. 28-33.

[2] H. Hashemi, *"The Indoor Radio Propagation Channel,"* Proceedings IEEE Vol. 81, No. 7, July 1993.

[3] J. M. Proakis, *Digital Communications,* McGraw Hill, 1995.

[4] G. L. Stüber, *Principles of Mobile Communications,* Kluwer Academic Publishers, 1996.

[5] R. Price and P. E. Green Jr., *"A Communication Technique for Multipath Channels,"* Proc. IRE, March 1958, pp. 555-570.

[6] P. Withington II and L. W. Fullerton. An Impulse Radio Communications System, in H. L. Bertoni, L. Carin, and L. B. Felsen, editors, *Ultra-Wideband, Short-Pulse Electromagnetics,* Plenum Press, 1993.

[7] J. Schandle, *" Impulse Radio System bid for PCS Communications Role,"* Electronic Design, February 4, 1993, pp. 32-34.

[8] R. A. Scholtz, *"Multiple Access with Time Hopping Impulse Modulation,"* invited paper, Proceedings of IEEE MILCOM conference, December 1993.

[9] L. B. Milstein and M. K. Simon, Spread Spectrum Communications, in J. D. Gibson, editor, *Mobile Communications Handbook,* IEEE press, 1996.

[10] F. Ramírez-Mireles and R. A. Scholtz, *"System Performance of Impulse Radio Modulation,"* in Proceedings IEEE RAWCON conference, August 1998.

[11] R. A. Scholtz and M. Z. Win, *"Impulse Radio,"* invited paper, Proceedings of IEEE PIMRC conference, September 1997. Printed in *Wireless Communications: TDMA versus CDMA,* S. G. Glisic and P. A. Leppänen, eds., Kluwer Academic Publishers, 1997.

[12] M. Z. Win and R. A. Scholtz, *"Impulse Radio: How It Works,"* in IEEE Communications Letters, vol. 2, no. 2, February 1998.

[13] M. Z. Win and R. A. Scholtz, *"Ultra-Wide Bandwidth (UWB) Signal Propagation for Indoor Wireless Communications,"* in Proceedings IEEE ICC'97, June 1997.

[14] M. Z. Win, F. Ramírez-Mireles, R. A. Scholtz and M. A. Barnes, *"Ultra-Wide Bandwidth (UWB) Signal Propagation for Outdoor Wireless Communications,"* in Proceedings IEEE VTC conference, May 1997.

[15] R. Jean-Mark Cramer, M. Z. Win and R. A. Scholtz, *"Impulse Radio Multipath Characteristics and Diversity Reception,"* in Proceedings IEEE ICC conference, June 1998.

[16] R. Jean-Mark Cramer, M. Z. Win and R. A. Scholtz, *"Evaluation of the Multipath Characteristics of the Impulse Radio Channel,"* submitted to PIMRC'98.

[17] M. Z. Win and R. A. Scholtz, *"Statistical Characterization of Ultra-Wide Bandwidth Wireless Communications Channels,"* in Proceedings IEEE ASILOMAR conference, November 1997.

[18] M. Z. Win and R. A. Scholtz, *"Characterization of Ultra-Wide Bandwidth Wireless Indoor Communications Channels: A Communications Theoretic View,"* submitted to IEEE Transactions on Communications.

[19] F. Ramírez-Mireles, M. Z. Win and R. A. Scholtz, *"Signal Selection for the Indoor Impulse Radio Channel,"* in Proceedings IEEE VTC conference, May 1997.

[20] F. Ramírez-Mireles and R. A. Scholtz, *"Performance of Equicorrelated Ultra-Wideband Pulse-Position-Modulated Signals in the Indoor Wireless Impulse Radio Channel,"* in Proceedings IEEE PACRIM conference, August 1997.

[21] F. Ramírez-Mireles, R. A. Scholtz and M. Z. Win, *"Performance of Ultra-Wideband Time-Shift-Modulated Signals in the Indoor Wireless Impulse Radio Channel,"* in Proceedings 31st Asilomar conference, November 1997.

[22] M. Z. Win and R. A. Scholtz, *"On the Robustness of Ultra-Wide Bandwidth Signals in Dense Multipath Environments,"* in IEEE Communications Letters, vol. 2, no. 2, February 1998.

[23] F. Ramírez-Mireles and R. A. Scholtz, *"Performance of Impulse Radio Modulation in the Presence of Dense Multipath,"* to be submitted to IEEE Transactions on Communications.

[24] F. Ramírez-Mireles and R. A. Scholtz, *"N-Orthogonal Time-Shift-Modulated Signals for Ultra-Wide Bandwidth Impulse Radio Modulation,"* in Proceedings IEEE CTMC conference, in conjunction with GLOBECOM conference, November 1997.

[25] F. Ramírez-Mireles and R. A. Scholtz, *"Time-Shift-Keyed Equicorrelated Signal Sets for Impulse Radio Modulation,"* in Proceedings WIRELESS conference, July 1998.

[26] F. Ramírez-Mireles and R. A. Scholtz, *"Wireless Multiple-Access Using SS Time-Hopping and Block Waveform Pulse Position Modulation, Part 1: Signal Design,"* in Proceedings ISITA symposium, October 1998.

[27] F. Ramírez-Mireles and R. A. Scholtz, *"Wireless Multiple-Access Using SS Time-Hopping and Block Waveform Pulse Position Modulation, Part 2: Multiple-Access Performance,"* in Proceedings ISITA symposium, October 1998.

[28] F. Ramírez-Mireles and R. A. Scholtz, *"Multiple-Access with Time Hopping and Block Waveform PPM Modulation,"* in Proceedings IEEE ICC conference, June 1998.

[29] F. Ramírez-Mireles and R. A. Scholtz, *"Multiple-Access Performance Limits with Time Hopping and Pulse Position Modulation,"* in Proceedings IEEE MIL-COM conference, October 1998.

[30] M. Z. Win and R. A. Scholtz, *"Ultra-Widebandwidth (UWB) Time-Hopping Spread-Spectrum Impulse radio for Wireless Multiple-Access Communications,"* accepted, pending revision, by IEEE Transactions on Communications.

[31] M. Z. Win, R. A. Scholtz, and L. Fullerton, *"Time-Hopping SSMA Techniques for Impulse Radio with an Analog Modulation Data Subcarrier,"* in Proceedings IEEE ISSSTA symposium, September 1996.

[32] M. Z. Win and R. A. Scholtz, *"Comparisons of Analog and Digital Impulse Radio for Wireless Multiple-Access Communications,"* in Proceedings IEEE ICC conference, June 1997.

[33] M. Z. Win and R. A. Scholtz, *"Energy Capture Vs. Correlator Resources in Ultra-Wide Bandwidth Indoor Wireless Communications Channels,"* in Proceedings of MILCOM conference, November 1997.

[34] M. Z. Win and R. A. Scholtz, *"On the Energy Capture of Ultra-Wide Bandwidth Signals in Dense Multipath Environments,"* in IEEE Communications Letters, vol.2, no. 9, September 1998.

[35] M. Z. Win and R. A. Scholtz, *"Design of an Ultra-Wide Bandwidth Rake Receiver for Time-Hopping SSMA Impulse Radio and Its Application to Wireless Indoor Multipath Communications,"* in preparation, to be submitted to IEEE Transactions on Communications.

[36] L.-K. A. Tee, *"Time Hopping Spread Spectrum System,"* M.S. Thesis, Department of Electrical Engineering, Univ. of Southern California.

[37] M. Z. Win, J.-H. Ju, X. Qiu, V. O. K. LI and R. A. Scholtz, *"ATM Based Ultra-wide Bandwidth (UWB) Multiple-Access Radio Network for Multimedia PCS,"* in Proceedings Fourth Annual Engineers Conference at NetWorld+Interop, May 1997.

[38] M. Z. Win, J.-H. Ju, X. Qiu, V. O. K. LI and R. A. Scholtz, *"ATM Based Time-Hopping Spread-Spectrum Multiple-Access Network for Multimedia,"* conditionally accepted in IEEE JSAC, special issue on "Networking and Performance Issues of Personal Mobile Communications."

[39] S. S. Kolenchery, J. K. Townsend, J. A. Freebersyser and G. Bilbro, *"Performance of Local Power Control in Peer-to-Peer Impulse Radio Networks with Bursty Traffic,"* in Proceedings GLOBECOM conference, November 1997.

[40] S. Kolenchery, J. Townsend and J. Freebersyser, *"A Novel Impulse Radio Network for Tactical Military Communications,"* in Proceedings IEEE MILCOM conference, October 1998.

[41] S. W. Golomb, *"Construction of signals with favorable correlation properties,"* in Surveys in Combinatorics, London Mathematical Society Lecture Notes Series 166, Cambridge University Press, 1991.

[42] R. M. Gagliardi, *Introduction to Telecommunications Engineering,"* John Wiley and Sons, 1988.

[43] H. Stark and J. W. Woods, *Probability, Random Processes, and Estimation Theory for Engineers,"* Prentice Hall, 1986.

[44] C. L. Weber, G. K. Huth and B. H. Batson, *"Performance Considerations of Code Division Multiple-Access Systems,"* IEEE Trans. on Vehicular Technology, Vol. VT-30, No. 1, pages 3-9, February 1981.

[45] H. V. Poor, *"Signal Processing for Wideband Communications,"* IEEE Information Society Newsletter, June 1992.

[46] S. Verdu, Recent Progress in Multiuser Detection, in *Multiple Access Communications: Foundations for Emerging Technologies,* IEEE Press, 1993, pp. 164-175.

[47] J. M. Wozencraft and I. M. Jacobs, *Principles of Communication Engineering,* John Wiley, 1965, Chapter 4.

[48] A. Papoulis, *Signal Analysis,* McGraw-Hill, 1984.

[49] M. K. Simon, S. H. Hinedi and W. C. Lindsey, *Digital Communication Techniques,* Prentice Hall, 1996.

[50] I. S. Reed and R. A. Scholtz, *"N-Orthogonal Phase-Modulated Codes,"* IEEE Transactions on Information Theory, Vol. IT-12, No. 3, July 1966.

[51] A. J. Viterbi and J. J. Stiffler, *"Performance of N-Orthogonal Codes,"* IEEE Transactions on Information Theory, July 1967, pp. 521-522.

[52] C. L. Weber, *Elements of Detection and Signal Design,* corrected reprint, Springer Verlag, 1987.

[53] M. J. Steiner, *Contributions to Statistical Communication Theory,* Ph.D. Dissertation, Department of Electrical Engineering, University of Maryland, 1994.

[54] J. E. Dennis, Jr. and D. J. Woods, *New Computing Environments: Microcomputers in Large-Scale Computing,* edited by A. Wouk, SIAM 1987, pp. 116-122.